ESTIMATING RECHARGE AND STORAGE COEFFICIENT IN A FRACTURED ROCK AQUIFER, TURKEY CREEK BASIN, JEFFERSON COUNTY, COLORADO

by

Greg A. VanderBeek

A thesis submitted to the Faculty and Board of Trustees of the Colorado School of Mines in partial fulfillment of the requirements for the degree of Master of Science (Geological Engineering).

Date:_____

Signed: _____
Greg A. VanderBeek

Approved: _____
Dr. Eileen Poeter
Thesis Advisor

Golden, Colorado
Date:_____

Approved: _____
Dr. Murray Hitzman
Professor and Head
Department of Geology and
Geological Engineering

ABSTRACT

Turkey Creek Basin is located 20 miles west of Denver. This front-range area is experiencing rapid development, thus water quantity and quality is a concern. Data collected from monitoring wells over the past 25 years show an average water-level decline of 1 ft/yr, indicating the Turkey Creek Basin is not in a state of equilibrium. The sustainable level of water use is unknown. Evaluation of the sustainability of the aquifer requires reasonable estimates of water use, recharge rates, transmissivities, and storage coefficients. Sustainability requires that the average rate of water usage be less than the average recharge rate. During droughts usage may exceed recharge and sustainability is dependent on the volume of water that can be drawn from storage. This research focuses on the evaluation of the magnitude and distribution of recharge and storage of the Turkey Creek Basin.

Water use is estimated using a combination of ranges for pumping and return-flow yielding a minimum (106 AFY) and maximum (518 AFY) for water consumption. This range includes the consumption (190 AFY) estimated by a recent Mountain Ground Water Study (MGWRS, 2002).

Recharge is estimated to be between 250 and 5,700 AFY. Several methods of estimating recharge are evaluated by comparing residuals of a calibrated ground-water model using MODFLOW and UCODE. These methods include: 1) a uniform recharge distribution; 2) a function relating recharge to elevation; 3) a function relating recharge to elevation and slope aspect; 4) a PRMS (Precipitation-Runoff Modeling System) model, created by the USGS; and 5) a SWAT (Soil & Water Assessment Tool) model. The magnitude and distribution of recharge calculated by surface water models, SWAT and PRMS were determined independently of the ground-water model. The average recharge value from PRMS modeling is larger than field observations can support. In order to

evaluate the spatial distribution of recharge determined with the surface water models, their results were incorporated into the ground-water model and calibrated with a recharge multiplier, constrained by a stream base flow observation. Although it was anticipated that the surface water models would provide the best estimate of recharge, the Elevation/Aspect based recharge model produced the best model fit as evaluated by comparing the sum of weighted squared residuals (SOS) and considering residual bias. The decline in model fit for the surface water models could be due to: independent calibration of the spatial distribution of recharge; and/or the use of larger zones of constant recharge by the surface water models (average of 0.42 mi^2) while the other functions apply a unique recharge value to each model cell (0.01 mi^2).

Transmissivity for individual geological units was estimated from aquifer test analysis and model calibration. Multi-well aquifer tests conducted in the granitic rock group yielded larger transmissivities (326 ft^2/day and 260 ft^2/day) as compared to two single-well tests (5 ft^2/yr and 1.5 ft^2/yr) and results from the preferred ground-water model (2.1 ft^2/day) for the granitic rock group. Multi-well aquifer tests were only successful in water district wells, thus the biased values. Single well test results are from individual domestic wells, for which drawdown was not measurable in observation wells. The calibrated model represents average transmissivity for the entire granitic rock group.

Specific yield was evaluated by comparing simulated water level declines to those observed in the field during the summer drought of 2002. A single value of specific yield was assigned to the entire basin in a transient ground water model, a value of 0.6% provided the best fit. This value is comparable to those calculated from aquifer test data, but is larger than the value estimated from fracture characterization on outcrops.

Given that current water use is at the low end of the range of estimated recharge to TCB, the long-term water level declines likely reflect a transition to a new equilibrium condition. Given that the long-term average recharge is likely greater than average water

consumption in TCB and storage is estimated to be relatively high for a fractured rock aquifer, current population appears sustainable in TCB. However, the maximum estimated current water use exceeds the minimum estimated recharge, therefore additional work to refine these estimates are needed before further development of the Turkey Creek Basin.

TABLE OF CONTENTS

LIST OF FIGURES

LIST OF TABLES

ACKNOWLEDGEMENTS

I would like to give special thanks to my advisor, Dr. Eileen Poeter whose unwavering dedication to my project and me have been amazing. I have valued Dr. Poeter's opionon as my advisor, mentor and as a friend through my career at the Colorado School of Mines and hopefully for years to come.

I would also like to thank Geoff Thyne and John McCray my committee members for their time and effort they have spend on my thesis and also the time they have spent with me outside of my research.

I would like to thank my Mom and Dad and the rest of my family for their advice, love and support. My parents have been true role models for me throughout my life. I would like to thank my girlfriend Janine for her love, patience and unbelievable support she has given me. Janine has always made me smile.

I would also like to thank my friends for their support and for being who they are. I couldn't have hoped for a better group of people to surround myself with. I would like to give special thanks to Samantha Tokash who from my first day at Mines has helped me as a friend and a colleague.

CHAPTER 1: INTRODUCTION

The Turkey Creek Basin, (TCB) is located in Jefferson County Colorado (Figure 1.1). This Front Range basin has experienced rapid population growth. Most of TCB's growth occurred in the last four decades, as documented by completion dates of individual wells from the State Engineers Office (SEO). Annual growth is shown (Figure 1.2), grouping growth by decade: 19% of the current population occurred before 1960, 16% in the 1960's, 38% in the 1970's, 11% in the 1980's and 16% in the 1990's. According to the USGS (Bossong et al., 2003), Turkey Creek Basin is currently home to 11,440 people and will need to supply water for 13,186 residents in 2010 and over 15,000 residents by the year 2020. Their prediction was based on an estimated 2% growth per year. Although it is difficult to predict population, current immigration into TCB suggests population will continue to increase, warranting a better understanding of water resources in the basin.

TCB encompasses 47 square miles and ranges in elevation from approximately 6,500 feet above sea level at the mouth to over 10,500 feet at the head of the basin. The aquifer is composed almost entirely of fractured bedrock to 1100 ft depth. Fractured bedrock is predicted below these depths but has not been confirmed by drilling. An aquifer composed almost exclusively of fractured rock with high topographic relief is challenging to characterize and model. Large variability in physical features of the basin is believed to cause local differences in precipitation, evapotranspiration, runoff, and vegetation, which, in combination, cause heterogeneous recharge. Rock type also varies and likely influences recharge rate, as well as storage coefficient.

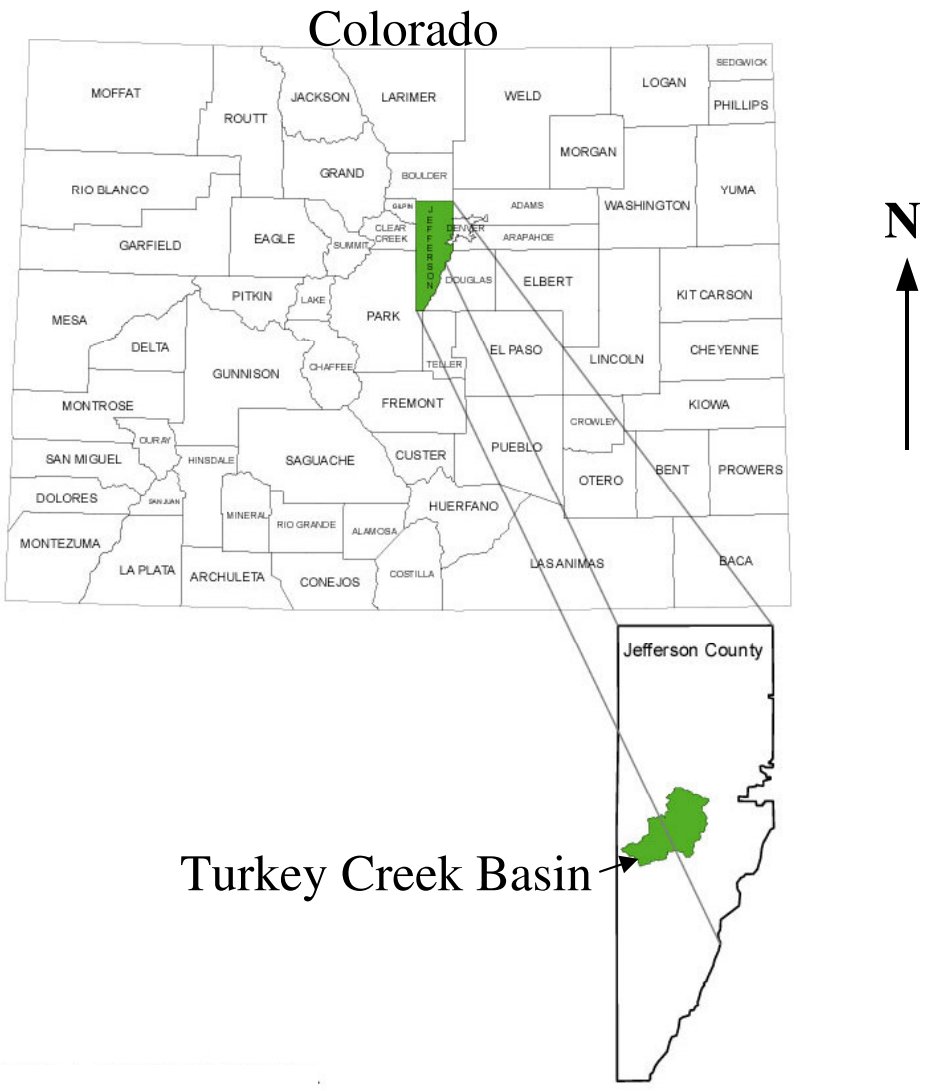

Figure 1.1 Location of the Turkey Creek Basin [Taken from Morgan 2000].

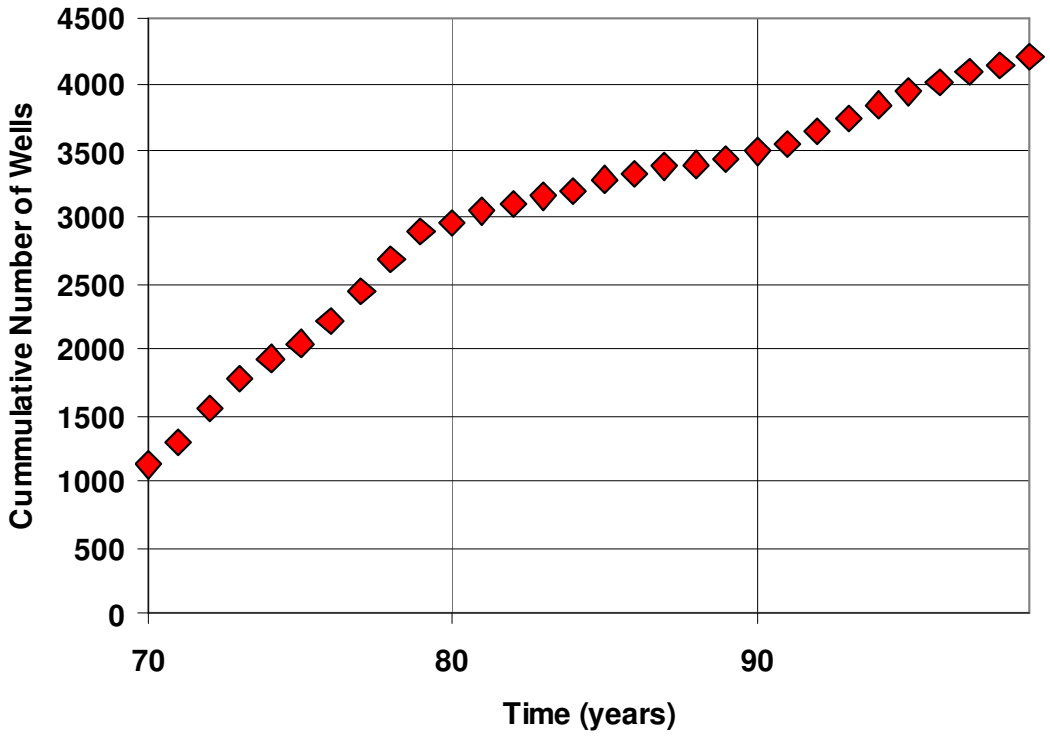

Figure 1.2 Population increase in the Turkey Creek Basin as documented by first beneficial use of wells from the Colorado State Engineers Office.

1.1 Purpose

This research focuses on using low-cost, presently-available, data to increase understanding of this system and investigate recharge, storativity and the water budget of the Turkey Creek Basin.

1.2 Previous Work

Hofstra and Hall (1975) investigated the hydrology and geology of Jefferson County including overviews on climate, vegetation, soils and depth to bedrock. The report contains a water budget for all of Jefferson County; recharge was estimated at 0.6 in/yr.

The Mountain Groundwater Research Study, a collaboration between the United States Geological Survey (USGS), Jefferson County, and the Environmental Protection Agency (EPA) attempted to quantify TCB's water quality and quantity. The study lasted several years involving several phases. Initial phases collected and analyzed water samples, depth to water (DTW), precipitation, stream flow and evapotranspiration. Bossong et al., (2003) constructed a surface water model estimating the spatial distribution of recharge for TCB.

Reports by Caine (2003), suggest that the Turkey Creek Basin aquifer has a low porosity, and thus stores only a small volume of water. Caine (2003) gave a porosity range to each rock unit within the Turkey Creek Basin based on fracture aperture. Caine (2003) estimated that the Metamorphic units range from 0.0016 – 0.51%, the intrusive rock units 0.002 – 0.24% and the Fault Zone units 0.028 – 2.78%.

CHAPTER 2: DESCRIPTION OF THE TURKEY CREEK BASIN

2.1 Geology

The Turkey Creek Basin is composed almost exclusively of fractured crystalline bedrock. The United States Geological Survey Quadrangle (Bryant, 1974) displays the complex local geology and was used to group four crystalline rock units and one surficial alluvial unit (Figure 2.1)(Bossong et al., 2003). The four major rock groups are granitic rocks, gneissic rocks, coarse-grained granitic rocks and fault zone rocks. The granitic rocks are primarily composed of the Silver Plume Quartz Monzonite, a unit composed of coarse to fine grained muscovite-biotite quartz monzonite. The unit includes numerous-crosscutting inclusions of biotite gneiss, migmatite and muscovite biotite schists. The gneissic rock group includes several units ranging from gneissic quartz monzonite, gneissic granodiorite with quartz monzonite, to biotite rich gneiss and migmatites. This unit can be grossly generalized as coarse to fine-grained gneiss with numerous layers and lenses. The coarse-grained granitic rock group is composed of the Pikes Peak Granite and has limited spatial extent in the basin. The rock is coarse-to medium-grained and is composed of biotite and biotite-hornblende granite. The fault zone group overprints the granitic and gneissic rocks. This area is highly fractured and is composed of numerous shear zones. Descriptions of rock groups were summarized from Bryant (1974).

The current structure of the basin resulted from a predominantly plastic deformational event between 1.75 and 1.69 billion years (Hutchinson, 1976). Existing sediments were subjected to high-grade metamorphism resulting in schistose and gneissic formations. This deformation created north to northwest-trending fold systems and related joint systems (Hicks, 1987). For an estimated 300 million years the area was

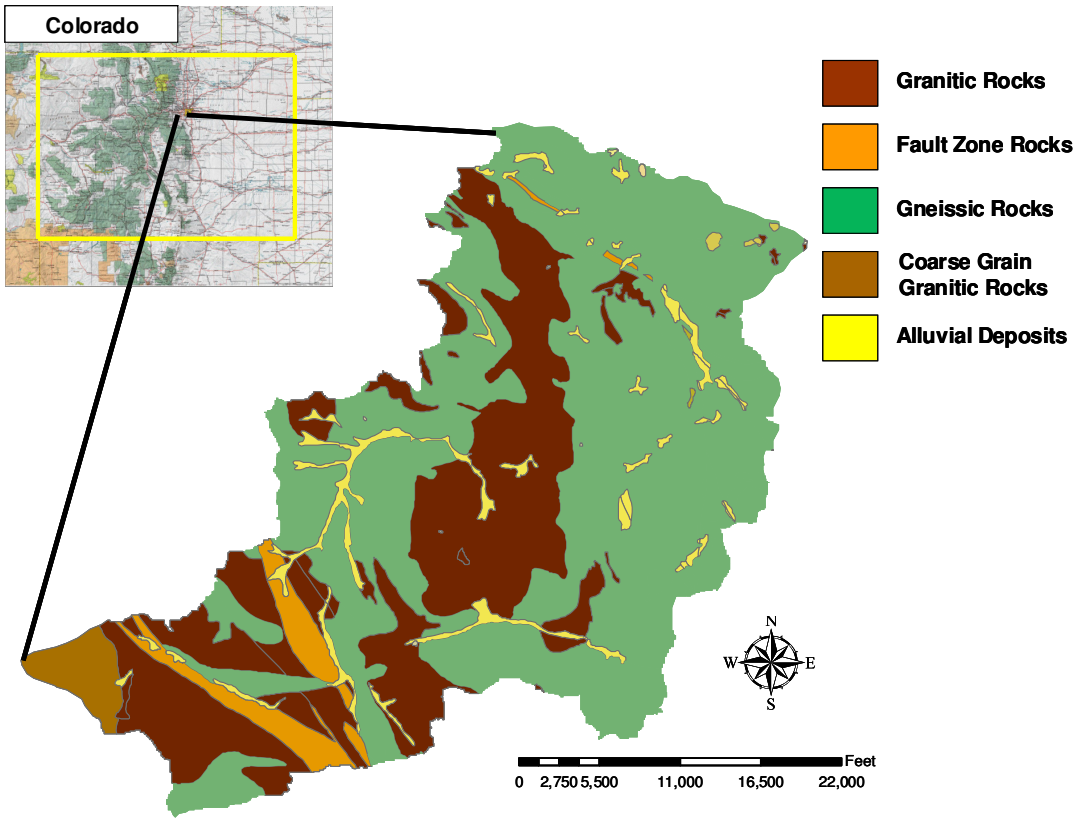

Figure 2.1 Geology of the Turkey Creek Basin [after Bossong et al., 2003]

tectonically inactive (Hicks, 1987). Late in the Precambrian a cataclastic deformational event created northeast trending folds, joint sets and shear zones (Hutchinson, 1976). During this period, 1 to 2.5 billion years ago, emplacement of the Silver Plume and Pikes Peak Batholiths occurred and numerous cooling joints were developed (Hicks, 1987). Since then the area has been affected by two major tectonic events causing folding and faulting. The ancient uplift of the ancestral Rockies, 300 million years ago and the Larmide Orogeny 80 million years ago resulted in northeast and northwest trending folds and superimposition of joints on the older Precambrian rocks (Hicks, 1987). Quaternary erosion is believed to have caused the observed unloading joints and local deposition of unconsolidated sand and gravel.

This sequence of events has created a sharp transition between the fractured crystalline bedrock in the Turkey Creek Basin and the sedimentary units at the mouth of the basin where Turkey Creek cuts through the Dakota hogback. The hydrology at the mouth of the basin is not fully understood.

2.2 Climate

The climate of the Turkey Creek Basin is influenced by topography, seasonal temperature variations, air movement and orogenic affects due to the location of TCB on the leeward side of the continental divide (Hofstra and Hall, 1975). Climate in the basin is classified as semi-arid, averaging approximately 20 inches of precipitation per year (Figure 2.2). The variations of elevation cause a wide range of temperature. Average temperatures fluctuate seasonally, with temperatures that fall below freezing in winter months and reach 90 degrees Fahrenheit in summer months. Temperature and precipitation extremes occur often, but are usually short lived.

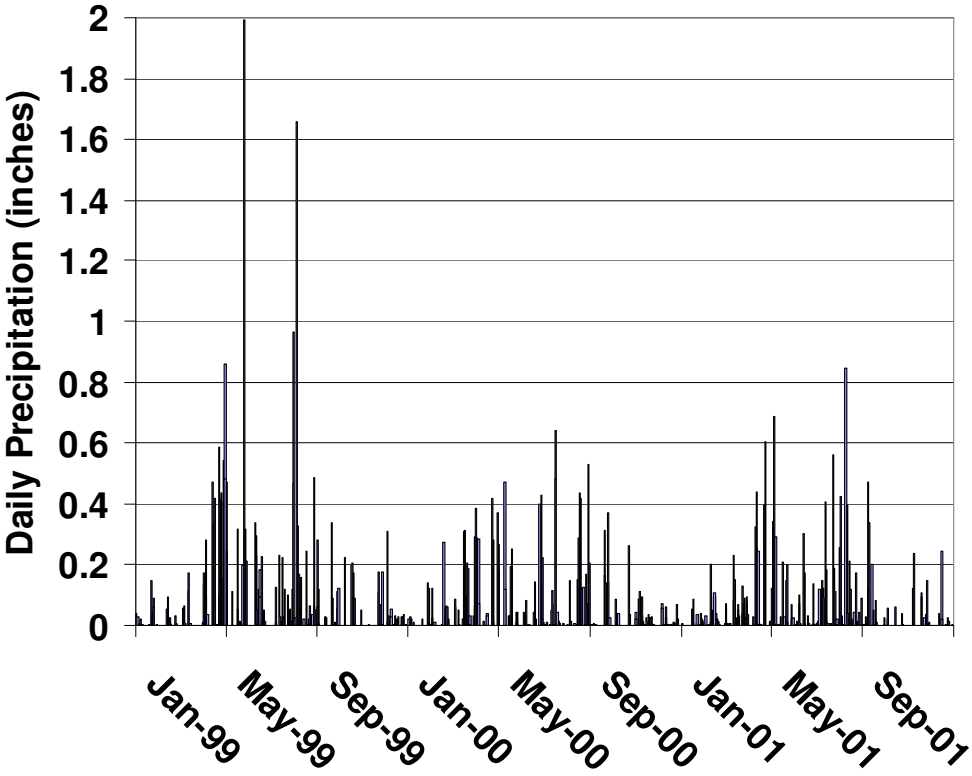

Figure 2.2 Daily values of precipitation from 1999 to 2002 reported by Bossong et al, (2003)

2.3 Vegetation

Vegetation within TCB varies with topography. Lowlands and valleys are composed mainly of trees, small shrubs and grasses. Agricultural activity is minimal. Some livestock is raised which feed on natural grasses in the basin. Higher elevations and steep slopes are composed mainly of a variety of evergreens with scattered pockets of aspen groves. Slopes with high relief can be void of all vegetation and south facing slopes have fewer trees.

2.4 Hydrology

Turkey Creek Basin is comprised of fractured crystalline rocks locally covered by thin soil/regolith. Quaternary deposits account for only 6% of the total basin surface area and are located along stream channels and valley floors (Morgan, 2000). These deposits have an estimated porosity of 20% and may form small local aquifers (Hofstra and Hall, 1975) that are not a significant source of water. However, these deposits may facilitate flow along the stream channel axis resulting in discharge from the basin not observed as open-channel flow in streams.

The fractured crystalline aquifer serves as the main source of water. Driller's logs indicate the average depth to water was less than 100 feet in the early 1970's (Figure 2.3) (Hofstra and Hall, 1975). The largest depths to water from the SEO logs are found along ridgelines and in topographic highs while the smallest depths to water occur in discharge zones near streams. Several hydrologic properties have been determined from well logs (Figure 2.4).

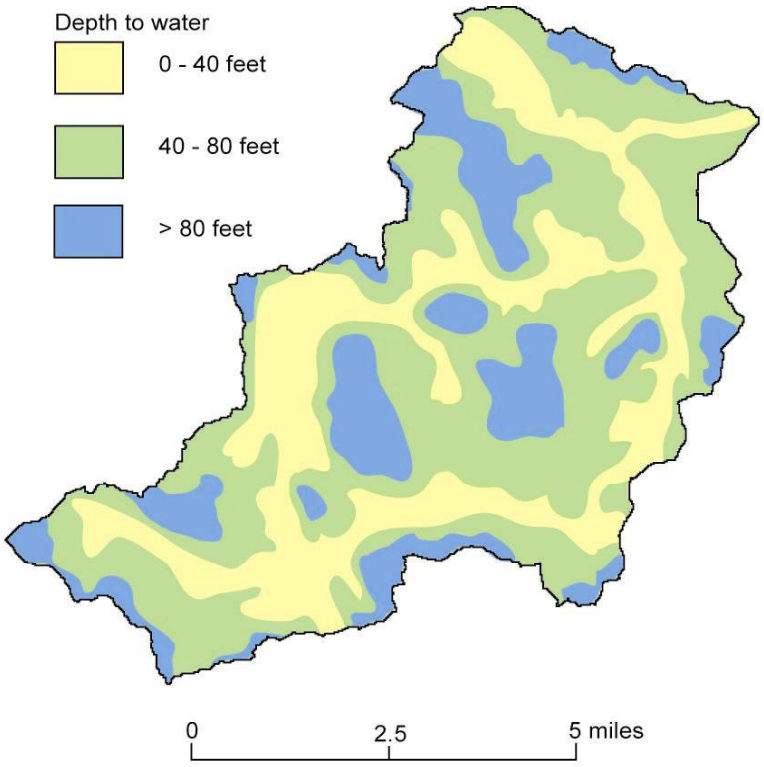

Figure 2.3 Average reported depth to water determined from State Engineers Office in 1975, Hofstra and Hall, [taken from Morgan 2000].

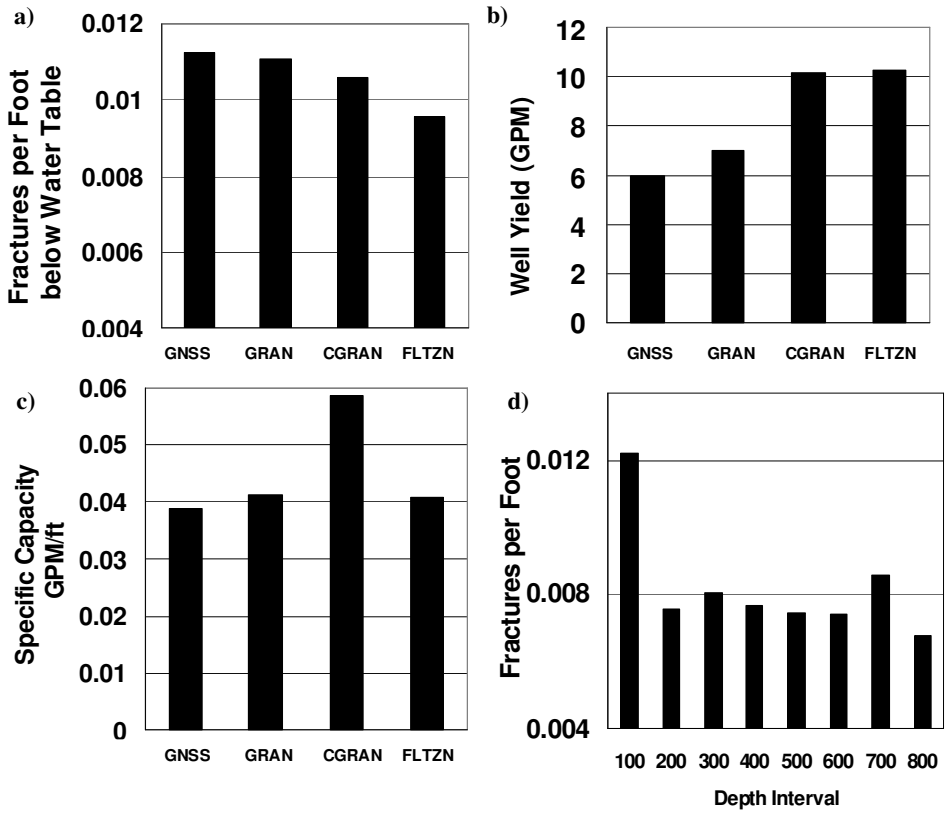

Figure 2.4 Distribution of well yield and fractures. a) Reported water bearing fractures per foot by rock group. b) Reported well yield by rock group. c) Reported specific yield broken by rock group. d) Number of reported water bearing fractures per foot per 100 ft interval below ground surface. [taken from Poeter et al., (2003)]

CHAPTER 3: HYDROLOGIC CHARACTERIZATION OF THE TURKEY CREEK BASIN

Collected data: discharge measurements, specific conductance, hydraulic head, single and multi-well aquifer test data was integrated with previous data to calculate the hydrologic properties of the aquifer and use in a ground-water model. The aquifer properties determined were used to quantifying the system.

3.1 Stream Measurements

Stream measurements were used to gain insight into seasonal variations in the temperature, specific conductance, and discharge of stream water to establish the contribution of ground water into the streams. Measurements were taken throughout the basin on a regular basis and combined with previously collected data.

3.1.1 Historical Discharge Measurements

Shifting locations of gauges, lapses in measurement periods, and stream diversions complicate historical discharge measurements for Turkey Creek. Turkey Creek was gauged, station 06711040 (Figure 3.1a and 3.1b) by the U.S. Geological Survey for periods in the 1940's, 1950's and 1980's. In April 1998, USGS gauge 06710995 (Figure 3.2) was installed for the MGWRS approximately 3 miles upstream from 06711040 (refer to section 1.2). This station was determined to be unstable due to diversions (Bossong et al., 2003), and was removed in April of 2001. Current measurements are from USGS gauge 06710992 (Figure 3.2) established in April 2001. The two most recent stations have overlapping data for a period of six days

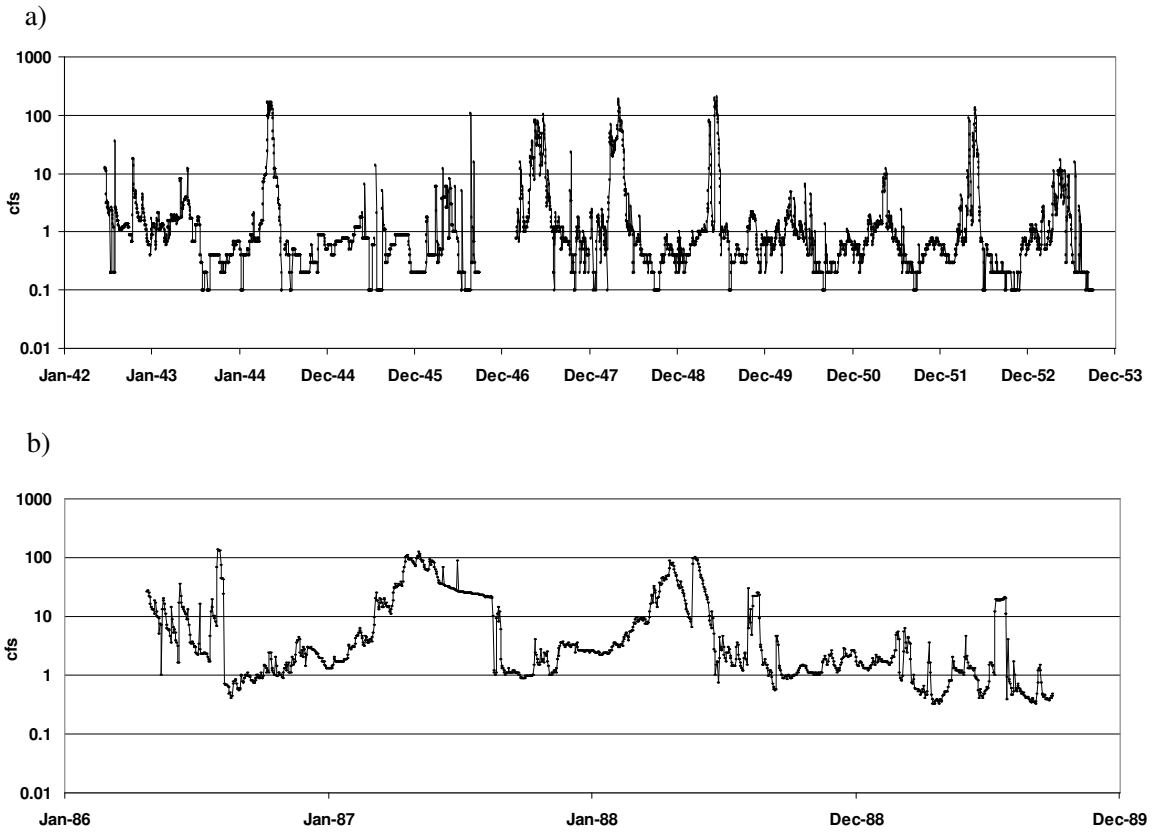

Figure 3.1 U.S.G.S. gauging stations in Turkey Creek. a) Discharge measurements taken from U.S.G.S. gauging station 0611040 from January 1943 to December 1953 for Turkey Creek. B) Discharge measurements taken from U.S.G.S. gauging station 0611040 from January 1986 to December 1989 for Turkey Creek.

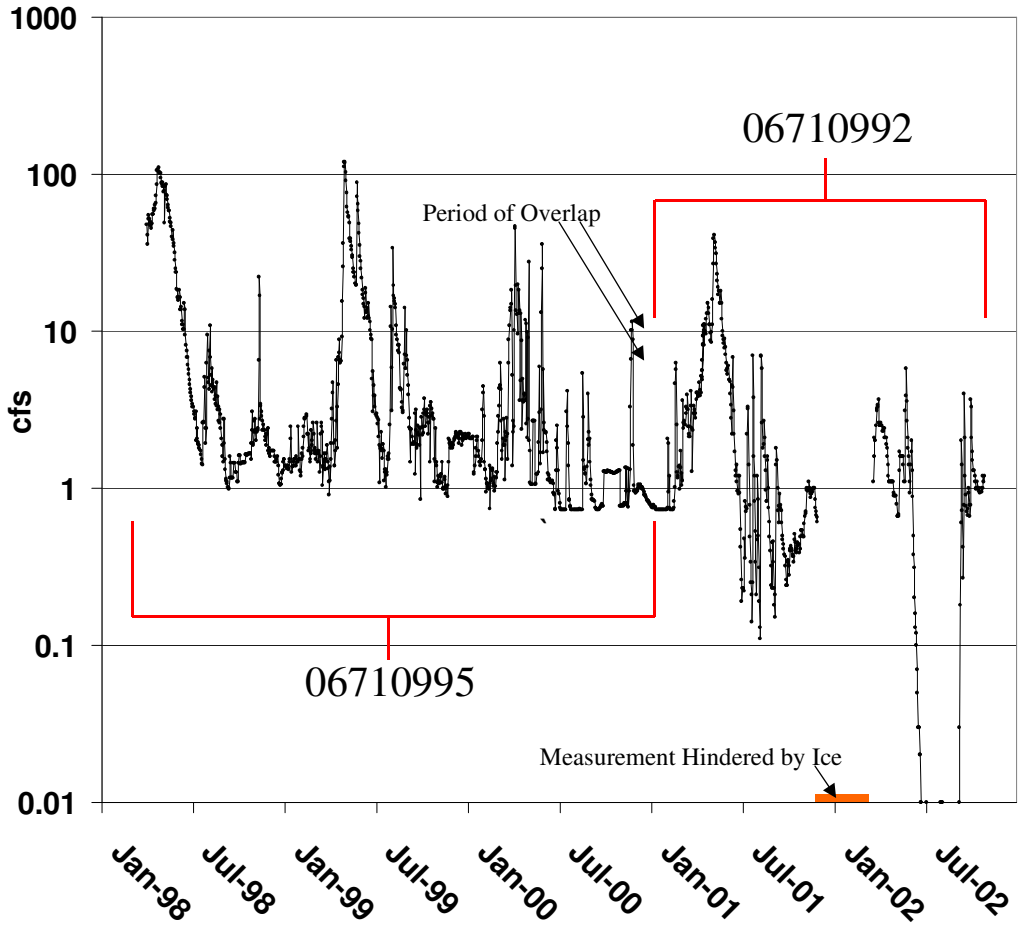

Figure 3.2 Discharge measurements from U.S.G.S gauging stations 06710995 and 06710992 with a small period of overlap for the Turkey Creek Basin.

3.1.2 Colorado School of Mines Discharge Measurements

Stream discharge measurements were collected on a weekly basis for the first three months (May, June and July) of the summer of 2002 and subsequent samples were collected bi-monthly for a 10-month period (Figure 3.3). Discharge measurements were taken with a Gurley pygmy flow meter mounted on a wading rod system. During some of the winter month's (December, January, February) measurements were hindered or prohibited by ice. This sampling schedule identified high flow and low flow (dry) conditions. Personal communication with local residents suggests that Turkey Creek has not been dry in recent history. Stream sampling locations were chosen to coincide with previous U.S.G.S locations (Figure 3.4). Locations were intended to document spatial patterns of discharge.

3.1.3 Specific Conductance and Temperature

Specific conductance and temperature measurements were taken at the same time intervals and locations as discharge measurements (Figure 3.5a and 3.5b). Specific conductivity changes dramatically along North and South Turkey Creek. Reasons for these changes are unknown, but one tributary labeled, Tatonka Tributary in figure 10 contributes elevated levels of total dissolved solids. For a more in depth discussion of the surface water chemistry of the Turkey Creek Basin refer to Hofstra and Hall (1975) or Bossong et al., (2003).

3.1.4 Analysis of Stream-Discharge Measurements

Stream hydrographs were constructed (Figures 3.1, 3.2, 3.3) to evaluate seasonal response to recharge. Water exiting the basin through North Turkey Creek can be separated into baseflow and overland flow/interland flow. Base flow originates from ground water and is considered to be available for domestic use. It appears that down-

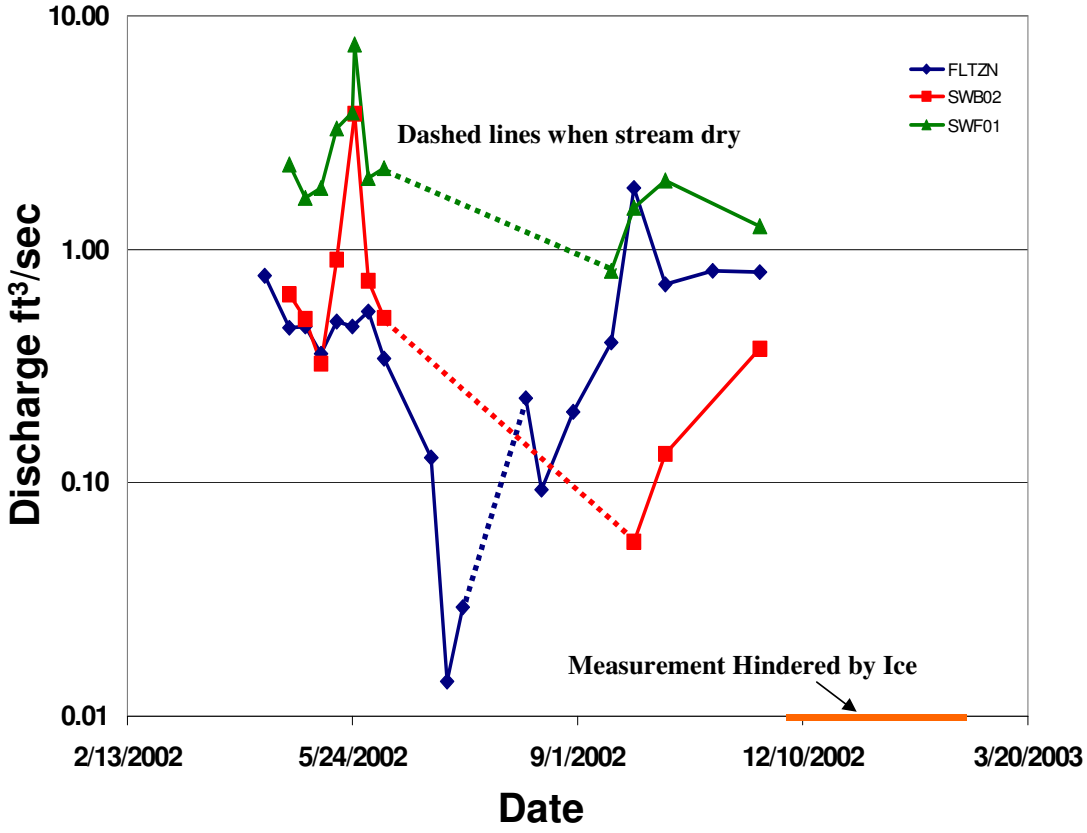

Figure 3.3 Discharge measurements at three locations in the Turkey Creek Basin.

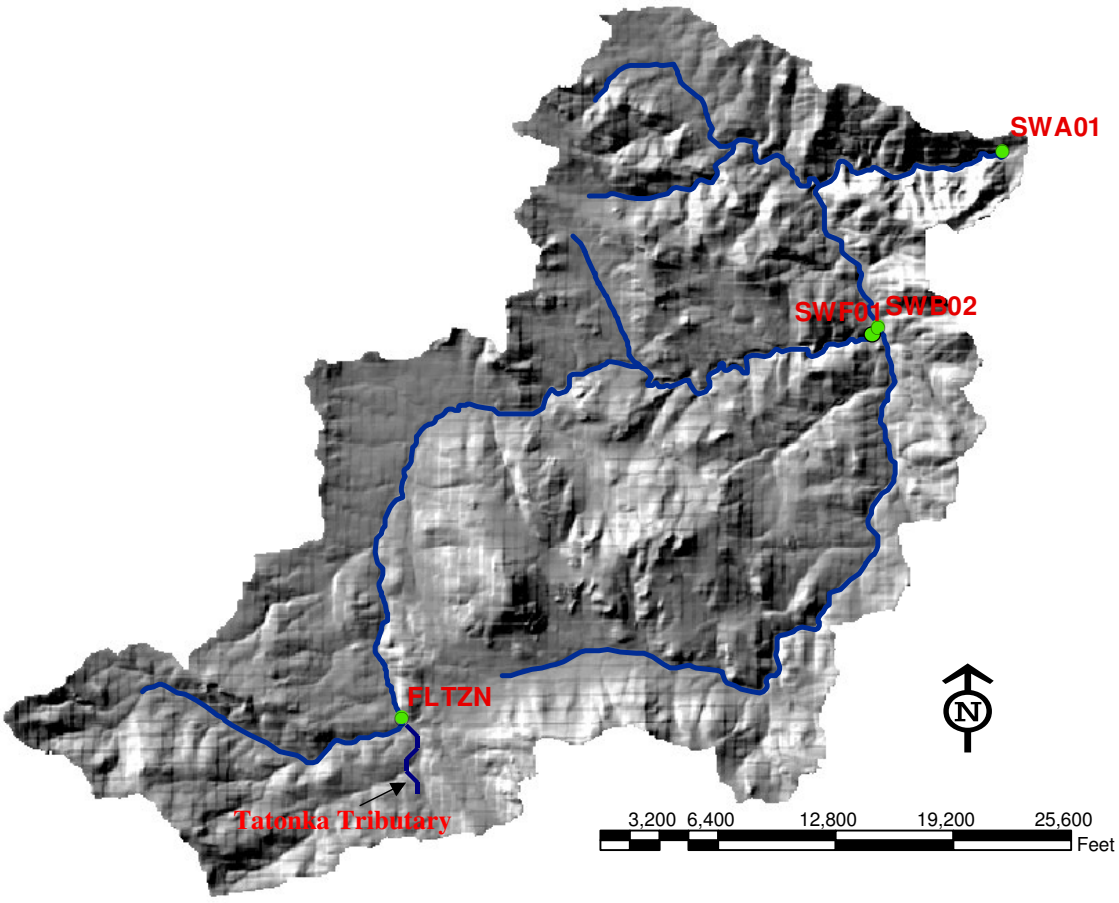

Figure 3.4 Stream gauging locations for Colorado School of Mines measurements in the Turkey Creek Basin.

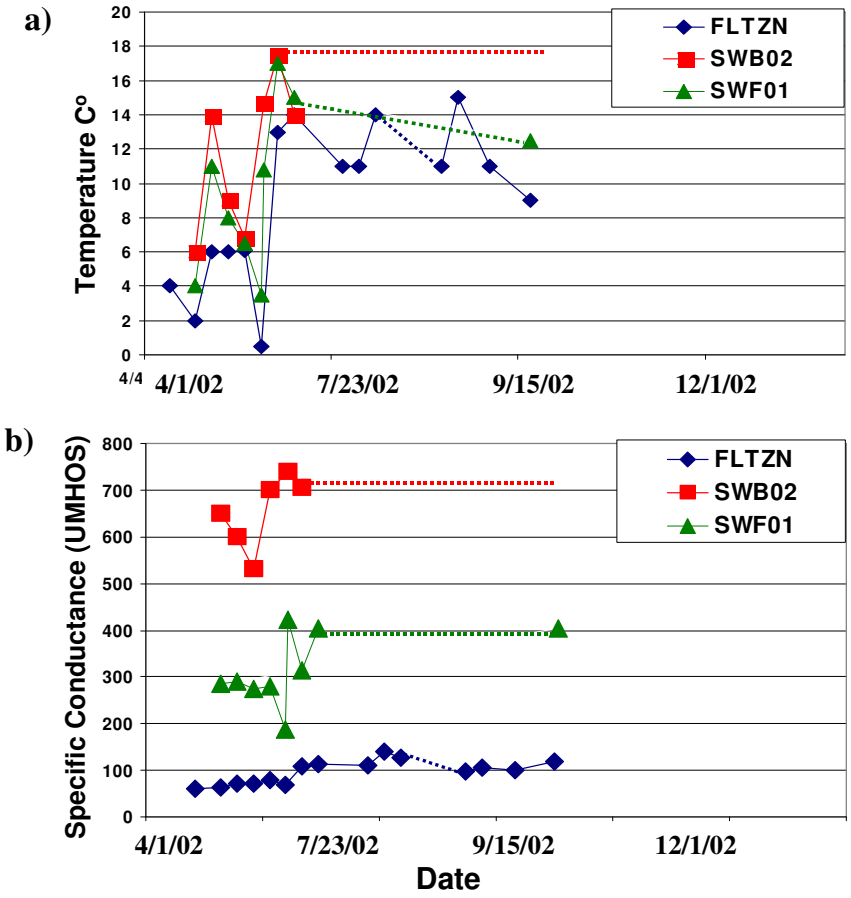

Figure 3.5 Stream sampling conducted by Colorado School of Mines. a) Temperature measurements taken at three stream locations in the Turkey Creek Basin. b) Specific conductance of stream water taken at three different stream locations in the Turkey Creek Basin.

gradient gauges, 06711040 and 06710995, have larger stream flow. This could be due to differences in precipitation during the gauged years. There were 6 days of coincident discharge measurements at 06710992 and 06710995 (Figure 3.6) (Poeter et al, 2003). There is a reasonable relationship between the two gauges but a longer overlap is required to use this relationship to estimate historical flow at 06710992. Given the limited data available from the gauging stations it appears that Turkey Creek gains as it exits the basin.

Estimation of Baseflow

Based on the limited data, baseflow is estimated to range from 0.3 ft^3/sec (cfs) to 1.3 cfs. This was determined from stream hydrographs (Figure 3.1, 3.2, 3.3) and is intended to encompass the maximum and minimum possible baseflow values. This value includes the baseflow value (1.12 cfs) calculated using the Soil and Water Assessment Tool's baseflow filter (USDA, 2000). This yields a range of effective uniform depth (EUD) of 0.10 to 0.34 in/yr. Effective uniform depth is a measure of volume averaged over the entire basin area. These numbers are consistent with baseflow (1 cfs, 0.30 in/yr) reported in Poeter et al., (2003).

3.2 Aquifer Tests

Two types of aquifer tests, single- and multi-well aquifer tests were conducted and analyzed to estimate aquifer properties. During the aquifer tests, one well is pumped at a known discharge rate while it and surrounding wells are monitored for decrease of hydraulic head (drawdown). The recorded drawdown is plotted vs. time and fit with a type curve. The Theis equation (C.V. Theis 1935) (3.1) for a fully confined system was used and drawdown was corrected equation (3.5) for an unconfined system. Specialized plots in the pumping well vs. square root of time, $t^{¼}$, and $t^{-¼}$, which are used to determine

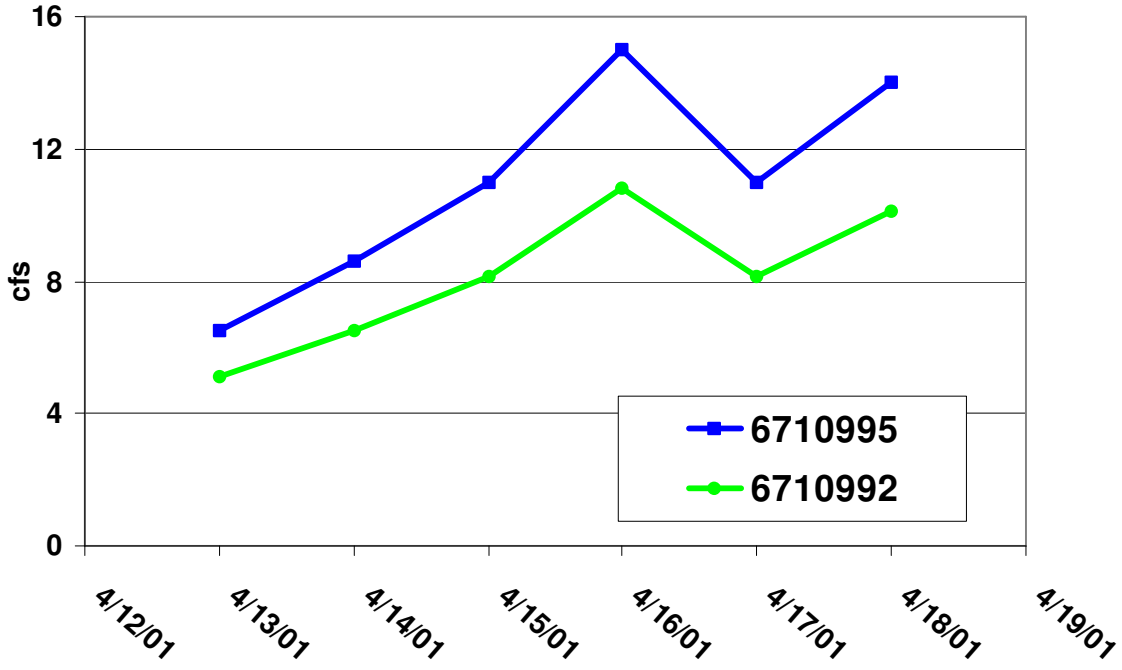

Figure 3.6 Discharge measurement overlap for U.S.G.S gauging stations 6710995 and 6710992 for the Turkey Creek Basin.

possible fracture characteristics, yielded the same plot as the Theis equation.

$$s = \frac{Q}{4\pi T}\int_{u}^{\infty}\frac{e^{-y}dy}{y} = \frac{Q}{4\pi T}W(u) \tag{3.1}$$

Matching calculated s vs. observed s, equation 3.1 is rearranged to solve for T and S.

$$T = \frac{QW(u)}{4\pi s} \tag{3.2}$$

Where: T = transmissivity
Q = discharge
W(u)= well function (dimensionless), based on match of Theis-type curve
s = drawdown at any time after pumping begins

$$u = \frac{r^2 S}{4Tt} \tag{3.3}$$

Once T is known equation 3.3 is rearranged to solve for S.

$$S = \frac{4Ttu}{r^2} \tag{3.4}$$

Where: S = storativity
T = transmissivity
t = time
u = dimensionless time, based on match of Theis-type curve
r = radial distance from the pumping well to observation well

$$s' = s - \left(\frac{s^2}{2b} \right) \tag{3.5}$$

Where: s' = corrected drawdown
s = observed drawdown
b = original saturated thickness of the aquifer

The Theis equation assumes the medium is porous. Therefore using this solution for this study assumes that the fracture system can be represented as an equivalent porous medium.

3.2.1 Single-Well Aquifer Tests

Multi-well aquifer tests that did not yield measurable drawdown in the observations wells were analyzed as single-well tests. Two tests (Newton and Vogal/Johnston) yielding single well data were analyzed (Appendix A,B).

Newton Single-Well Aquifer Test

The Newton aquifer test consisted of one pumping well of unknown depth and two monitoring wells located over 600 ft away from the pumping well. Pumping was constant, 8 gallons per minute (GPM) for one hour. The Theis solution was fit (Figure 3.7) to drawdown data and hydraulic conductivity was estimated to be 0.025 ft/day using a saturated thickness of 200 ft.

Vogal/Johnston Single-Well Aquifer Test

The Vogal/Johnston aquifer test consisted of one pumping well over 580 ft total depth and one monitoring well located about 100 ft away from the pumping well. Pumping was constant, 6 GPM for one hour. The Theis solution was fit (Figure 3.8) to drawdown data and hydraulic conductivity was estimated to be 0.0025 ft/day using a saturated thickness of 582 ft.

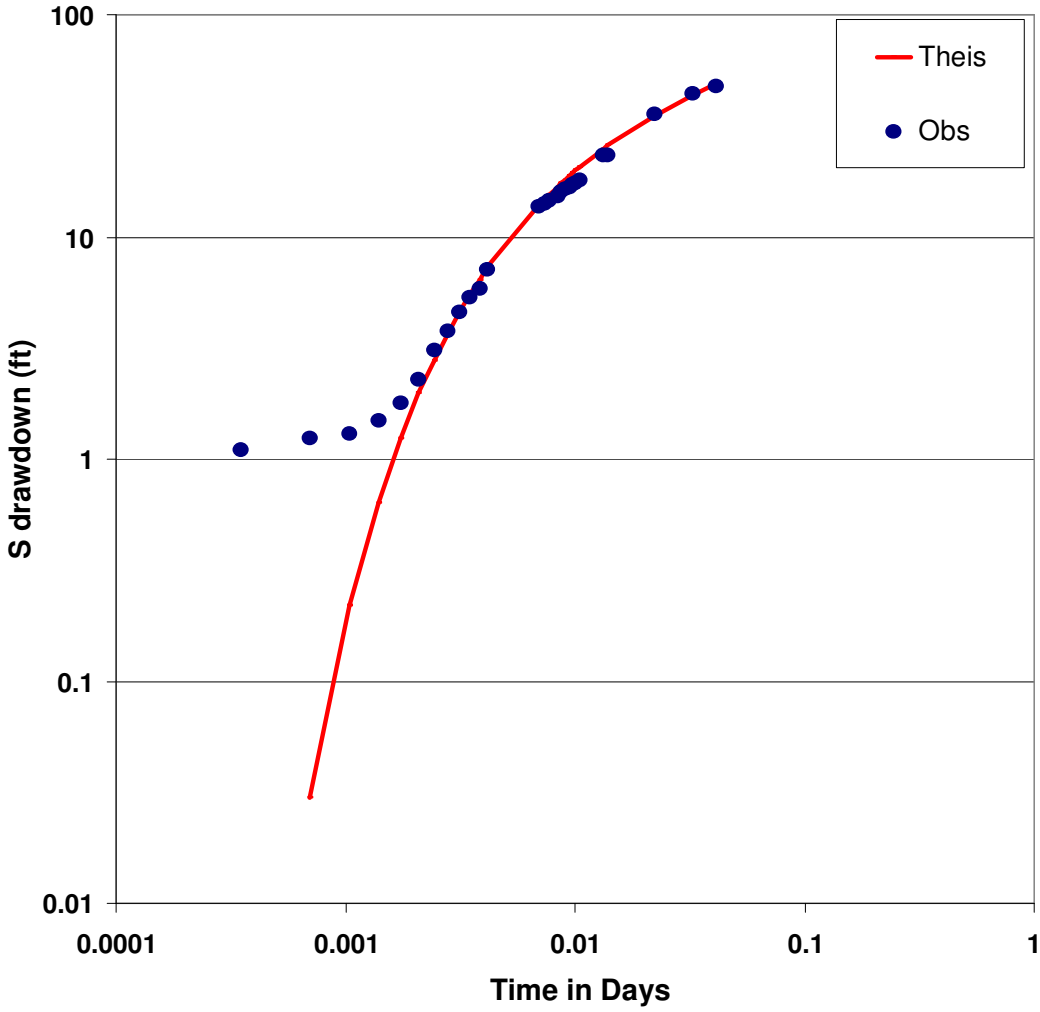

Figure 3.7 Newton single well aquifer test, Theis curve in red and observation points in blue.

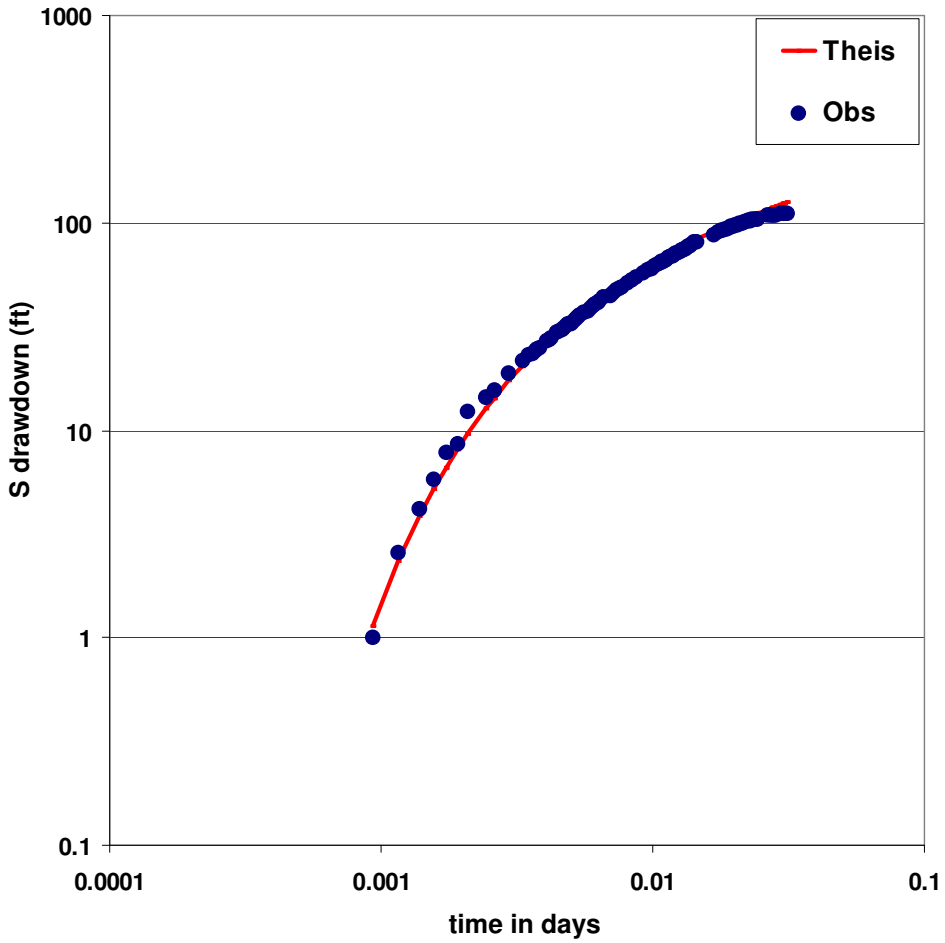

Figure 3.8 Johnston/Vogal single well aquifer test, Theis curve in red and observation points in blue.

3.2.2 Multi-well Aquifer Tests

Two multi-well aquifer tests were analyzed for transmissivity, hydraulic conductivity and storage coefficient, a thirty-day aquifer test (IHWD) conducted in the 1980's and a three-day multi-well aquifer test (Lewis) from the summer of 2003 (Appendix C, D).

Indian Hills Water District

The 30-day aquifer test was in the Indian Hills Water District (IHWD). It was conducted because residents expressed concern about a proposed district well. Parmalee Gulch, where IHWD resides, has a higher average well yield 9 GPM (Wellman, 2003) relative to the average well yield for TCB (5.8 GPM), as determined from well logs recorded with the State Engineers Office. Pumping continued for 30 days at a constant rate of 21.8 GPM, but was compromised by additional pumping of 5.1 GPM from a nearby district well. Observation wells were corrected for a negative water level trend observed over an 8-day period prior to pumping. Monitoring wells ranged 220 to 750 ft from the primary pumping and 150 to 1,000 ft from the second district well. After correction for the negative water level trend, four of the thirteen wells showed a direct response to the induced stress (Figure 3.9). One well (BO) (Figure 3.10), used a continuous recorder; therefore early time data are available. Using the Theis solution for two superposed pumping wells (#10 and #5) this well showed two distinct response periods to pumping, early and late time. Data suggest a classic delayed yield response to pumping an unconfined aquifer; however early time data are sparse. Interpretation yields an extremely high transmissivity, (3500 ft^2/day) and an elastic storage coefficient of 0.0065, and specific yield of 0.01, 1.0%. After a couple of hours the extent of the high T zone is reached as indicated by the positive deviation from the Theis curve. The other three wells that show response to pumping are more coincident with one another yielding

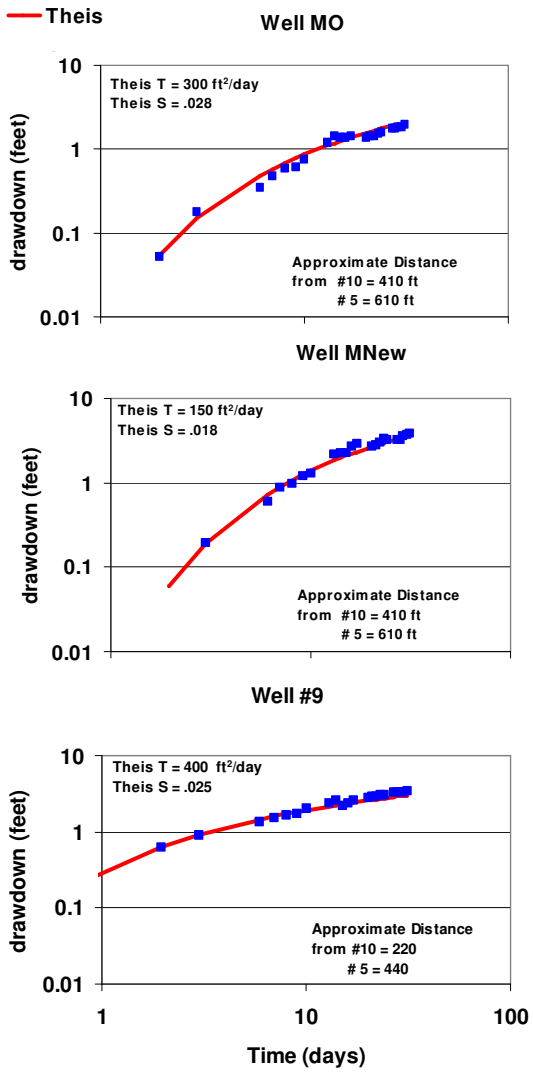

Figure 3.9 IHWD multi-well aquifer test results. Wells are labeled for proximal distance from pumping wells and resultant transmissivity and storage values. Well MO and Mnew are located fifteen feet apart and are listed as the same proximal distance from pumping wells.

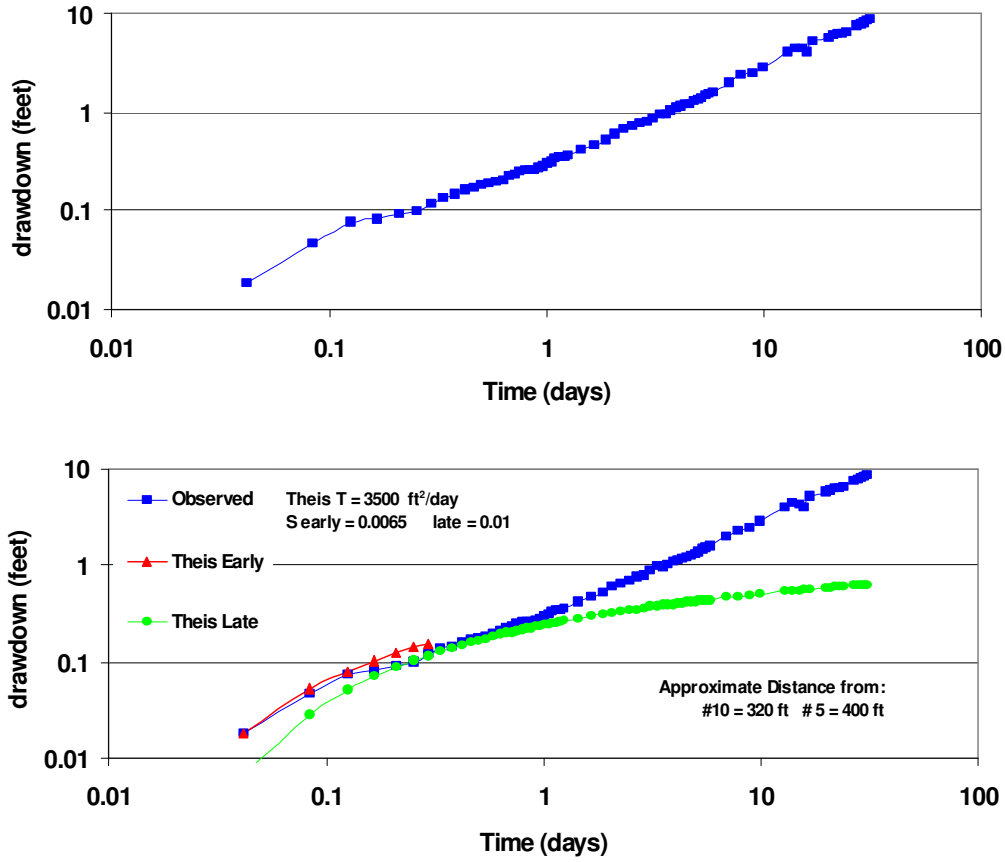

Figure 3.10 IHWD multi-well aquifer test results for BO well. Early time data are available indicating an unconfined aquifer with delayed yield, thus early and late time matches yield one value of T as well as S and Sy.

a geometric mean transmissivity of 260 ft^2/day, and an average specific yield of 0.024, 2.4%.

Some parameters for this test were unclear. Several errors were identified in the final report presented to IHWD. The test was done before global positioning system (GPS) was available and estimations for radial distance were used. Total well depth was not reported for all wells. One well, which did not show a response, was reported as two different total depths. The report made it unclear whether nearby domestic wells were pumped. A small intermittent pond is located near pumping well #10 and observation wells. It was not noted in the report whether the pond was dry or could have been a source of recharge. Monitoring of pond stage in subsequent years noted the pond is dry during this time of the year.

Lewis Well

A 3-day aquifer test (Lewis test) was conducted in the summer of 2003. The well was pumped for a total of 60 hours at approximately 12 GPM. An observation well was located 9.2 ft away and drawdown was measured with a continuous recorder at 3-second intervals for the first 24 hours. The Theis equation was fit to the data (Figure 3.11). Early time data predicted a specific yield of 0.05, 5.0% and a transmissivity of 350 ft^2/day. A positive deviation from the Theis curve was noted after about 2 minutes of pumping. Fitting a second Theis curve to late time data predicted a specific yield of 0.025, 2.5% and a transmissivity of 325 ft^2/day. Differences between early and late time curves could result because water is coming from well bore storage before water is pulled from the aquifer thus yielding a higher calculated transmissivity and specific yield.

3.2.3 Summary

The summation of the aquifer properties as presented in section 3.2 are provided in Table 3.1. Hydraulic conductivities (K) calculated by multi-well aquifer tests are much

Test Name	Test Type	Transmissivity (ft^2/day)	Hydraulic Conductivity (ft/day)	Storage Coefficient
Newton	Single Well	5	0.025	NaN
Vogal/Johnston	Single Well	1.48	0.0025	NaN
IHWD	Multi-Well	260*	32	0.025
Lewis	Mult-Well	325	2.6	0.024

Table 3.1 Summary of results from single and multi-well aquifer test in the Turkey Creek Basin. * Several wells tested and the geometric mean of results displayed.

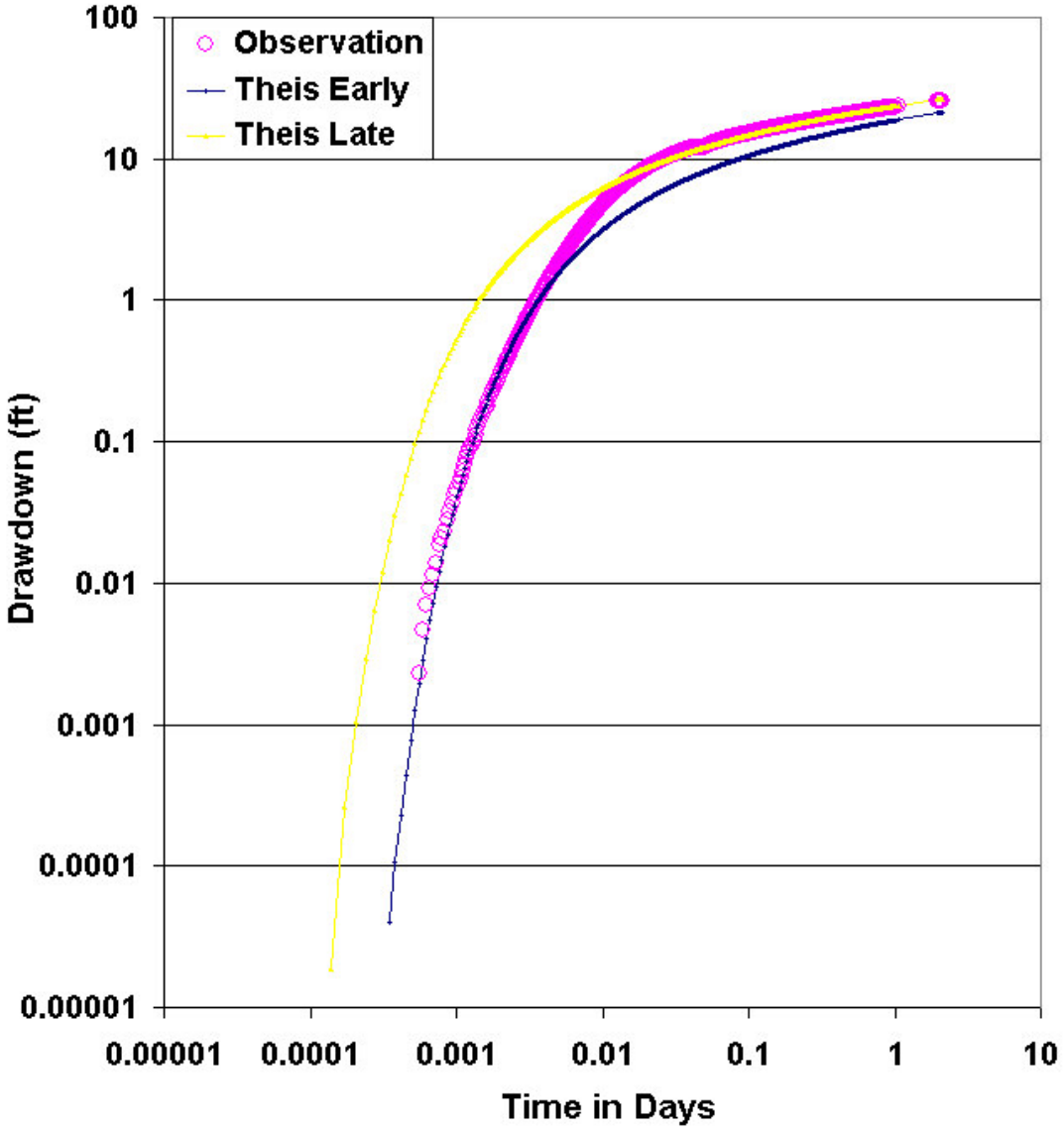

Figure 3.11 Lewis multi-well aquifer test results. Two Theis curves fit to early and late time data.

larger than K's calculated by single well aquifer tests. This is believed to occur because multi-well aquifer tests were only successful in water district wells. Wells are only used for distribution if they have high sustainable yield, which would result in larger hydraulic conductivities. For this reason hydraulic conductivities measured in domestic wells (single-well aquifer tests) are believed to be more representative of the rock mass as a whole.

Having a lack of response in observation wells due to pumping may indicate either a high storage coefficient or no fracture connection between wells. Using the Theis equation and the specific storage estimated by Bossong et al., (2003) drawdown of 0.88 ft would be expected in the observation well of the Vogal/Johnston aquifer test (Table 3.2). The specific storage calculated from the Lewis and IHWD tests indicate immeasurable drawdown.

Johnston/Vogal Aquifer Test			
Q GPM	Transmissivity (ft^2/day)	Specific Yeild	Expected drawdown (ft) after 1 hour of pumping
6	325	0.027%	0.88
6	325	2%	0.01

Table 3.2 Comparisons of predicted drawdown in the observation well of the Johnston/Vogal aquifer test using the Theis equation with S_y observed in multi-well tests and that estimated from fracture outcrop studies by Bossong et al., (2003).

3.3 Hydraulic-Head Measurements

Measuring depth to water in wells maps the water table and provides calibration data for ground water flow models. Hydraulic head was determined by subtracting depth to water measurements from a surface elevation as interpreted from a DEM given the GPS coordinates of the well. Depth to water was measured in pumping and abandoned wells by several groups and continues to be measured.

3.3.1 Historical Head Measurements

Historical head measurements are available from the U.S. Geological Survey, local volunteers, CSM, and well logs from the State Engineers Office.

U.S.G.S Water-Level Measurements

Hofstra and Hall collected data from over 700 hundred wells in the mountainous area of Jefferson County. Depth to water measurements in TCB were taken in 6 abandoned wells (Figure 3.12).

Mountain Ground Water Research Study

For the Mountain Ground Water Resource Study Bossong et al., (2003) collected synoptic measurements in 131 domestic wells. Some participants (homeowners) agreed to limit water use before measurement. Bossong created a water table elevation map (Figure 3.13).

Indian Hills Water Level District

After installing pumping well #10 and conducting an aquifer test (See section 3.2.2) the IHWD began monitoring the surrounding domestic wells. Nine wells have been monitored on a monthly basin since 1994 (Figure 3.14).

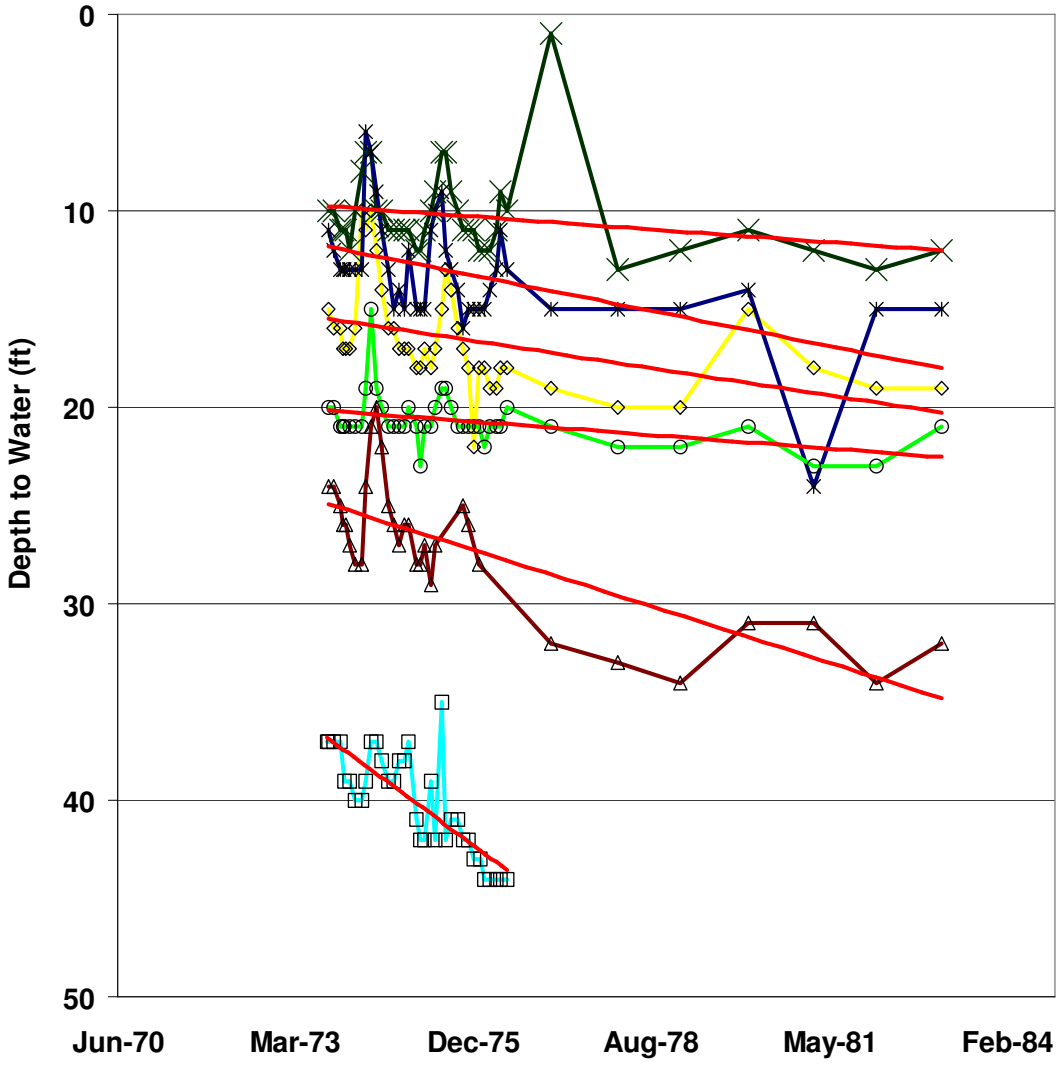

Figure 3.12 Depth to static water level measured in abondended wells from Hofstra and Hall 1976 combined with measurements collected later in same wells.

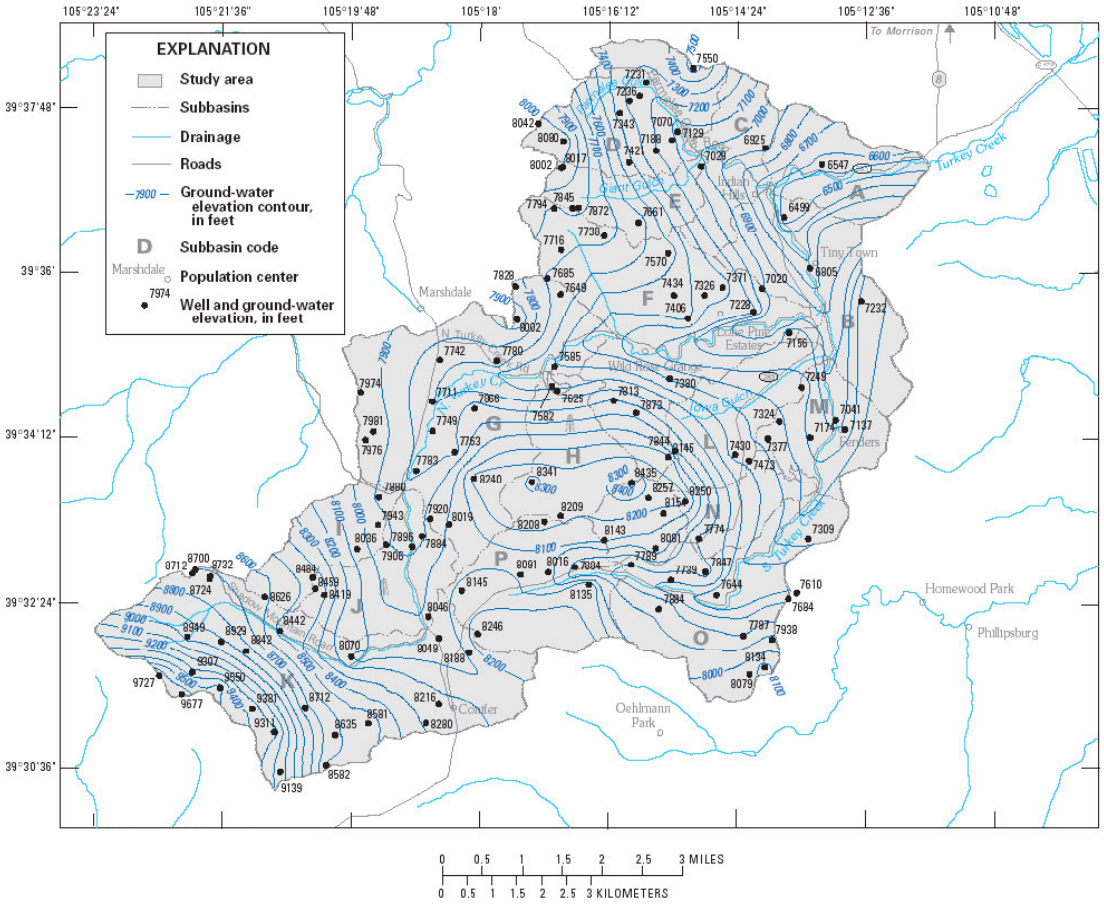

Figure 3.13 Water table elevation map calculated by Bossong et al., (2003).

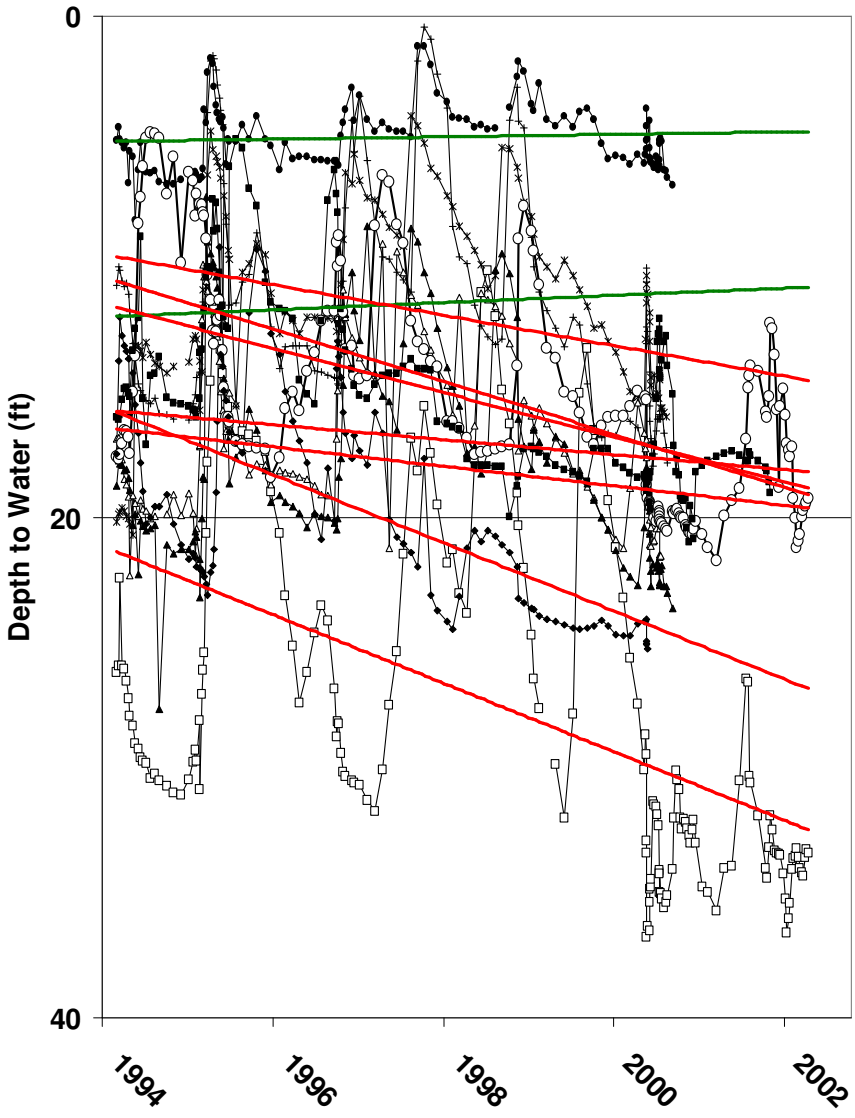

Figure 3.14 Wells monitored by the Indian Hills Water District after IHWD aquifer test.

State Engineers Office

The SEO maintains well logs for the State of Colorado. Drillers are required to report a static water level for every completed well. The static water levels were used to create a water table elevation map (Figure 3.15). Which can be compared to the surface water divide (Figure 3.16) The depth to water on well logs (which are known to include errors) were subtracted from a surface elevation interpolated from a Digital Elevation Model (DEM) (National Elevation Database, 2003) given (x,y) coordinates determined by a GPS. The resultant distribution of head is not synoptic because wells were drilled at different times over a period of 50 years.

3.3.2 Abandoned Wells

Measuring water level in abandoned wells is preferred because it is not impacted by drawdown from pumping. Measurement of water levels in pumping wells as done by Bossong et al., (2003), may result in biased measurements. Frequently water levels in pumping wells will be lower than the true value because the water level is still recovering from prior pumping at the time of measurement.

Abandoned Wells Monitored by Jefferson County Volunteers

As part of the MGWRS, a volunteer from Jefferson County made monthly water level measurements in 15 unpumped wells (Figure 3.16). Although the MGWRS project is completed, the volunteer continues to take measurements.

Abandoned Wells Monitored by CSM

Eleven abandoned wells have been monitored since September of 2002. One well was discontinued because it was decommissioned (filled –in) and three, owned by a local developer, were converted to pumping wells. Continuous recorders, sampling every hour, originally monitored eight wells, but presently two have been removed.

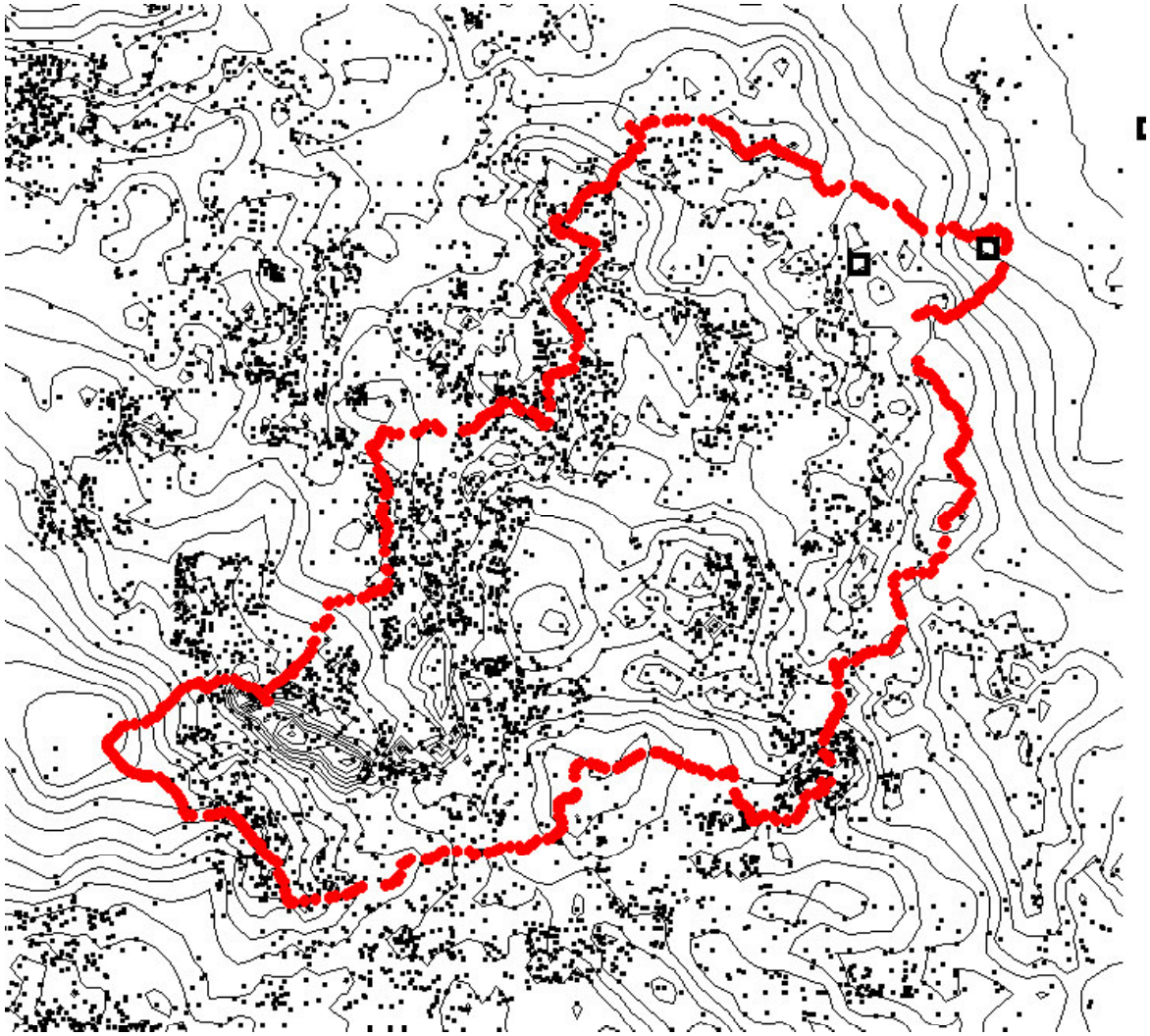

Figure 3.15 Ground-water divide contoured from static water levels. Small boxes represent a domestic well.

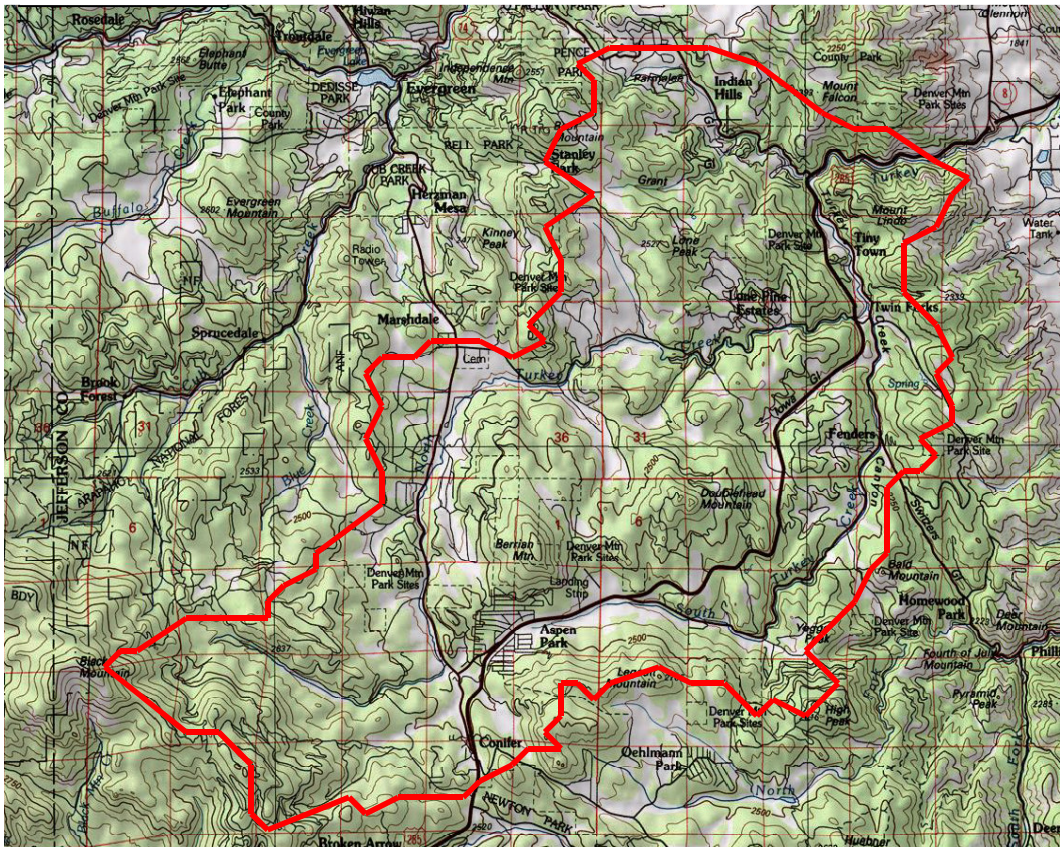

Figure 3.16 Approximate surface water divide as determined from 1:24,000 topography map.

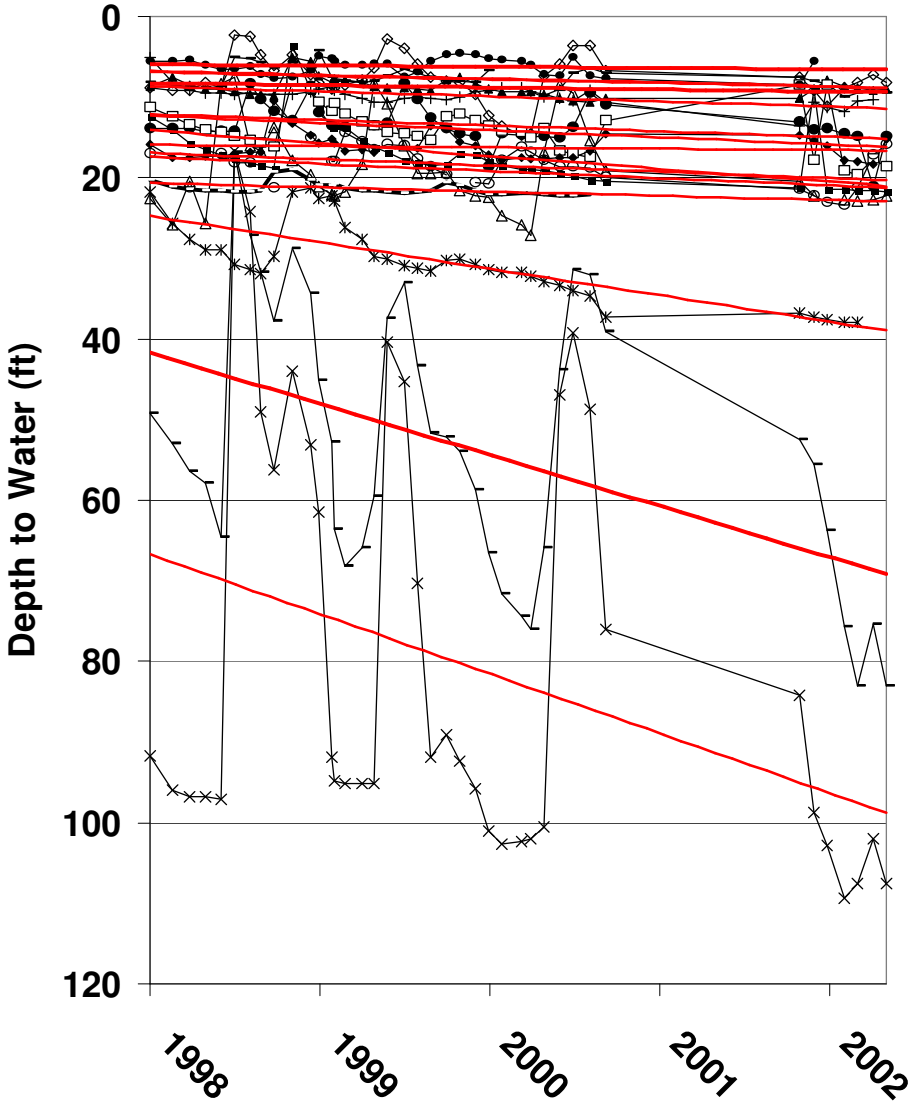

Figure 3.17 Depth to water measurements taken by Jefferson County volunteer

3.3.3 Analysis of Water Levels

The water level distribution map (Figure 3.15) created from the SEO logs displays contours that emanate from the head of the basin and are perpendicular to the surface water divide. Figure 3.15 is similar to the water level map created by the U.S.G.S. (Figure 3.13), suggesting the surface and phreatic divides coincide. Water-level measurements in unpumped wells show that water levels are responsive to seasonal fluctuations in recharge and that water levels are declining in the Turkey Creek Basin. Water levels in five wells (MH 1, 5, 8, 9, 10) with measurements from the 1970's that exhibit a water level decline show an average drop in head of 1 ft/yr from 1973 to 1998 (Figure 3.17). One well (MH2) exhibits a sharp rise in water table elevation but is most likely due to a change in the local pumping regime. Of the nine IHWD wells monitored, two show a slight increase in water level, one shows no change, but 6 show an average decline of 0.5 ft/yr (Figure 3.14). The IHWD wells show a lower average water level decline than the MH wells. This could be due to the fact that the wells monitored by IHWD are located within or close to a discharge zone which has been shown to have a higher average well yield as compared to the rest of the basin. Differences could also stem from 25 years ago when Jefferson County signed a resolution prohibiting the issuance of septic system permits on designated lots, essentially banning residential development in this area (Laws, 2003) and many homes have begun using the IHWD supply some of which comes outside of the sub-basin.

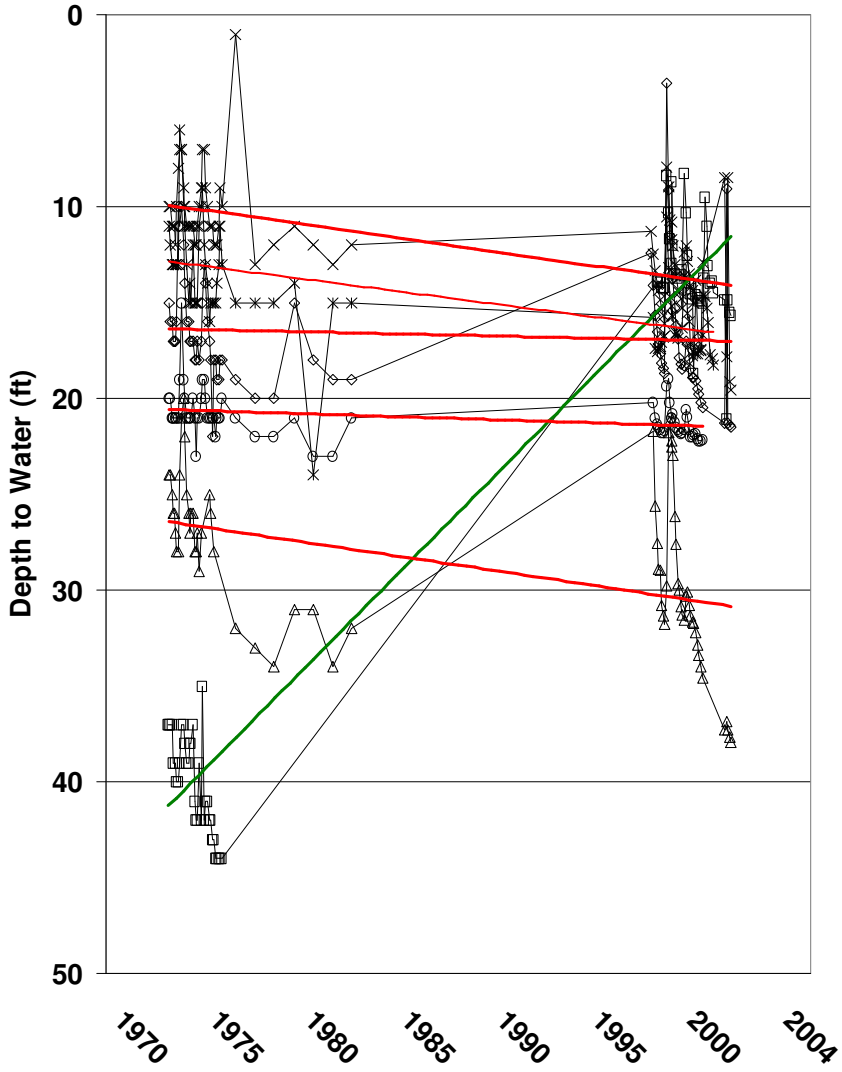

Figure 3.18 Long term depth-to-water measurements. Hofstra and Hall (1976) combined with Jefferson County volunteer measurements.

CHAPTER 4: MODELING THE HYDROLOGY OF THE TURKEY CREEK BASIN

Models were constructed in order to better understand the ground-water system and estimate K, recharge, and S_y. Water budget calculations provide a framework for development and calibration of steady state and transient numerical models of ground-water flow in TCB.

4.1 Water Budget

For this project, a sustainable water resource is defined as a system where recharge exceeds consumption. In order to estimate the range of total recharge to the basin, a water budget for the ground-water system was constructed (Equation 4.1). A water budget accounts for the inputs and outputs of water to a defined domain. In this case the domain is the saturated zone of TCB and an average annual steady condition is evaluated.

$$\text{Inflow} = \text{Outflow} \tag{4.1}$$

Where: Inflow = (recharge), water that enters the aquifer and is available for use
Outflow = (flow to streams, alluvial outflow at the mouth of the basin, consumption).

4.1.1 Ground Water Outflow

Ground-water outflow is the volume of water exiting the basin through fractured bedrock. TCB was shown earlier (section 3.3.3) to be a closed basin with ground water only exiting at the mouth. High, low and medium discharge values (Table 4.1) were calculated using Darcy's Law (Equation 4.2) for a range of cross-sectional area, hydraulic conductivity and gradient. Cross-sectional area was assigned as the product of estimated

width and depth of the ground water discharge zone perpendicular to the axis of the stream at the mouth of the basin. The ground-water gradient near the mouth of the basin was determined to have a maximum value of 0.1 based on water levels from driller's logs.

	Cross Sectional Area ft^2	**Gradient**	**Hydraulic Conductivity (ft/yr)**	**Discharge (ft^3/day)**
Low	500x700 Product (350,000)	0.01	0.01	35
Medium	2640x700 Product (1,848,000)	0.05	1	92,400
High	5280x700 Product (3,696,000)	0.1	500	184,800,000

Table 4.1 Ground water outflow from bedrock calculated using Darcy's law and the variables used for calculations. Estimated cross sectional area of ground water outflow, range of hydraulic conductivities based on aquifer test and modeling results and the ground water gradient calculated from water table map and surface contours.

$$Q = KIA \tag{4.2}$$

Where: Q = Discharge
K = Hydraulic conductivity
I = Gradient

4.1.2 Baseflow

Stream baseflow calculations are described in section 3.1.4.

4.1.3 Alluvium Outflow

Alluvium outflow is the volume of water exiting the basin through the alluvium perpendicular to the axis of the stream at the mouth of the basin. High, low and medium discharge values (Table 4.2) were calculated using Darcy's Law (Equation 4.2) from a range of cross-sectional area, hydraulic conductivity and gradient. Cross-sectional area of the alluvium was assigned as the product of estimated width and depth of the alluvium. Published values of hydraulic conductivity for alluvial materials were used to estimate a range for hydraulic conductivity (Fetter, 2000). The same gradients used in section 4.1.1 for ground-water outflow calculations were used for alluvium outflow.

	Cross Sectional Area ft^2	**Hydraulic Conductivity ft/yr**	**Gradient**	**Discharge ft^3/yr**
Low	5x10 Product (50)	1	0.01	50
Medium	15x20 Product (300)	5,173	0.05	77,600
High	30x50 Product (1,500)	10,346	0.1	1,552,000

Table 4.2 Alluvium outflow calculated using Darcy's law and the variables used for calculations. Estimated cross sectional area of alluvial outflow, range of hydraulic conductivities (Fetter, 2000). Gradient calculated from water table map and surface contours.

4.1.4 Water Consumption

The present population in TCB uses individual water wells and individual septic disposal systems (ISDS). An average household is estimated to pump as much as 300 gallons per day (GPD) (MGWRS, 2002). Of the estimated 300 GPD, 90% is assumed to return as effluent to the system via ISDS effluent. For the entire basin, this yields an estimated consumption of 165 acre-feet per year (AFY)(MGWRS 2002). The Indian Hills Water District (IHWD) operates a collective residential system; consumption is estimated at 24 AFY (MGWRS 2002) bringing total water consumption in TCB to 190 AFY.

These numbers are estimated using several assumptions: 1) An average household uses 300 GPD and 2) 90% of what is used is returned to the aquifer. Neither of these estimates to date has been rigorously tested. For the purpose of estimating values of water consumption three different values of pumpage and return were used (Table 4.3). In addition to each of these values the reported consumption from IHWD community residential system was added.

	Water Consumption (ft^3/yr)	
Low	**Medium**	**High**
10% of 150 GPD /home + 10% of (240 AFY)	20% of 225 GPD /home + 20% of (240 AFY)	30% of 300 GPD/ home + 30% of (240 AFY)
4,632,000	12,850,572	24,655,705

Table 4.3 Estimates calculated for water consumption within the Turkey Creek Basin.

4.2 Concepts of Numerical Modeling

A model is a simplified representation of a system. Mathematical models of ground water have been used for over a century (Wang and Anderson, 1982). Mathematical ground-water models are based on differential equations that describe ground-water flow (Wang and Anderson, 1982). The ground-water modeling code, MODFLOW 2000 (McDonald and Harbaugh, 2000), a modular three-dimensional finite-difference ground water flow model is used. Selection of this model is based on (1) MODFLOW is an industry standard and the physical and mathematical concepts are widely accepted; (2) The Graphical User Interface (GUI), Groundwater Modeling System (GMS) (Brigham Young University, 2000) facilitates use of MODFLOW; and (3) the source code and executable are public domain.

As discussed by McDonald and Harbaugh (1988), the three-dimensional movement of an incompressible fluid of a constant density through a porous or equivalent porous media may be described by the partial differential equation:

$$\frac{\partial}{\partial x}\left(K_{xx}\frac{\partial h}{\partial x}\right)+\frac{\partial}{\partial y}\left(K_{yy}\frac{\partial h}{\partial y}\right)+\frac{\partial}{\partial z}\left(K_{zz}\frac{\partial h}{\partial z}\right)-W=S_s\frac{\partial h}{\partial t} \qquad (4.3)$$

Where: K_{xx}, K_{yy} and K_{zz} = hydraulic conductivity in the x, y and z direction respectively
h = hydraulic head
W = source or sink term, volumetric flux per unit volume
S_s = Quotient of storage coefficient and saturated thickness
t = time

In combination, Equation 4.3 and boundary conditions such as flow and/or hydraulic head specifications, and initial conditions, constitutes a mathematical representation of a ground-water flow system (McDonald and Harbaugh, 1988).

4.2.1 Steady-State Modeling

In a steady-state model, parameters and boundary conditions do not change with respect to time, heads and flows are constant, and water does not move in, or out, of storage. A steady state model does not provide insight into the rate of change of a system, in response to an induced stress rather an average equilibrium condition. A steady-state ground water model solves equation (4.3) for head (h) or discharge (W) for each node in the model. Where W is known, the equation is solved for h; if h is known, W is determined. In most locations the flows balance and thus W is known to be zero. Steady-state models calibrated to evaluate different recharge models. Each model calibrated used UCODE (Poeter et al, 1998) a modified Gauss-Newton inversion tool. Steady-state models were used to estimate average parameter values for hydraulic conductivity and recharge given a number of different spatial distributions.

4.2.2 Transient Modeling

In transient modeling the dependent variables and sometimes the parameters and boundary conditions change with respect to time. Transient modeling gives insight into the rate of change of the system in response to an induced stress. When solving the governing flow equation (4.3) for each node, the equation is altered so the total volume inflow equals the total volume outflow plus the volume of water that goes into storage.

A transient simulation of the summer drought of 2002 was used to estimate specific yield. During this time little precipitation occurred and water level declines were noted. A transient simulation was calibrated to estimate the specific yield that provided the best match between simulated and observed water level declines.

4.3 Model Assumptions

In order to model the TCB ground-water system, several assumptions where made when field data were limited or to simplify the system. These include:

Assumptions about: **4.3.1** Representing a fractured system as an equivalent porous medium.

4.3.2 Ground water outflow

4.3.3 Total depth of the system

4.3.4 Hydraulic conductivity

4.3.1 Representing a Fractured System as an Equivalent Porous Medium

The representative elementary volume of fractured aquifers is much larger than for porous aquifers. At small scales, ground water flow is dominated by the pattern and interconnectedness of the fractures. At larger scales an average value of hydraulic conductivity is representative of the rock mass and at this scale the fractured medium can be represented as an equivalent porous medium. Figure 4.1 illustrates a block of fractured rock represented in two dimensions. In samples represented by small squares, porosity and permeability vary from sample to sample. This sampling size is not large enough to incorporate enough fractures to yield a consistent average bulk property. At the size of the larger squares the rock mass includes enough connected fractures such that the calculated properties do not vary significantly from location to location. This area is equal to, or larger than, the representative elementary volume.

The Turkey Creek Basin is believed to be larger than a representative elementary volume of the fractured rock, although the size of the REV is not known. Recent preliminary work by Wellman (2003) suggests it is on the order of 400 meters, approximately 1200 by 1200 ft. Cells smaller than the REV can be used to obtain a

Figure 4.1 Two-dimensional representation of a fractured medium, squares represent sample areas.

solution, but predictions must be averaged (scaled-up) to the REV for management purposes.

4.3.2 Ground Water Outflow

Ground water outflow was limited to an area about 1500 ft by 700 ft at the mouth of the basin. The size of area was determined from Figure 3.5.

4.3.3 Total Depth of the System

The base of the ground water system was assumed to be 700 ft below ground surface. Water-bearing fractures in Turkey Creek have been identified at depths greater than 700 ft, but are believed be rare and not significant to the overall flow system. This assumption is based on SEO logs which show fracture intensity decreases with depth (Figure 2.4d).

4.3.4 Hydraulic Conductivity with Depth

Hydraulic conductivity is believed to vary with depth. Water-bearing properties are dependent on the presence of fractures and joints and the extent of weathering. Horizontal joints and fractures developed by unloading are usually concentrated near the surface along with the affects of weathering. Turk and Davis (1967) report porosity and specific yield to decline rapidly after 100 ft below ground surface (bgs) in two different fractured aquifers. Decreasing hydraulic conductivity with depth was initially attempted but did not improve model fit and data was insufficient to support use. Therefore, for the purpose of simplifying the model and reducing the number of total parameters, hydraulic conductivity and specific yield were considered constant with depth.

4.4 Model Construction

Model construction is the conditions used in the code to represent hydraulic features and the discretization and the zonation or method of distributing parameters. For this project construction was constant except for variations in parameterization.

4.4.1 Model Boundary Conditions

The surface and ground water divides of TCB coincide (section 3.3.3) and are represented by a no flow boundary (Figure 4.2). As discussed in section 4.3.3, the ground-water system is assumed to have minimal permeability below a depth of 700 ft., which is represented by a no flow boundary. The aquifer is unconfined and saturated thickness varies with water table elevation. If head within a cell falls below the bottom elevation of the cell, it is converted to a dry cell, which can rewet during future iterations. Water table elevation is the calculated head of the highest active cell at any (x,y) location and recharge is applied to the highest active cell. Ground-water outflow is considered to occur only at the mouth of the basin as described in sections 4.1.1 and 4.3.2, and is represented by constant head cells. River cells represent North and South Turkey creek and smaller seasonal tributaries are represented as drains in MODFLOW where water discharges when the water table reaches the ground surface but water does not recharge the system via drains.

4.4.2 Model Discritization

The model consists of a plain grid of 100 by 100 cells in five layers. Cell size is uniform throughout the model, (650ft in the Northeast- Southwest direction, 408ft in the Northwest-Southeast direction and 140ft vertically). The grid frame is rotated 42 degrees off horizontal to limit inactive cells. The top and bottom of each layer mimics surface

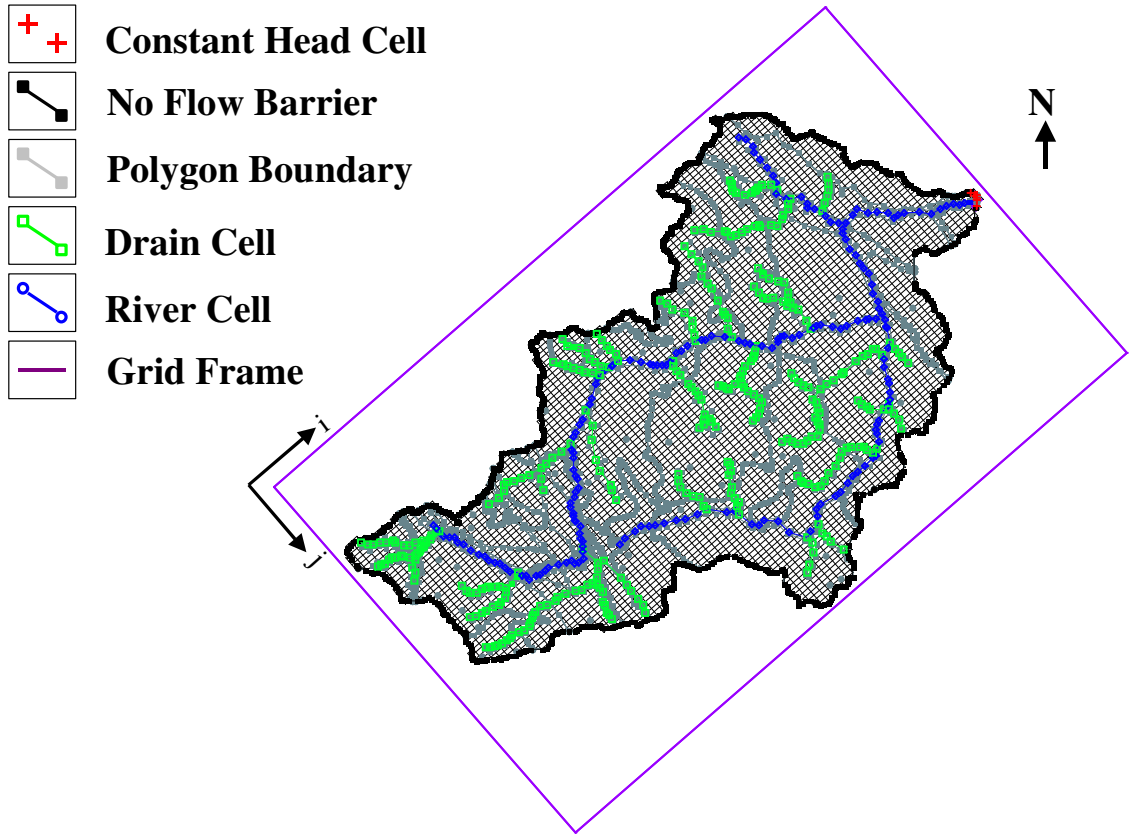

Figure 4.2 The grid frame, model construction and boundary conditions of the Turkey Creek Basin as viewed in GMS. Constant head cells, polygon boundaries and no flow boundaries extend five layers to the bottom of the model. Drain and river cells are located in the top layer.

topography (Figure 4.3). This was accomplished by subtracting layer thickness for each node from a surface elevation obtained from a digital elevation map.

4.4.3 Model Parameters

Hydraulic Conductivity

Hydraulic Conductivity for TCB was based on rock type. Rock type was determined from an unpublished USGS map of the Turkey Creek Basin compiled by Steve Char of the U.S.G.S in 1999. A hard copy of the U.S.G.S map was scanned into digital format and opened in GMS. Polygons of individual rock types were created and grouped (Figure 4.4). Files created by GMS were manipulated in a text editor to create MODFLOW input files.

Recharge

Recharge magnitude and spatial distribution in TCB were unknown. In order to determine the spatial distribution and, magnitude of recharge and the field parameters that affect recharge, several recharge models were evaluated.

Uniform Based Recharge Model

This recharge model assigned the same recharge value to each node within the MODFLOW model. An initial value was assigned to each cell in the recharge file and a recharge multiplier was adjusted until the best fit of observed heads, simulated heads and flows were obtained.

Elevation Based Recharge Model

Topography is believed to affect precipitation, vegetation, temperature and evaporation. Consequently recharge was calculated as a function of elevation. A DEM was imported to GMS and an elevation was assigned to each node within the model.

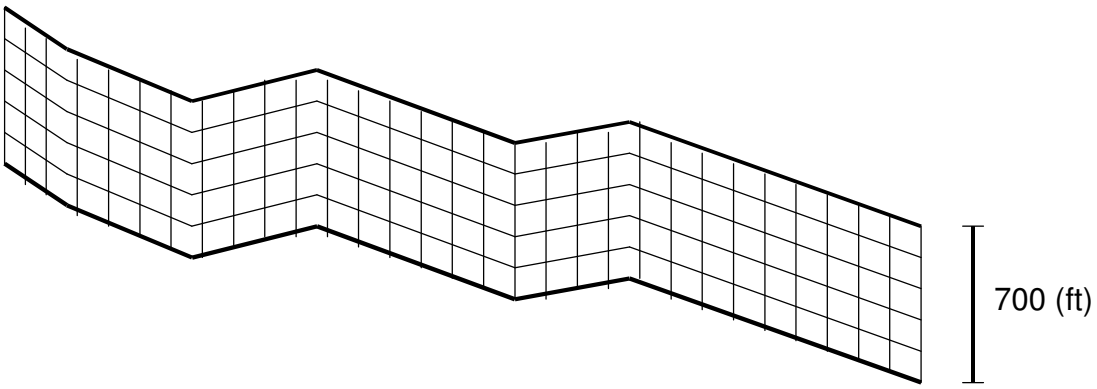

Figure 4.3 Schematic profile of MODFLOW model layers mimicking topography.

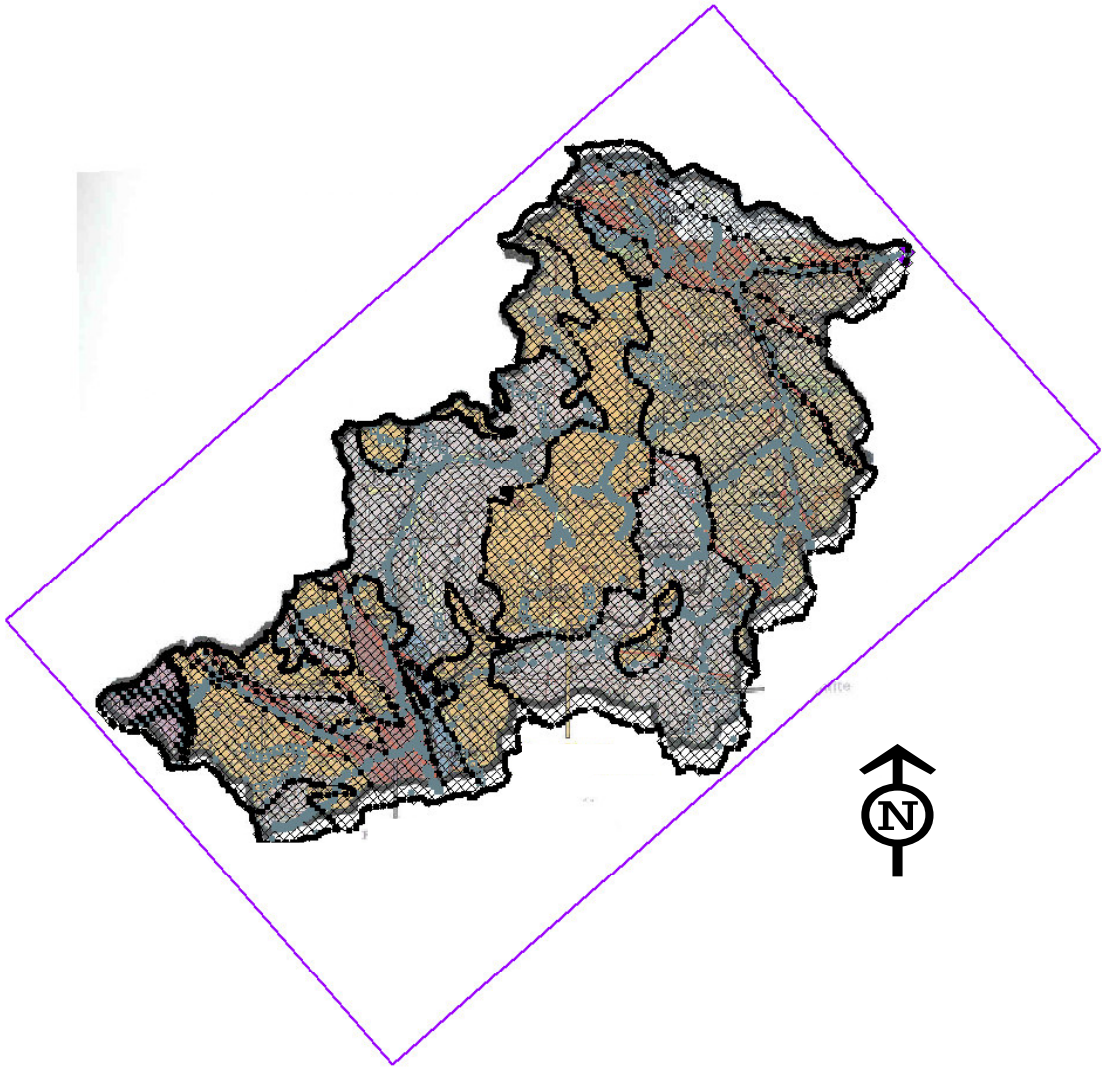

Figure 4.4 Grid frame with polygon boundaries drawn over an image of the geology of the Turkey Creek Basin. Turkey Creek Geological map from U.S.G.S. unpublished compiled by Steven Char of the U.S.G.S. in 1999.

The interpolated surface was output as a 2D array and read into a FORTRAN code (Appendix E). The FORTRAN code used equation (4.4) to manipulate the 2D elevation array to calculate recharge.

$$\text{Recharge} = \left[\left(\frac{\text{Elev} - \text{ElevMin}}{10{,}000} \right)^{a} \right] b \tag{4.4}$$

Where: Recharge = Recharge value assigned to MODFLOW cell in RCH file
Elev = Surface elevation determined for each node from a DEM by GMS
ElevMin = Minimum elevation of basin
a = Parameter calibrated by UCODE, (recharge spread factor)
b = Parameter calibrated by UCODE, (recharge multiplier)

Elevation/Slope/Aspect Based Recharge Model

Slope is believed to influence recharge. Given equal areas, greater slope will have more overland runoff resulting in less infiltration. To represent this, a value of slope was incorporated into the calculation of recharge. As with elevation, an average slope value (0-90deg) is calculated for each node within the model from a DEM. Equation (4.5) was used to manipulate the average slope values.

$$\text{Slp} = \left(\frac{1}{Slope} \right)^{c} \tag{4.5}$$

Where: Slp = Value calculated for slope
Slope = Average value of slope determined for each node
c = Parameter calculated by UCODE to represent importance of slope to the recharge function

The aspect of the slope is believed to affect recharge in several ways. Slopes that face south receive more direct sunlight than north facing slopes. Drastic differences in vegetation are noted between north and south facing slopes. Because of this, different soil types occur. These factors influence the rate of infiltration and evapotranspiration, thus affect recharge rates. From a DEM, an average value for aspect was assigned (0-359deg) for each node of the model. Equation (4.6) was used to manipulate the average slope aspect values.

$$\text{Asp} = x^{d} \tag{4.6}$$

Where: x = Slope aspect value ranging from 0-359 ^{o}.

For aspects within 10^{o} of south x is 0.5. For aspects outside that range, but within 20^{o} of south, x is 0.8. For each increase of 10^{o} of aspect x increases by 0.3. At the largest range which is 10^{o} of either side of north, x = 5.6.

A FORTRAN code (Appendix F) used equation (4.7) to combine Equations (4.4, 4.5, 4.6) to calculate the total recharge applied to an individual cell.

(4.7)

$$\text{Recharge} = \left(z^{a} * s^{c} * x^{d}\right)b$$

Where: z = The elevation of the node
s = The inverse value of slope of each node
x = The assigned value determined by average slope aspect
b = The recharge multiplier

Precipitation Runoff Modeling System Model

The Precipitation Runoff Modeling System (PRMS) (USGS, 2002) is based on estimated physical parameters throughout the watershed and is intended to distribute measured precipitation and gauged stream flow (MGWRS, 2002). HRUs were determined using a series of algorithms developed to work with a DEM (Jensen and Domingue, 1988). Bossong et al., (2003) defined 112 HRUs and incorporated the following parameters into PRMS for a three year period (1999, 2000 and 2001): soil data from Soil Survey Geographic database (SURGO); vegetation data including trees and grasses interpreted from digital orthophoto imagery provided by Jefferson County; movement of water, and energy-budget processes related to precipitation and evapotranspiration.

Bossong et al., (2003) gave values for total estimated evapotranspiration, overland flow and precipitation for each Hydrologic Response Unit (HRU). A residual value was given for the difference between precipitation and evapotranspiration for each HRU. Overland flow reported for each HRU was subtracted from the reported residual, multiplied by HRU area, and summed to determine total recharge to the basin. The calculated values of recharge for each water year (7.8 in/yr, 0.31 in/yr, and 0.16 in/yr EUD, respectively for 1999, 2000 and 2001) were averaged, yielding a value of 2.75 in/yr with spatial variation ranging from 0.49 to 8.9 in/yr. The water year was incomplete for 1999 and was adjusted accordingly. An image of the HRU distribution was scanned into GMS, polygons were drawn for each HRU, and the recharge value for each HRU was assigned to each MODFLOW cell in the HRU.

Soil Water Assessment Tool Model

SWAT stands for Soil Water Assessment Tool. SWAT is a distributed-parameter model designed to aid in long-term management of resources (King et al., 1999). An in-depth description of SWAT is provided by Arnold et al., (1998) or Arnold et al., (1999).

SWAT incorporates readily available physical parameters (i.e., slope, elevation, etc.) to simulate surface water runoff, ground-water recharge, soil water content, ET, and biomass production (Murray, 2003). Murray (2003) incorporated trends in precipitation and temperature based on elevation for individual HRUs. The SWAT model produced a recharge file for direct input to MODFLOW. Total recharge to the basin was equivalent to 0.67 in/yr EUD over the entire basin area, with spatial variation ranging from 0.043 in/yr to 1.53 in/yr.

Storage Coefficient

The storage coefficient or storativity of an aquifer is the volume of water drained from the pore space/fractures per unit surface area per unit change in head. Water levels (hydraulic head) will fall or rise with changes in the amount of water in storage. If water exits storage, water levels fall as water is drained from fractures. This release from storage is a function of the specific yield and specific storage of the material. Equation (4.8) represents the storage coefficient of an unconfined aquifer.

$$S = S_y + bS_s \tag{4.8}$$

Where: S = Storativity
S_y = Specific yield
b = Aquifer thickness
S_s = Specific storage

For unconfined aquifers S_y is several orders of magnitude larger than Ss. Often for unconfined systems storage coefficient is assumed to equal specific yield. The value of S_s was held constant (1.0×10^{-6}) for all model runs.

Distribution of Specific Yield

A uniform distribution of specific yield (S_y) was used. The same value of S_y was assigned to each node in the model and that value was calibrated by UCODE.

4.4.4 Observations

Observations are field data used to calibrate the model. The observations are used in steady-state and transient models as discussed below.

Hydraulic Heads for Steady-State Calibration

Hydraulic head is a dependent variable; parameters are adjusted until model results match observations. Heads were determined from depth to water measurements (section 3.3). The water table elevations at the 12 abandoned wells were individually averaged in an attempt to represent a steady state condition. The well locations were identified using a hand held Global Positioning System (GPS) and observation depth was determined as ¾ of the total well depth.

Initial attempts were made to incorporate the U.S.G.S. synoptic depth-to-water measurements. However, these measurements were taken in domestic wells (section 3.3.1), which resulted in model bias. Wells with low yields (<2 GPM) yielded larger residuals as compared to wells with larger yields (>2 GPM) indicating a lack of recovery from prior pumping therefore use was discontinued.

Flow for Steady-State Calibration

Stream discharge measurements taken for a 10-month period (section 3.1.2) were averaged at each sample location to determine the ratio between discharge at the measurement location and the discharge at the mouth of the basin. This was done in order to use a longer record of stream flow at the mouth of the basin. A discharge rate was then

assigned to each measurement location based on the determined ratio and an average baseflow value (section 4.1.2).

Hydraulic Heads for Transient Calibration

Hydraulic-head measurements taken over the summer of 2002 (section 3.3.2) were used to calculate a head decline for each month. Specific yield was estimated by matching simulated head decline with observed head decline.

4.5 Evaluation of Alternative Conceptual Models

Each conceptual model (water budget, five steady state models comparing different recharge scenarios and a transient model) was evaluated. The water budget was evaluated for recharge magnitude, steady state model for spatial distribution of recharge and the factors affecting it and the transient model for specific yield. Other models explored (homogeneous geology, varying K with depth, etc.), which yielded poor model fit, are not discussed.

4.5.1 Evaluation of the Water Budget

Summing individual terms of the water budget (section 4.1) yields a range for potential long-term recharge (Table 4.4) (Appendix G). The largest calculated recharge value is the maximum value from each component. The smallest recharge value is composed solely of baseflow, which could occur if all other terms are negligible. Both the maximum and minimum recharge values are unlikely to occur, but provide a possible range for long-term recharge.

4.5.2 Evaluation of Steady-State Models

UCODE, a modified Gauss-Newton inversion tool, was used for steady state calibration. Parameter estimation converged when the user defined closure criterion was satisfied. Calibration results produced for each model were compared to evaluate which model produced the best overall model fit. Analyses of individual calibration results are above. Appendix H-L contains MODFLOW and UCODE files from calibration for each individual model.

	Low Baseflow	Low	Medium	High
Alluvium Outflow		50 ft^3/yr	77,595 ft^3/yr	11 $x10^6 ft^3/yr$
Bedrock Outflow		35 ft^3/yr	92,400 ft^3/yr	184 $x10^6 ft^3/yr$
Stream Baseflow	9,460,800	$11x10^6 ft^3/yr$	23 $x10^6 ft^3/yr$	37 $x10^6 ft^3/yr$
Water Consumption		24 $x10^6 ft^3/yr$	12 $x10^6 ft^3/yr$	24 $x10^6 ft^3/yr$
Total AFY	253	360	818	5,565
Total in/yr (EUD)	0.09in/yr	0.14 in/yr	0.33 in/yr	2.27 in/yr

Table 4.4 Summation of individual water budget components. High, medium and low recharge values were determined by summing the components in section 4.1. The low baseflow value is considered the lowest possible recharge value and is composed solely of the lowest baseflow value, assuming ground-water outflow from bedrock and alluvium outflow are zero.

Global Measures of Model Fit

Global model fit was evaluated by considering the magnitude of the weighted residuals and their spatial distribution. Large errors or residual bias can indicate a poor conceptual model of the system.

Residual Statistics

Residuals are the difference between observed and simulated values. The sum-of-squared weighted residuals (SOS) are often used as a general indication of model fit. Equation (4.9) is used to determine SOS.

$$SOS = \sum_{i=1}^{n} W\left(y_m - y_s\right)_i^2 \tag{4.9}$$

Where: y_m = Measured value observed in the field
y_s = Simulated value produced by model
W = Observation weight, 1/variance of measurement, y_m

Using the sum-of-squared weighted residuals prevents positive and negative residuals from canceling out in the measure of fit and emphasizes large residuals. Weighting the observations reflects the uncertainty in field measurements and allows for the synoptic use of different types of measurements such as hydraulic head and flow observations. The (SOS) for each model can be viewed in Figure 4.5.

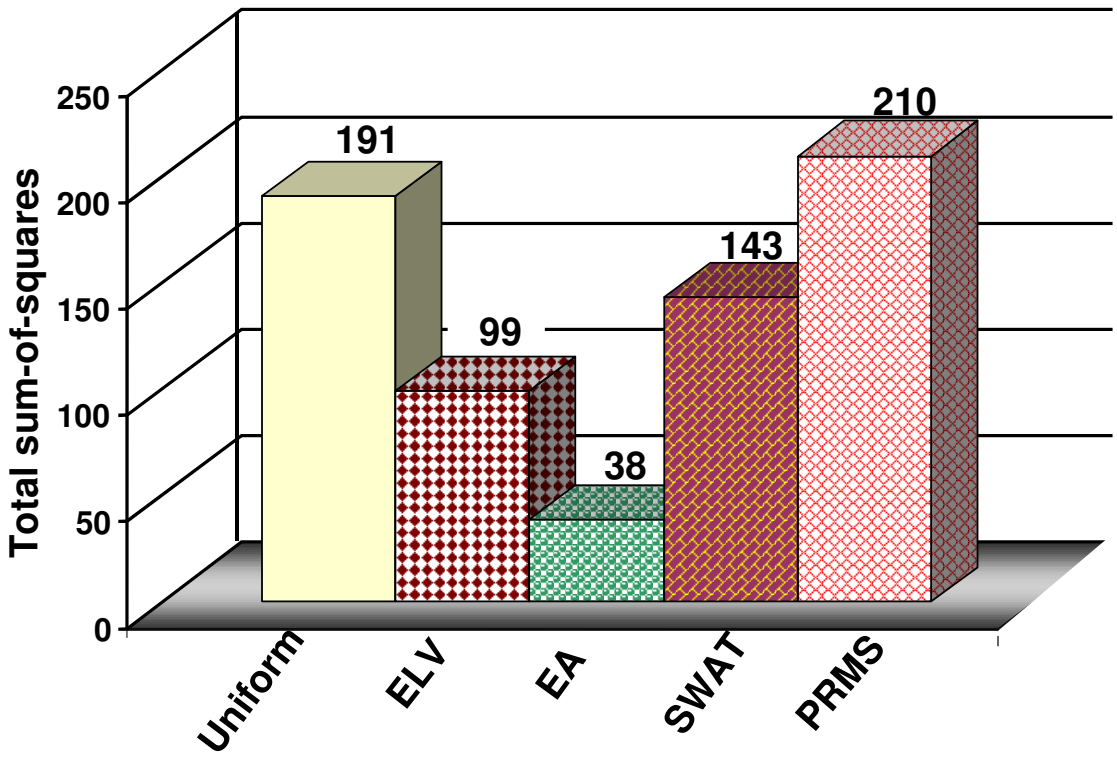

Figure 4.5 The total sum-of-squared residuals produced by UCODE for each recharge model.

Graphical Measures of Model Error

It has been shown (Draper and Smith, 1981) that for most modeled systems the weighted residuals and weighted simulated values, weighted observation and weighted simulated, and spatial bias of unweighted head and flow residuals should be independent. Therefore it is beneficial to assess graphs comparing these to identify model bias, which may require reconceptualization.

Weighted Simulated Values vs. Weighted Residual Values

Plotting weighted residual values vs. weighted simulated values may identify model bias. An unbiased model has a uniform distribution of the residuals around zero with roughly equal number of negative and positive residuals. Trend lines should have a slope and Y-intercept of zero (Figures 4.6, 4.7, 4.8). Models are presented in order of decreasing spatial bias.

Weighted Observation Values vs. Weighted Simulated Values

Comparing the weighted observations and weighted simulated values evaluates residual bias. Ideally, points fall along a straight line with a slope of one and a Y-intercept of zero (Hill, 1998)(Figure 4.9, 4.10, 4.11). Models are presented in order of decreasing spatial bias.

Spatial Bias of Unweighted Head Residuals and Flow Residuals

Plotting unweighted residuals on a topographic image of the model surface gives insight into possible spatial bias with respect to observation location within the model. Figures 4.12- 4.16 display the unweighted head and flow residuals. Models are presented in order of decreasing spatial bias.

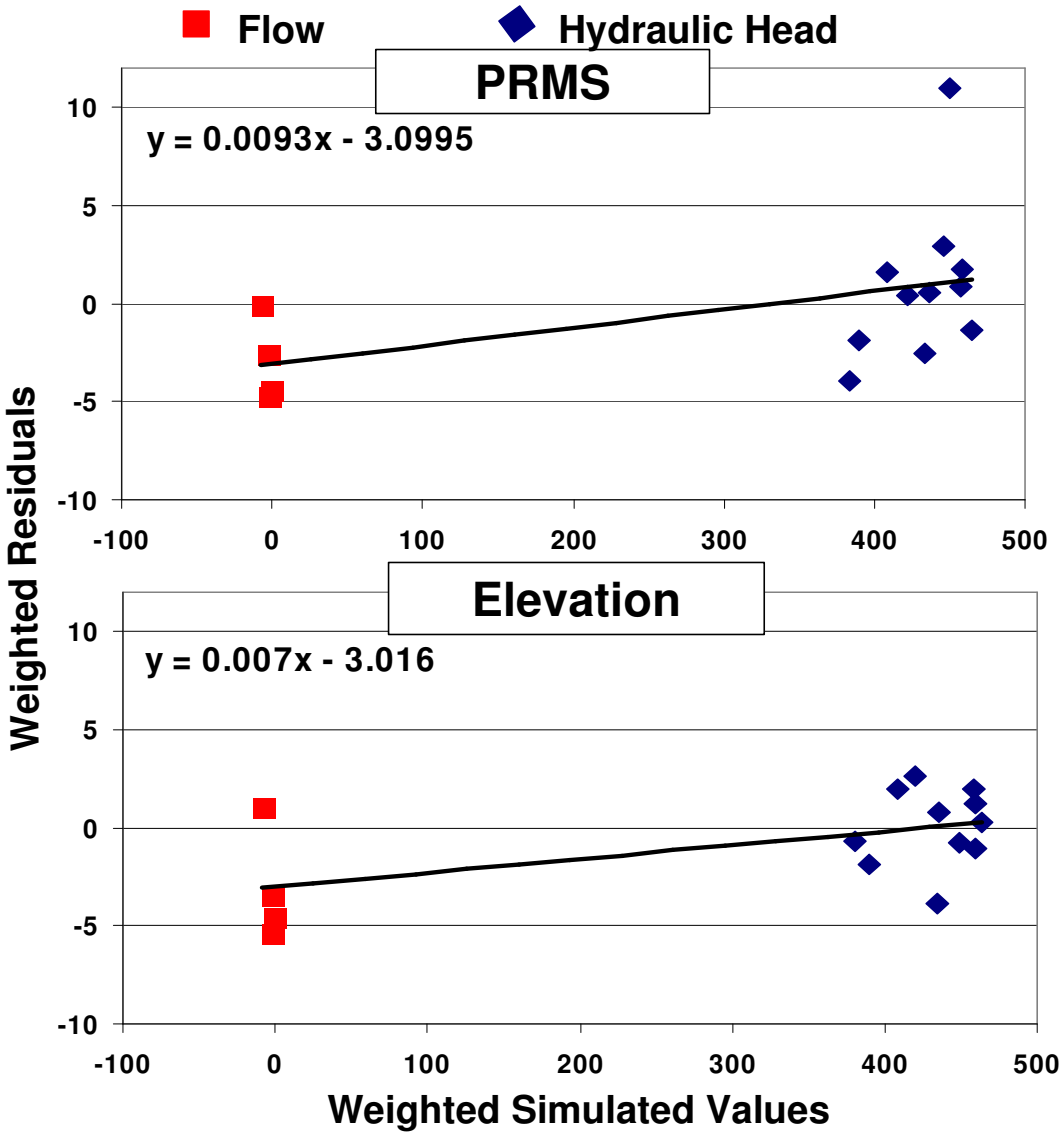

Figure 4.6 Weighted simulated values vs. weighted residual values produce by UCODE.

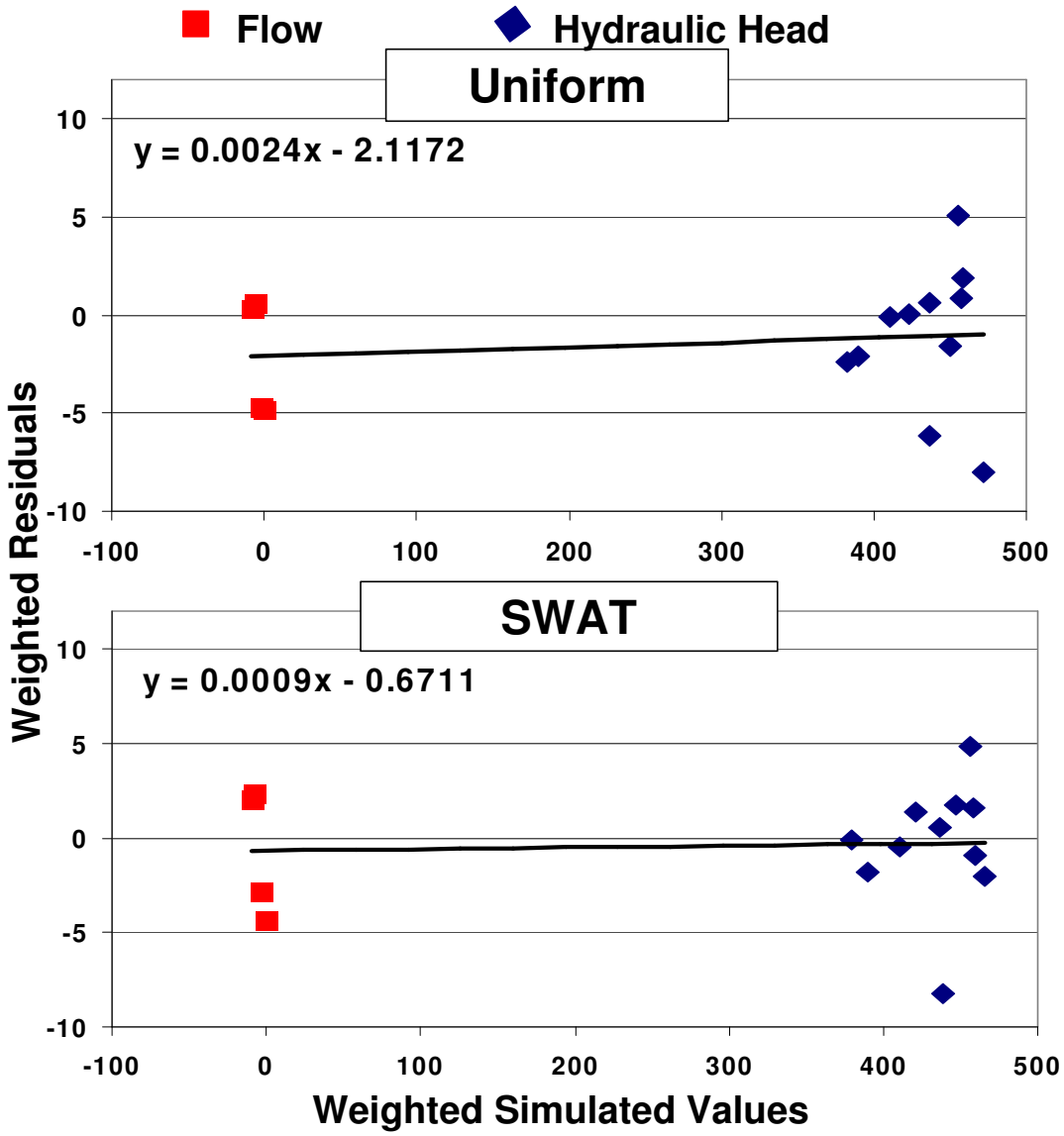

Figure 4.7 Weighted simulated values vs. weighted residual values produce by UCODE.

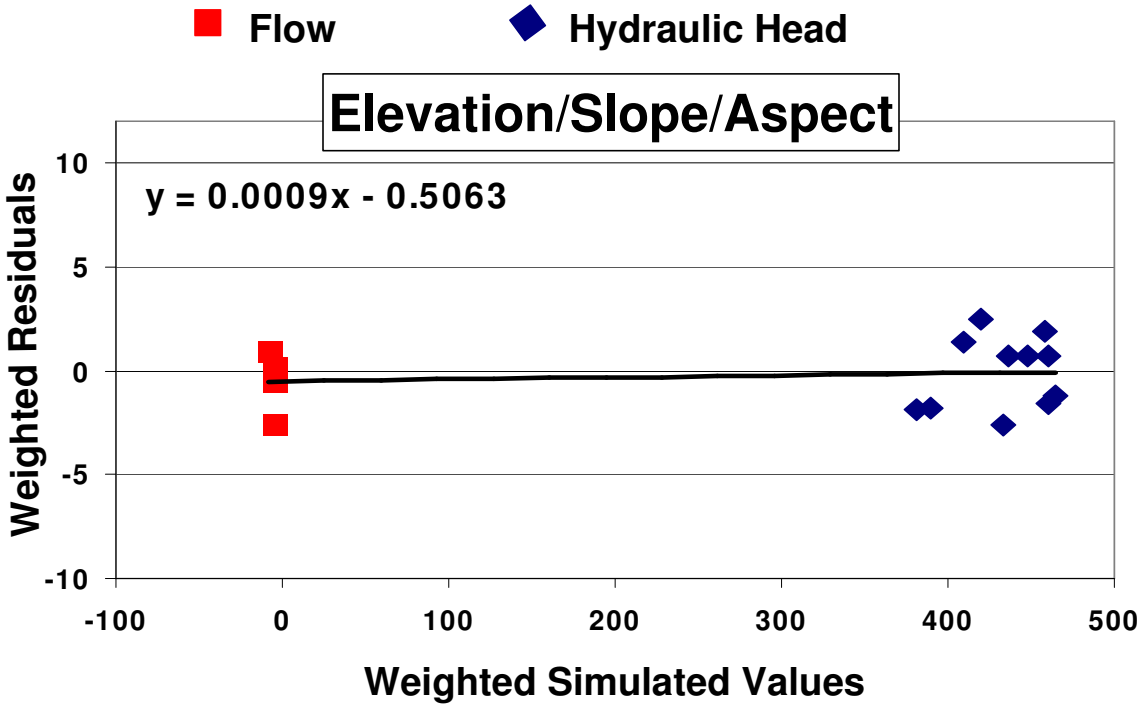

Figure 4.8 Weighted simulated values vs. weighted residual values produce by UCODE.

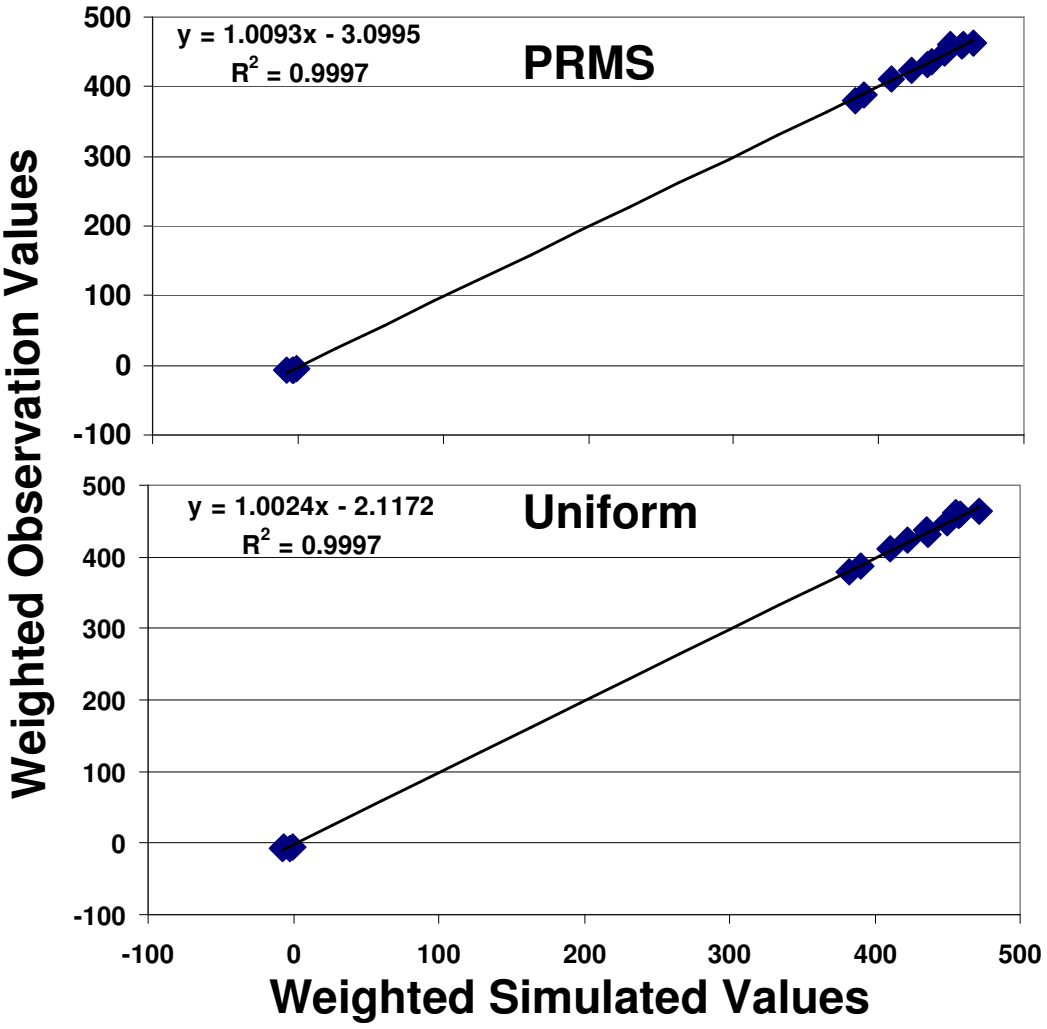

Figure 4.9 Weighted simulated values vs. weighted observed values. Equation for the line displayed in upper left corner.

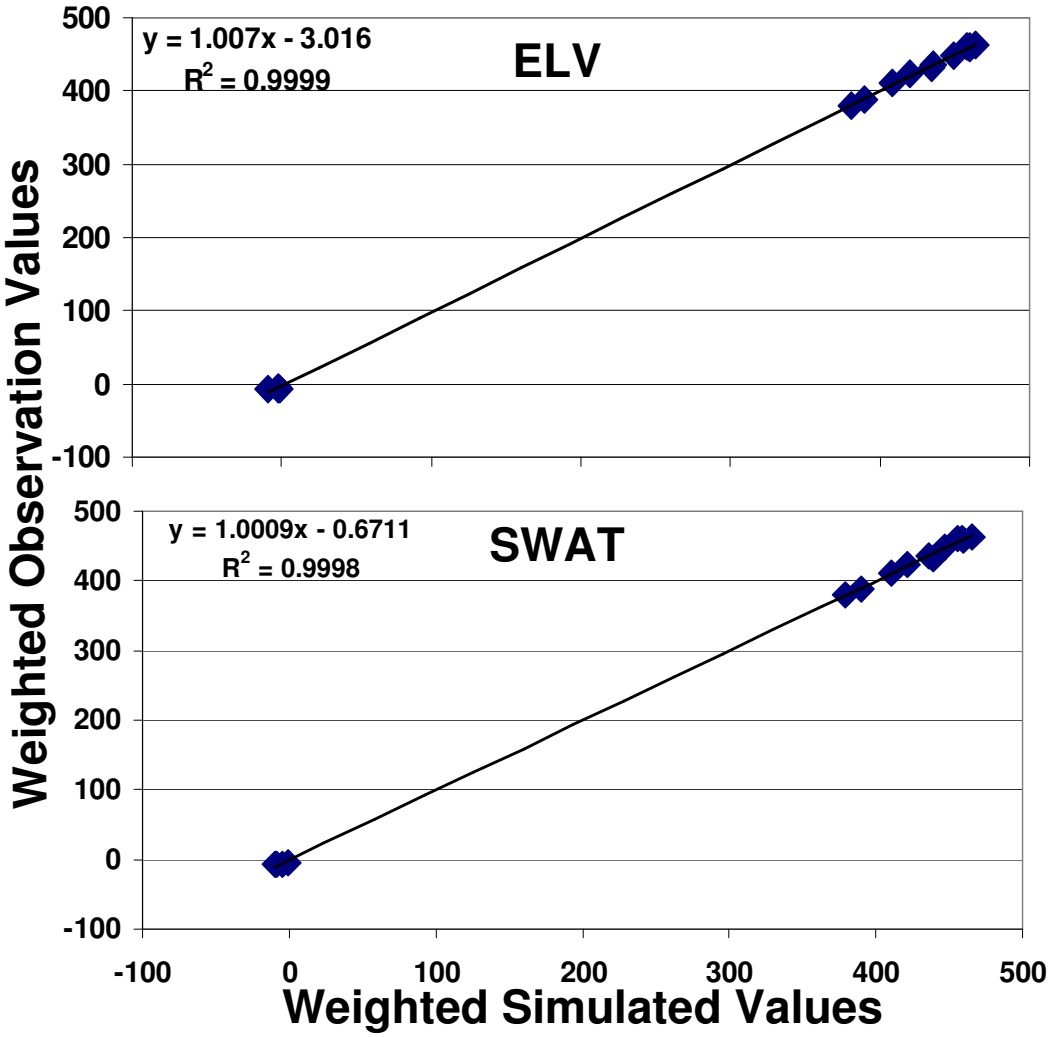

Figure 4.10 Weighted simulated values vs. weighted observed values. Equation for the line displayed in the upper left corner.

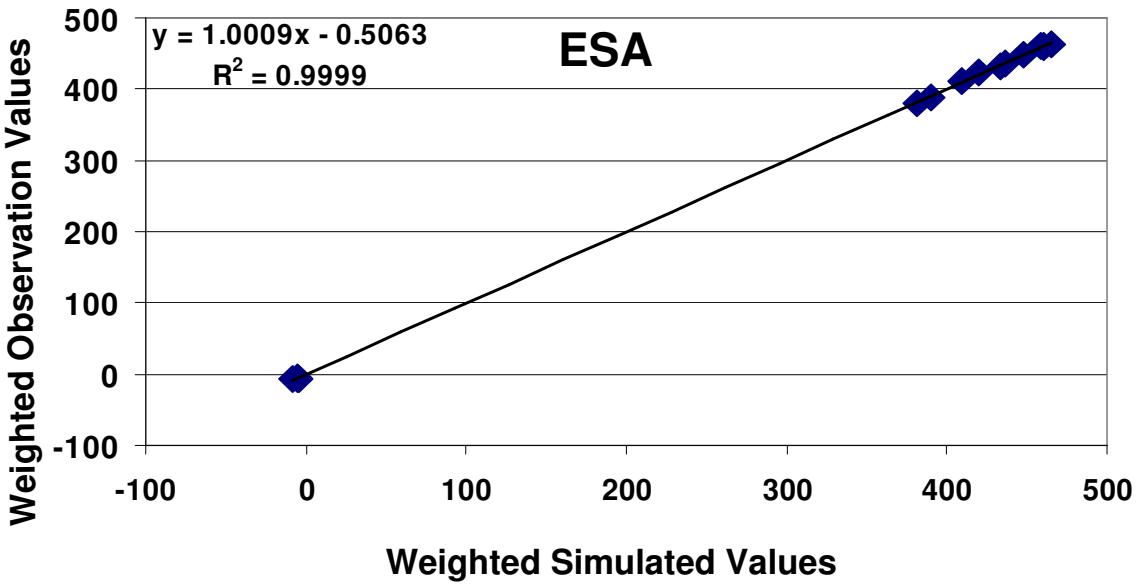

Figure 4.11 Weighted simulated values vs. weighted observed values. Equation for the line displayed in the upper left corner.

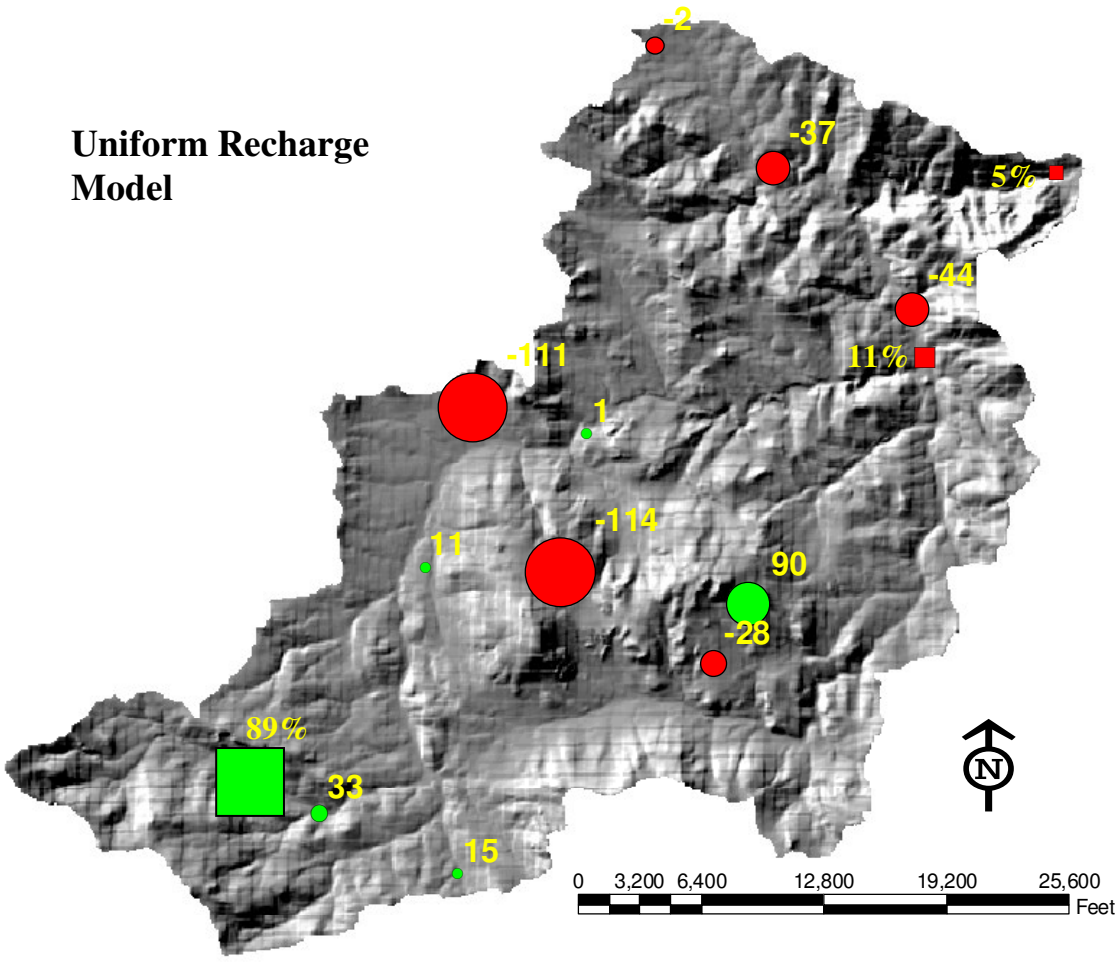

Figure 4.12 Spatial distribution of unweighted residuals for the Uniform recharge model. Squares represent flow residuals in percent error and circles represent head residuals in feet of error. Green represents a simulated value smaller than observed; red represents a simulated value larger than observed.

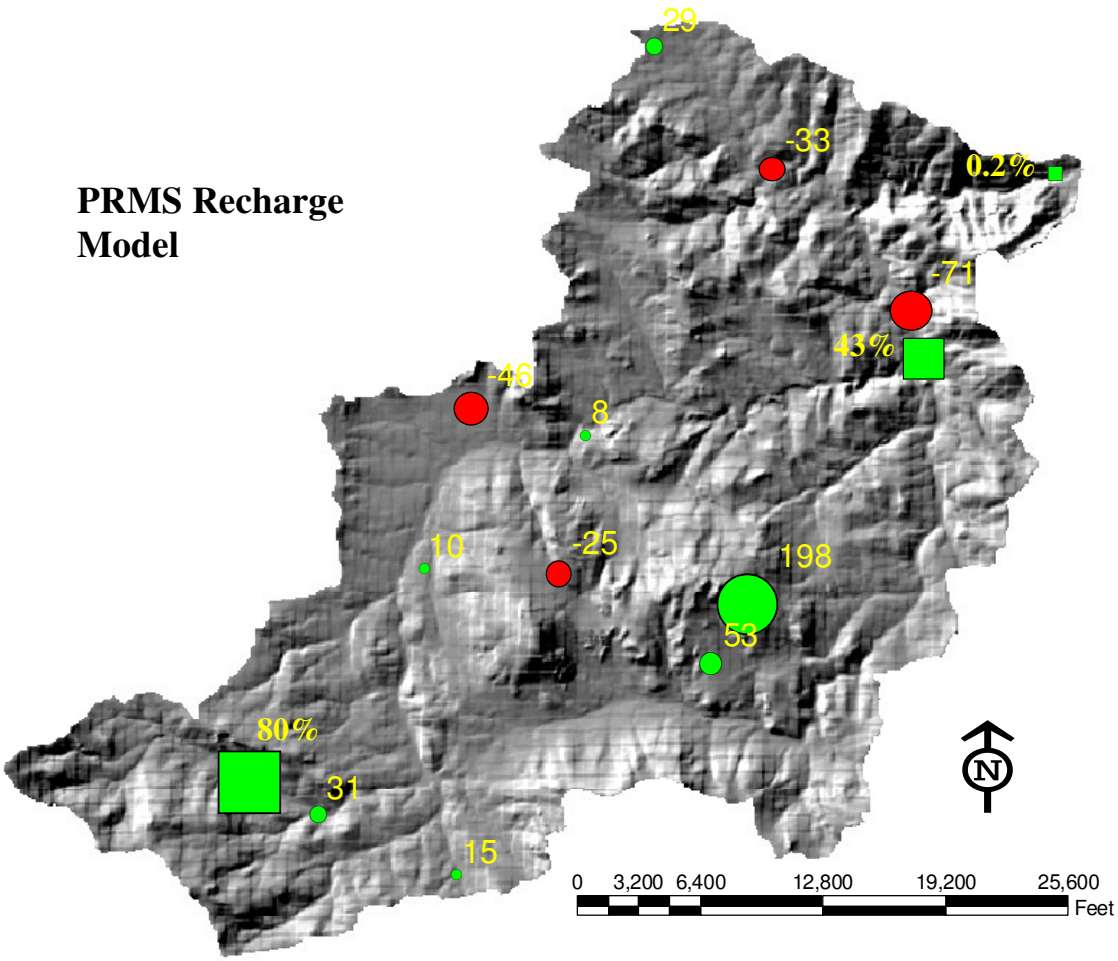

Figure 4.13 Spatial distribution of unweighted residuals for the PRMS recharge model. Squares represent flow residuals in percent error and circles represent head residuals in feet of error. Green represents a simulated value smaller than observed; red represents a simulated value larger than observed.

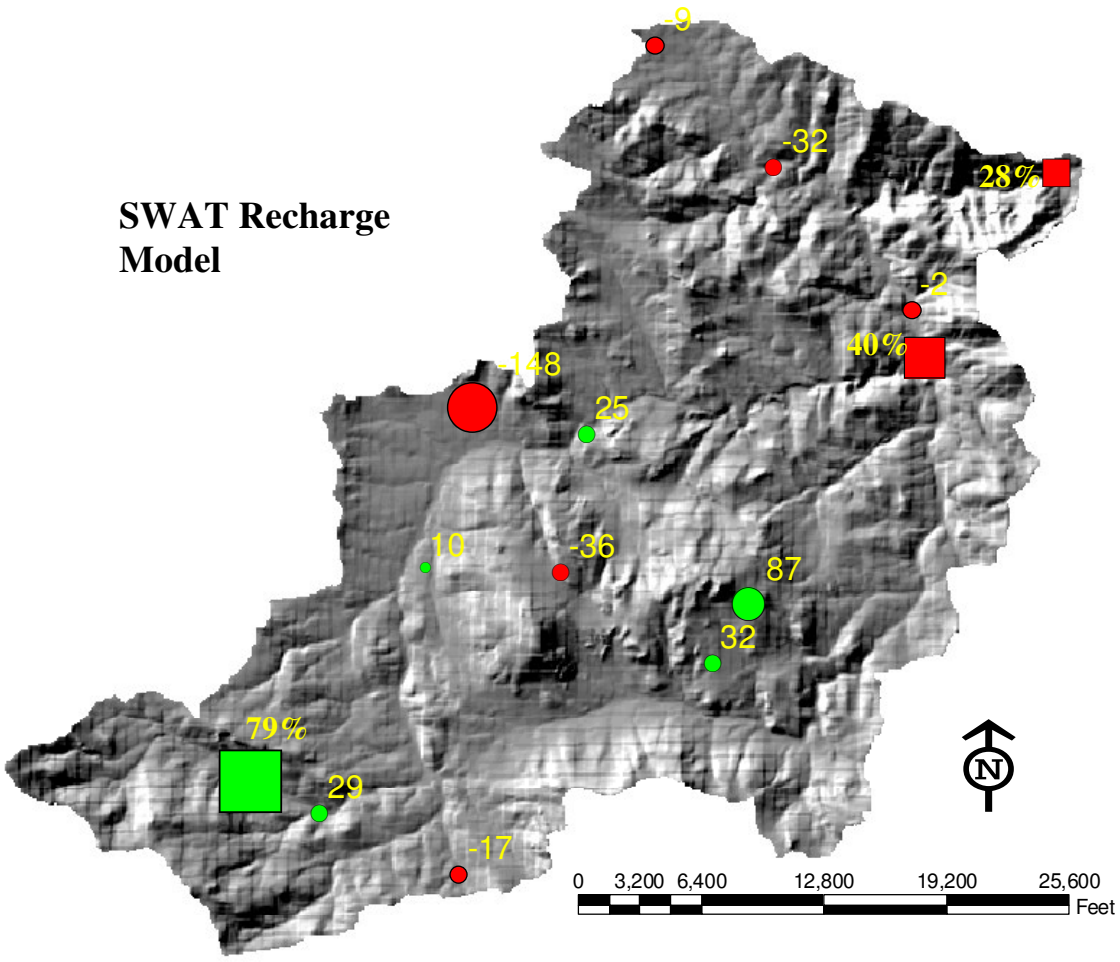

Figure 4.14 Spatial distribution of unweighted residuals for the SWAT recharge model. Squares represent flow residuals in percent error and circles represent head residuals in feet of error. Green represents a simulated value smaller than observed; red represents a simulated value larger than observed.

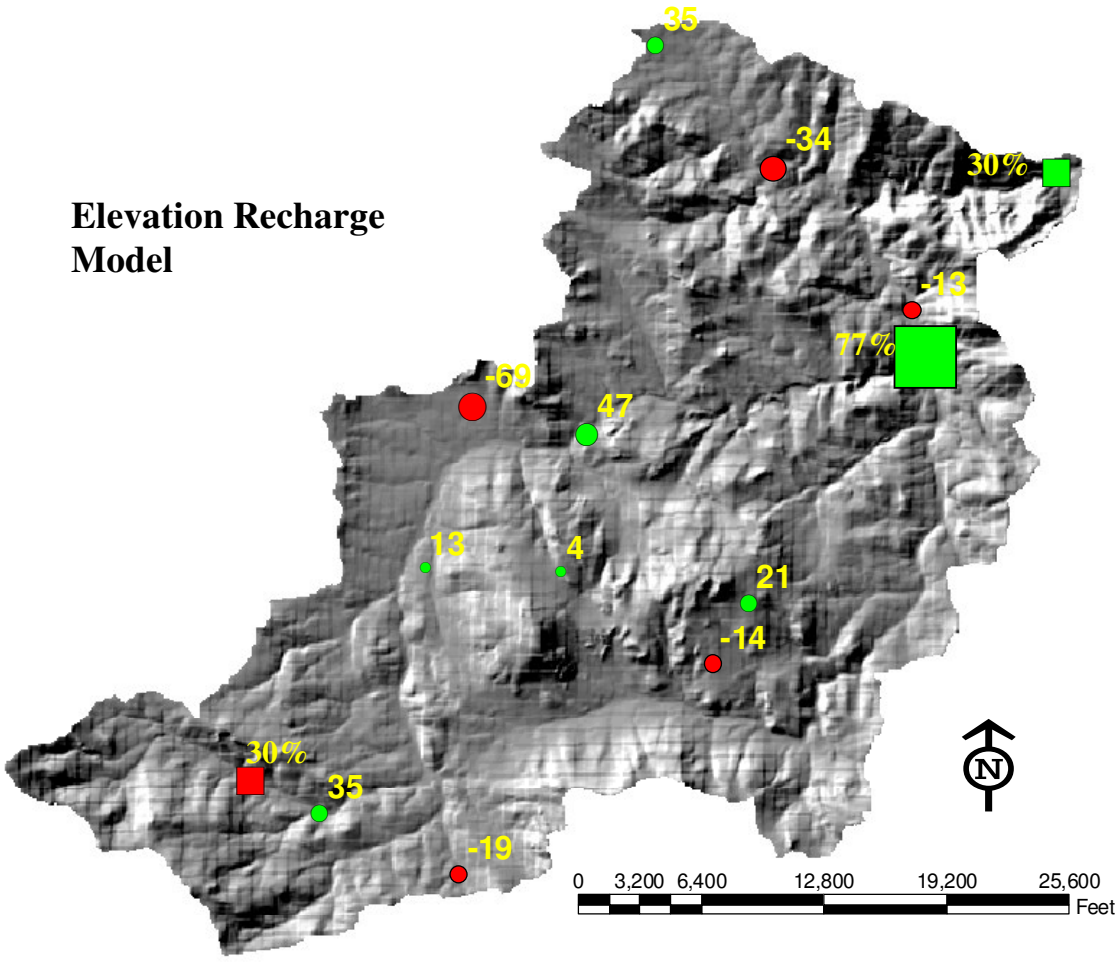

Figure 4.15 Spatial distribution of unweighted residuals for the Elevation recharge model. Squares represent flow residuals in percent error and circles represent head residuals in feet of error. Green represents a simulated value smaller than observed; red represents a simulated value larger than observed.

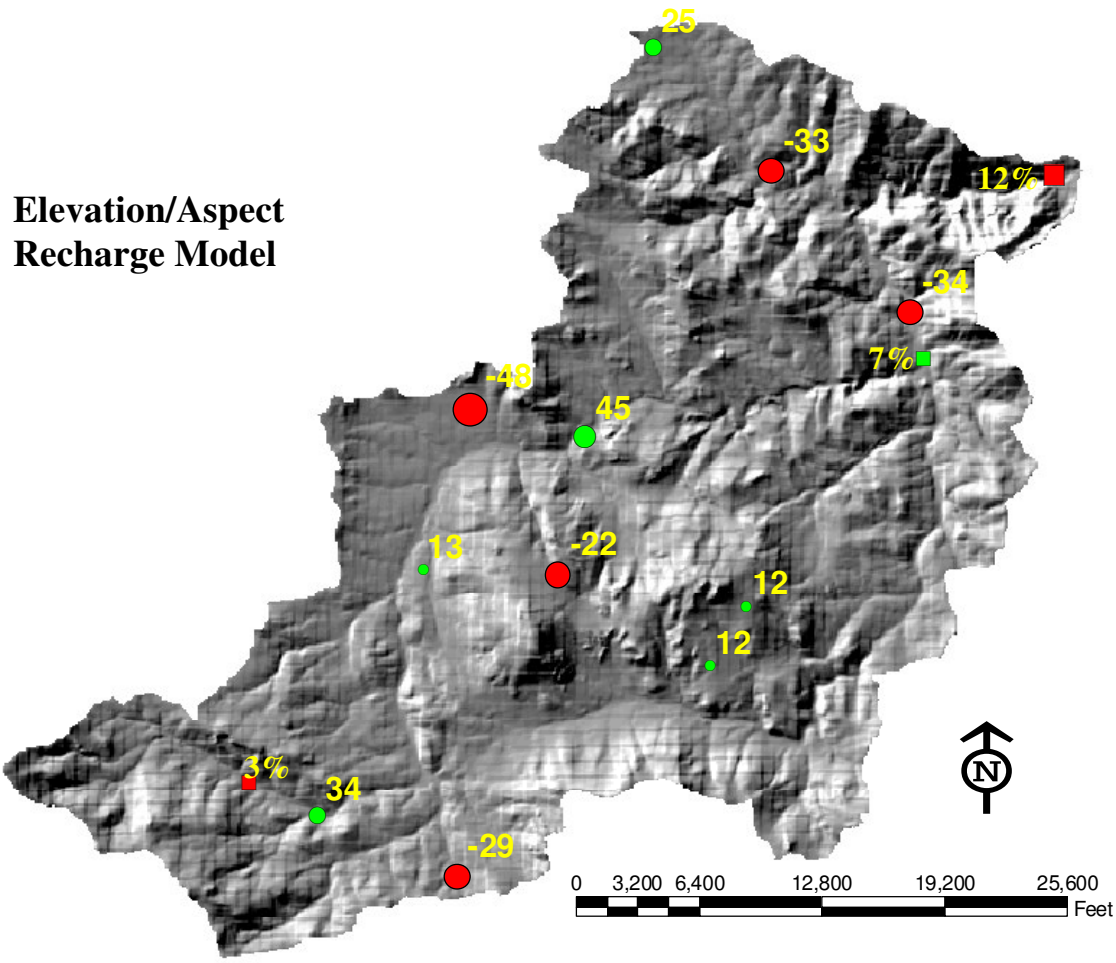

Figure 4.16 Spatial distribution of unweighted residuals for the Elevation/Aspect recharge model. Squares represent flow residuals in percent error and circles represent head residuals in feet of error. Green represents a simulated value smaller than observed; red represents a simulated value larger than observed.

Correlation Between Ordered Weighted Residuals and Normal Order Statistics

For regression to be valid, errors in the observations need to be random and uncorrelated (Hill, 1998). If the model is accurately representing the system, and weighted errors are random, then the weighted residuals are expected to be random and normally distributed or have a predictable relationship. After regression UCODE produces a value for correlation between ordered weighted residuals and normal order statistics, Rn^2. This value can be compared to a (5 and 10%) critical significance level, which is printed by the UCODE output file. If Rn^2 is greater than the critical value produced by UCODE, then it is likely the weighted residuals are independent and normally distributed (Poeter et al., 1998). This model however, only utilizes 15 observations, which is less than the published value of 35 for which the 5 and 10% significance level statistics are calculated (Table 4.5).

	Correlation between ordered weighted residuals and normal ordered statistics	5% Significance Level	10% Significance Level
Uniform	0.956	0.943	0.952
Elv/Asp	0.954	0.943	0.952
Elevation	0.947	0.943	0.952
SWAT	0.938	0.943	0.952
PRMS	0.845	0.943	0.952

Table 4.5 Correlation between ordered weighted residuals and normal ordered statistics calculated for 5% and 10% confidence intervals. If the calculated value is above the significance value then it is believed the weighted residuals are independent and normally distributed.

It can be seen in Table 4.5 that the Uniform, Elevation and Elevation/Aspect recharge models show an acceptable distribution while the SWAT and particularly the PRMS recharge models are less likely to exhibit normally distributed residuals.

Optimal Parameter Values

The combinations of parameter values yielding the lowest (SOS) are considered the optimal parameter values. Table 4.6 and 4.7 display the optimal parameter values resulting from each model.

Determining if the Optimal Parameter Values are Unique

Universal inversion codes calculate sensitivity by perturbation and so may not accurately calculate parameter correlation especially for extreme correlations. Consequently it is good practice to confirm uniqueness by repeating parameter estimation by starting with different initial parameter values and confirming that the same values are obtained from calibration. To do this, starting parameter values are set at the upper or lower confidence intervals reported by UCODE and regression is repeated. If the resultant optimal parameter values produced from calibration are within one standard deviation of the previously estimated optimal values then it can be assumed that the optimal parameter values are indeed unique. This process should be done numerous times using different combinations of starting values. Figure 4.18 and 4.19 present the results.

Model Analysis and Ranking

The PRMS and SWAT models were created independently of this research and had previously defined values for recharge magnitude, 2.78 and 0.67 in/yr EUD respectively. These estimates were believed to be too high and in order to compare results produced by different recharge models it was desirable for all models to have the same recharge magnitude. In order to accomplish this, recharge magnitude was constrained by stream flow observations. A baseflow value of 0.35 ft^3/sec was used at the mouth of the

	Pikes Peak Granite	Fault Zone	Longs Peak Granite	Migmatite	Biotite Gneiss
ESA (ft/yr)	1.0×10^{-3}	3.1×10^{-4}	3.0×10^{-3}	3.7×10^{-4}	1.0×10^{-4}
Elv (ft/yr)	3.1×10^{-4}	2.5×10^{-4}	2.1×10^{-3}	2.3×10^{-4}	7.0×10^{-3}
Uniform (ft/yr)	7.8×10^{-4}	2.8×10^{-3}	8.1×10^{-4}	4.0×10^{-4}	4.0×10^{-3}
SWAT (ft/yr)	7.8×10^{-4}	2.7×10^{-3}	1.4×10^{-3}	6.7×10^{-4}	3.1×10^{-4}
PRMS (ft/yr)	1.2×10^{-6}	5.9×10^{-3}	5.5×10^{-4}	2.9×10^{-4}	1.1×10^{-3}

Table 4.6 Optimal aquifer parameter values calculated by UCODE.

	Rch Multiplier	Elv Exponent	Asp Exponent	SOS
ESA	2.4×10^{-2}	4.4	0.31	38
ELV	6.8×10^{-3}	3.5	NaN	99
Uniform	8.8×10^{-1}	NaN	NaN	191
SWAT	2.8×10^{-1}	NaN	NaN	143
PRMS	6.8×10^{-2}	NaN	NaN	210

Table 4.7 Optimal recharge parameter values calculated by UCODE.

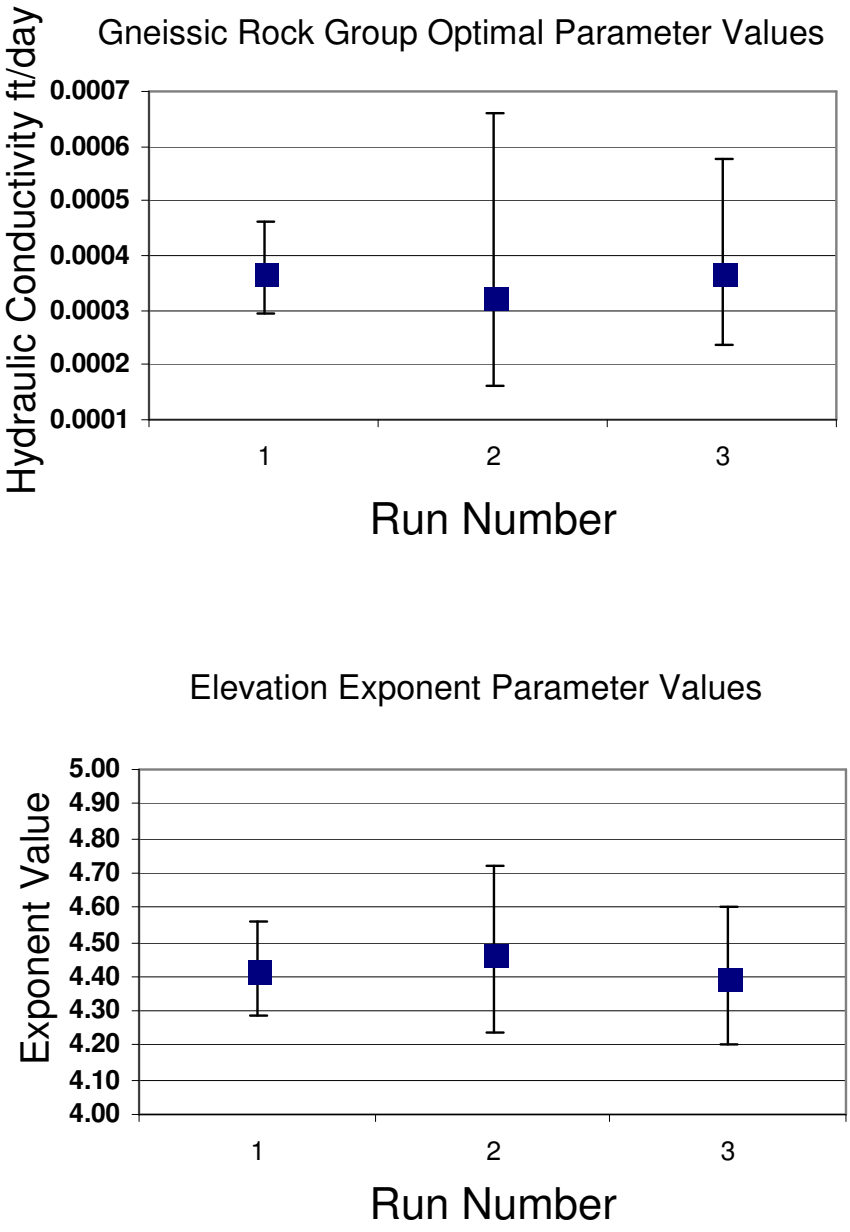

Figure 4.17 Optimal parameter values and their upper and lower linear confidence intervals as calculated by UCODE for the Gneissic rock group and elevation exponent. Blue squares are the optimal parameter value and error bars represent upper and lower confidence intervals. Ideally all points should fall within the next point's error bars.

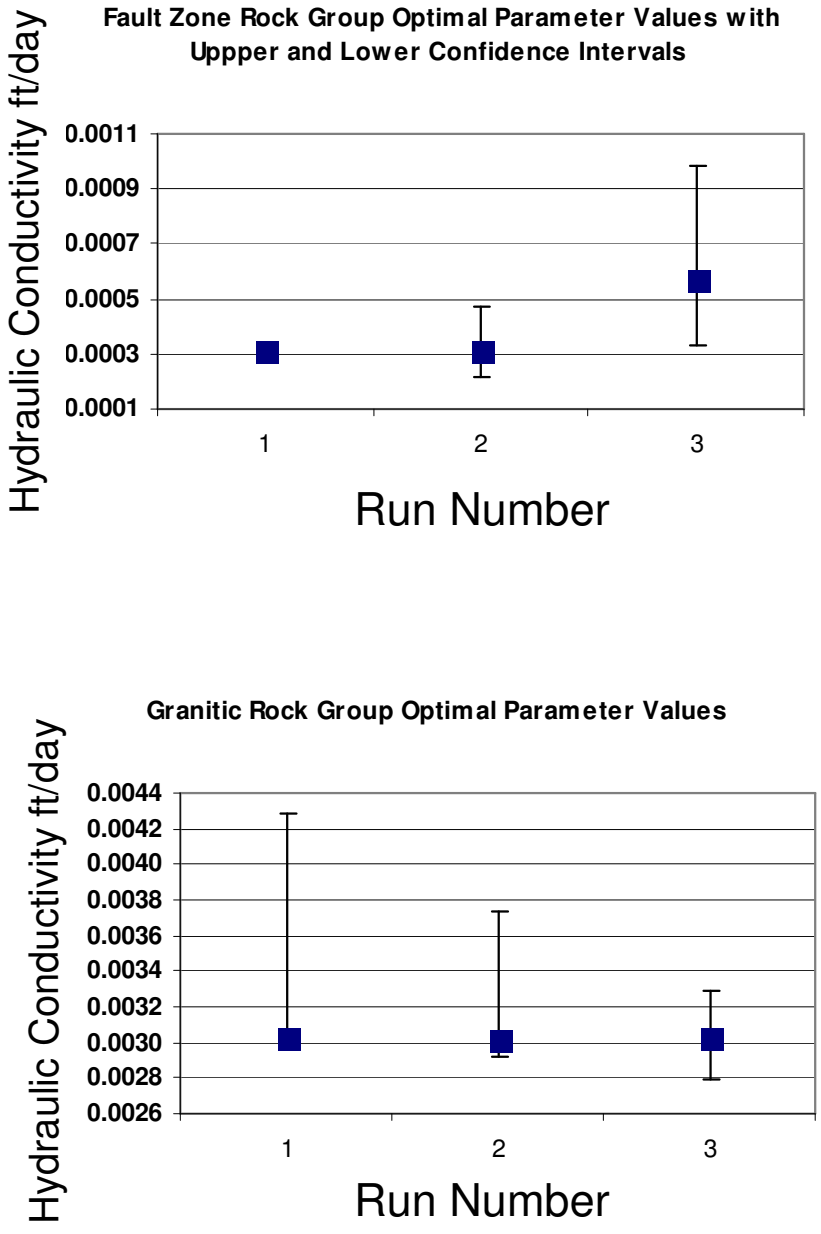

Figure 4.18 Optimal parameter values and their upper and lower confidence intervals as calculated by UCODE for the Fault zone rock group and granitic rock group. Blue squares are the optimal parameter value and error bars represent upper and lower confidence intervals. Ideally all points should fall within the next point's error bars.

basin and the recharge multiplier (defined in section 4.4.3) calibrated by UCODE determined the overall recharge magnitude. The range of recharge values, calibrated values of the recharge multiplier, and the resultant recharge magnitude for each model is shown in table 4.8.

	Maximum (in/yr) EUD	**Minimum (in/yr) EUD**	**Recharge Multiplier**	**Total Recharge (in/yr) EUD**
Uniform	0.16	0.16	0.79	0.16
Elevation	2.1	7.5×10^{-9}	0.0069	0.15
Elv/Asp	7.2	2.6×10^{-8}	0.024	0.22
SWAT	1.53	0.043	0.28	0.19
PRMS	8.9	0.49	0.069	0.16

Table 4.8 Recharge summary for the optimal parameters produced for each recharge model. Minimum and maximum recharge values are a product of the recharge multiplier so values displayed are effective uniform depth applied to the model.

Even when calibrating a multiplier to adjust the overall magnitude of recharge estimated by the surface water models and applied to the ground water models, the Elv/Asp recharge model produced the best overall model fit. This was followed by the Elevation recharge model, SWAT model, Uniform recharge model and last the PRMS recharge model. Figure 4.19 and Figure 4.20 are graphical summaries of calibration statistics.

Evaluation of the Elv/Slp/Asp recharge model showed the slope term of equation 4.7 had little sensitivity to recharge rate. This is believed be to an averaging affect. Slopes

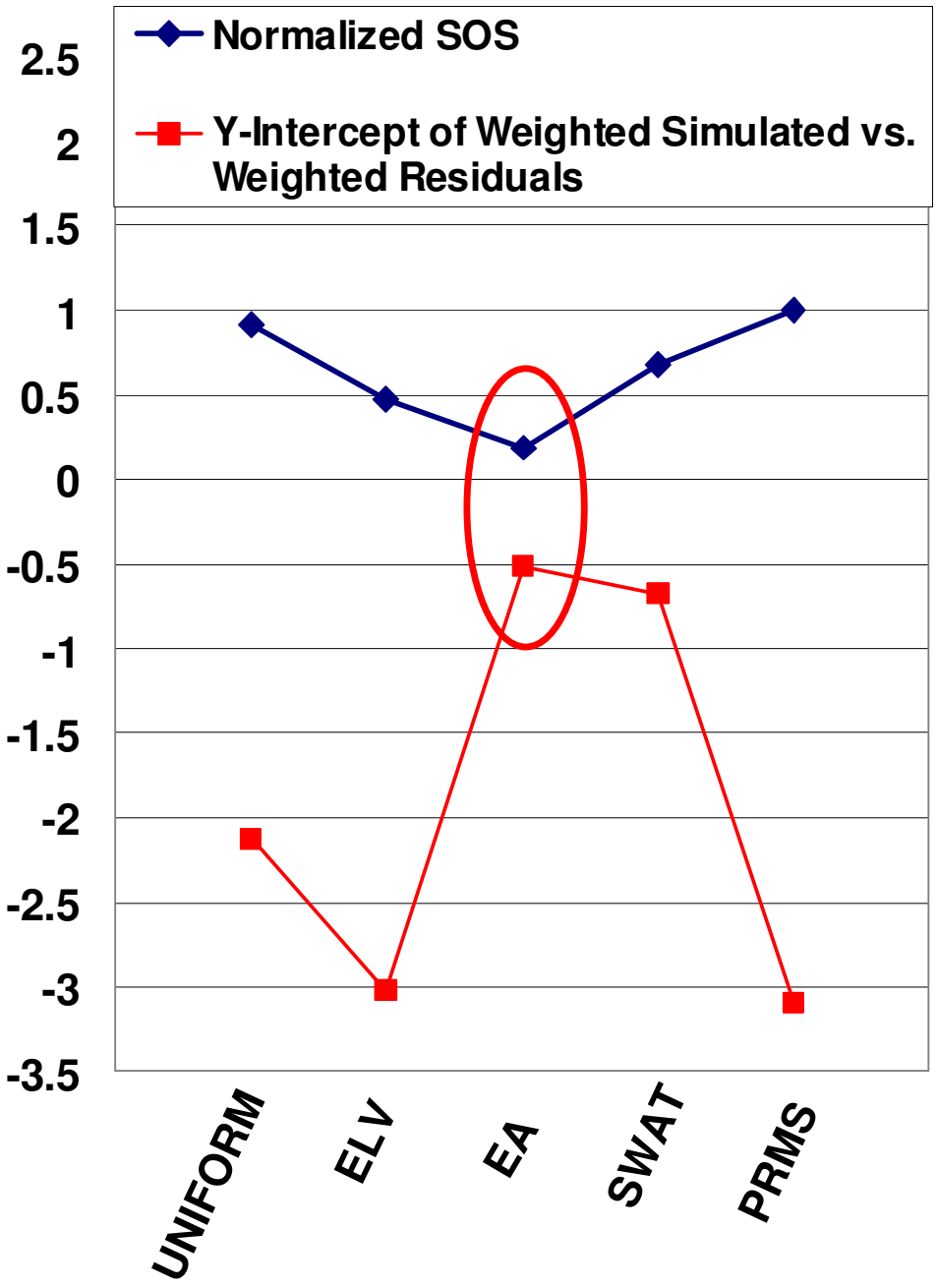

Figure 4.19 Normalized SOS and y-intercept of weighted simulated vs. weighted residuals for each recharge model. Dividing the largest SOS into each SOS for all models normalized SOS. Ideally the SOS and y-intercept should be zero.

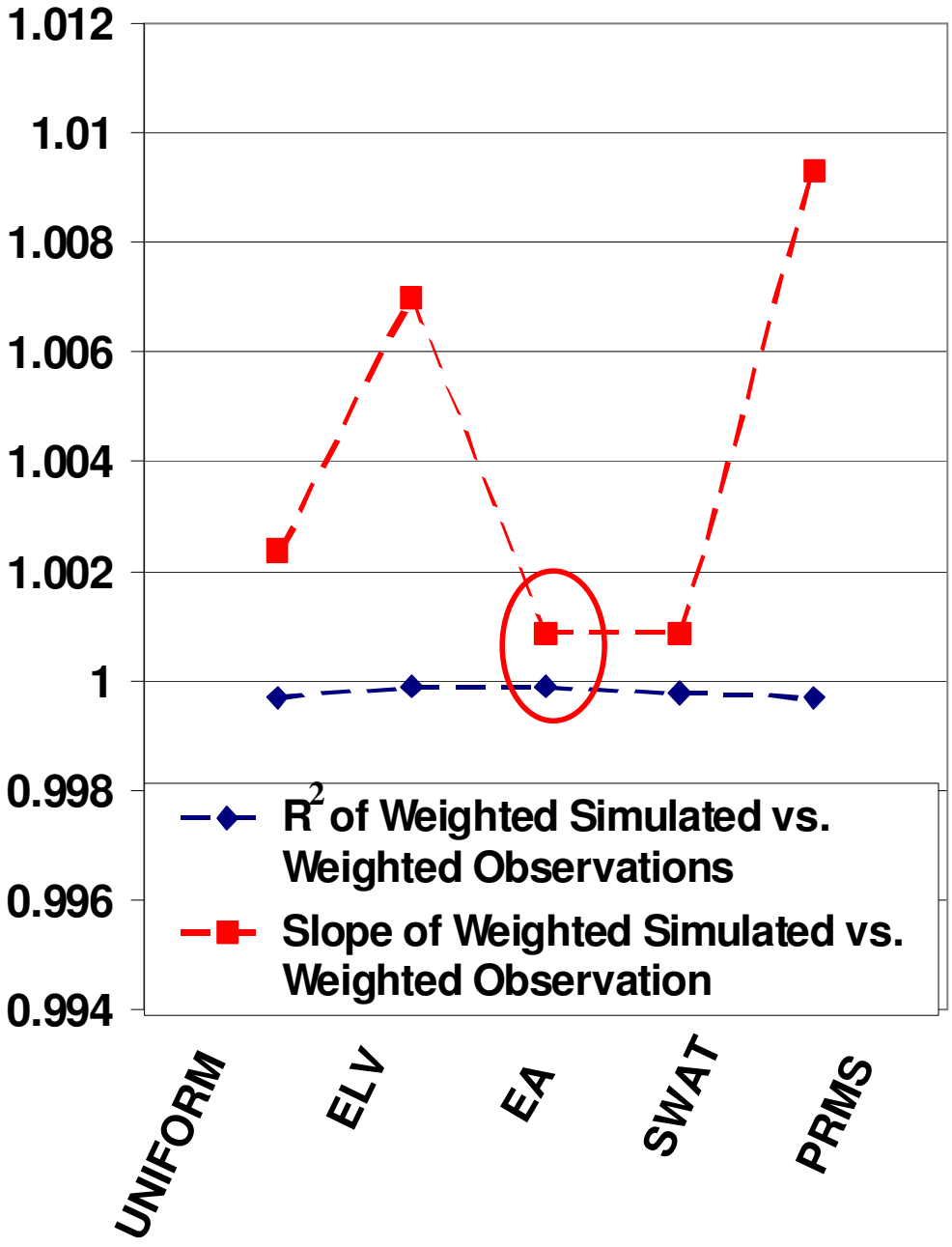

Figure 4.20 The R^2 of weighted simulated vs. weighted observations and the slope of weighted simulated vs. weighted observations. Ideally R^2 and slope should be one.

were calculated from a DEM, which has 30m by 30m (98.5ft by 98.5ft) resolution, which is then averaged again to obtain a value for the MODFLOW cells 650ft by 408 ft, such that steep slopes are averaged out (Figure 4.21).

The Elv/Asp and Elevation recharge models produced little spatial bias with their calculated recharge distribution. Unweighted head residuals were similar between the two models with the Elv/Asp model producing smaller residuals (Figure 4.5). The main difference between Elevation model results and Elv/Asp results was related to the flow observation errors. When aspect was incorporated into the recharge distribution, flow residuals were greatly reduced, 30% to 3% at FLTZN, 77% to 7% at SWBO2 and 30% to 12% at SWAO1. Reasons for this are presently unknown, but by incorporating slope aspect several possible parameters affecting recharge are incorporated. Slope aspect is believed to generically represent differences in vegetation, evaporation and possibly soil type. Incorporating another variable into the recharge equation (4.4) may give the Elv/Asp recharge model more flexibility to estimate the distribution of recharge. Comparing the minimum and maximum recharge values applied from each model (Table 4.7), the Elv/Asp had a much larger range of recharge values applied.

The Uniform recharge model, SWAT recharge model and PRMS recharge model all produced spatial bias with their calculated recharge distributions. The Uniform recharge model overestimates recharge in lower elevations while underestimating recharge in higher elevations and had large residuals in the middle elevations. Since it appears that higher elevations receive more recharge and the uniform recharge model cannot represent this, because it can only spread recharge uniformly throughout the basin, an average recharge value was estimated that underestimated recharge at the higher elevations and overestimated recharge at lower elevations. The SWAT and PRMS recharge models were created and calibrated outside of MODFLOW by other researchers therefore the reason for spatial bias is unknown. However, the SWAT model overestimated recharge in the lower elevations and the PRMS model underestimated recharge in the higher elevations.

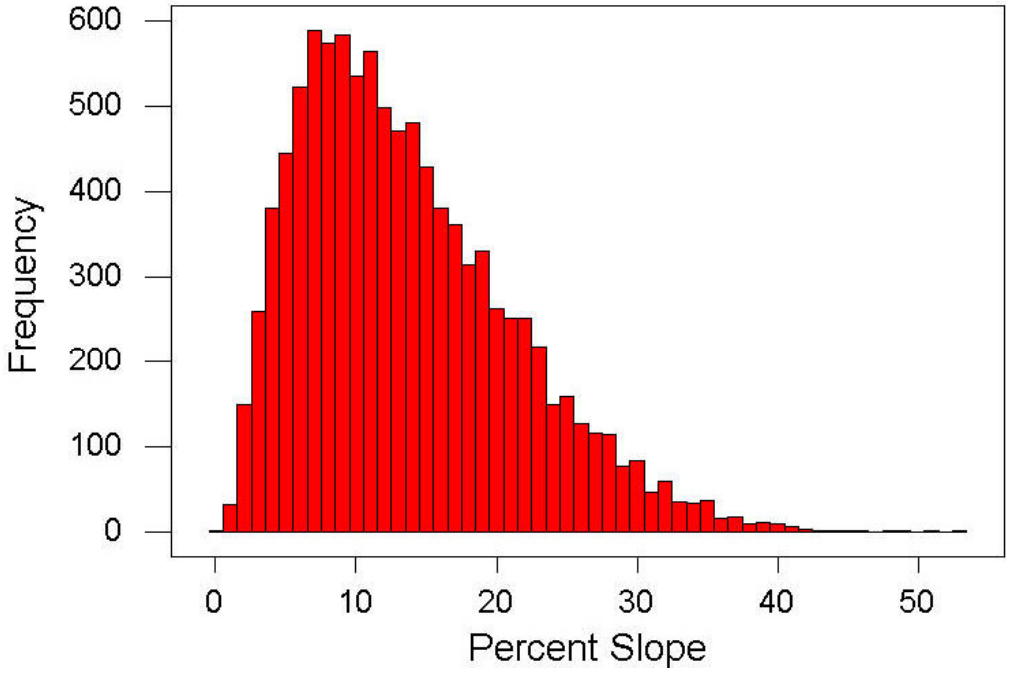

Figure 4.21 Histogram of percent slope values used in Elvation/Slope/Aspect recharge model.

4.5.3 Evaluation of Transient Model

Parameter values and water levels from the model producing the best model fit (Elv/Asp) were used as initial conditions for transient simulation. During simulation recharge was zero and water consumption (pumping rate of wells) remained constant while water levels in 6 wells was observed. Several of the wells (Mh 2, 4, 12, 13) were hand dug and reside only in soil. The model does not contain a soil layer, so these wells were excluded from the transient simulation.

UCODE was used for transient calibration. Parameter estimation converged when the user-defined closer criteria was satisfied. The total sum-of-squared residuals were 0.028. The unweighted residuals were plotted spatially in an attempt to identify spatial bias (Figure 4.23). The transient model does not appear to have spatial bias simulating water level declines, however this is difficult to evaluate with the limited number of points. Appendix M contains the transient model and UCODE results.

The optimal storage coefficient found by UCODE is approximatly 0.6%. Using this storage coefficient, three wells showed water level decline greater than simulated and three showed less (Figure 4.24). There appears to be spatial variability of storage coefficient, but the distribution cannot be determined with the limited number of points.

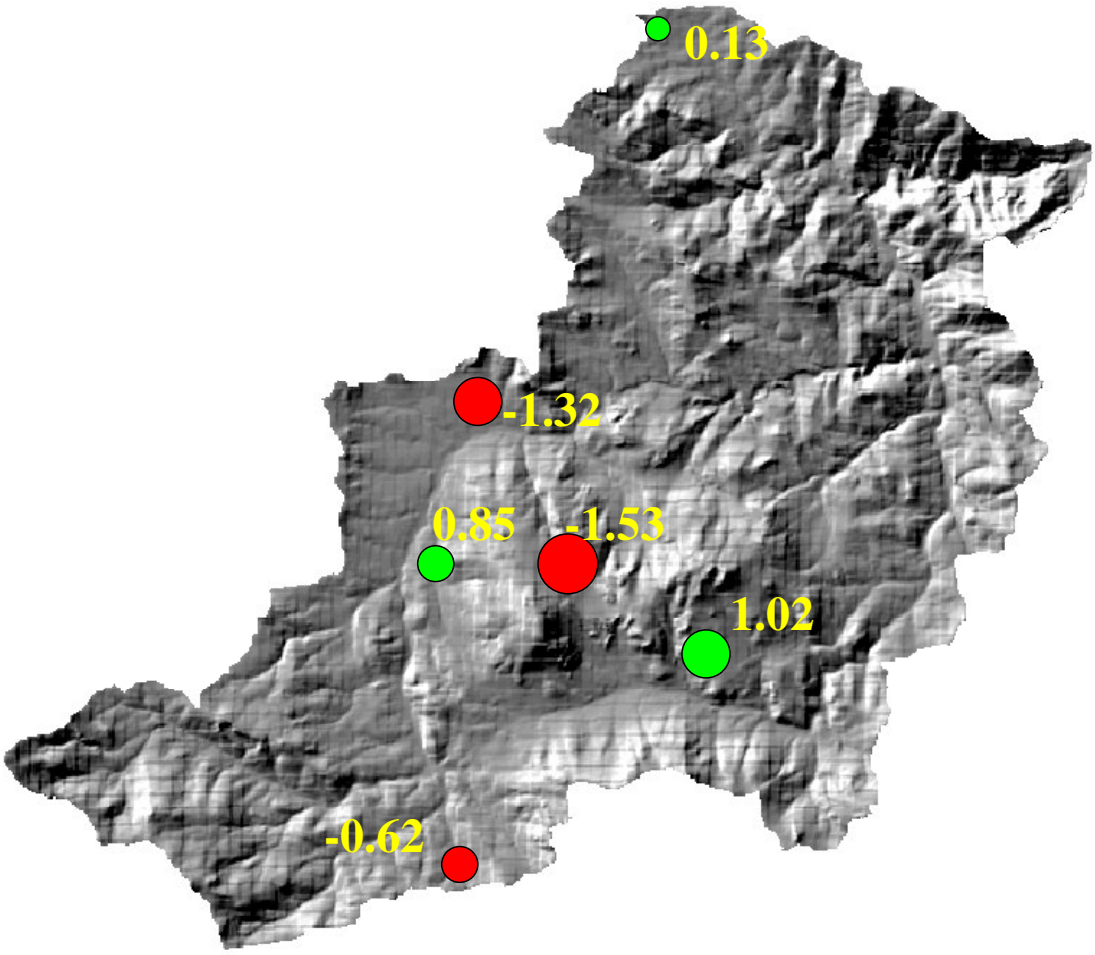

Figure 4.22 Spatial distribution of unweighted head residuals. Red represents the simulated water level decline was greater than observed and green means simulated water level decline was less than observed. The numbers represent error in feet of simulated water level decline for the last time step.

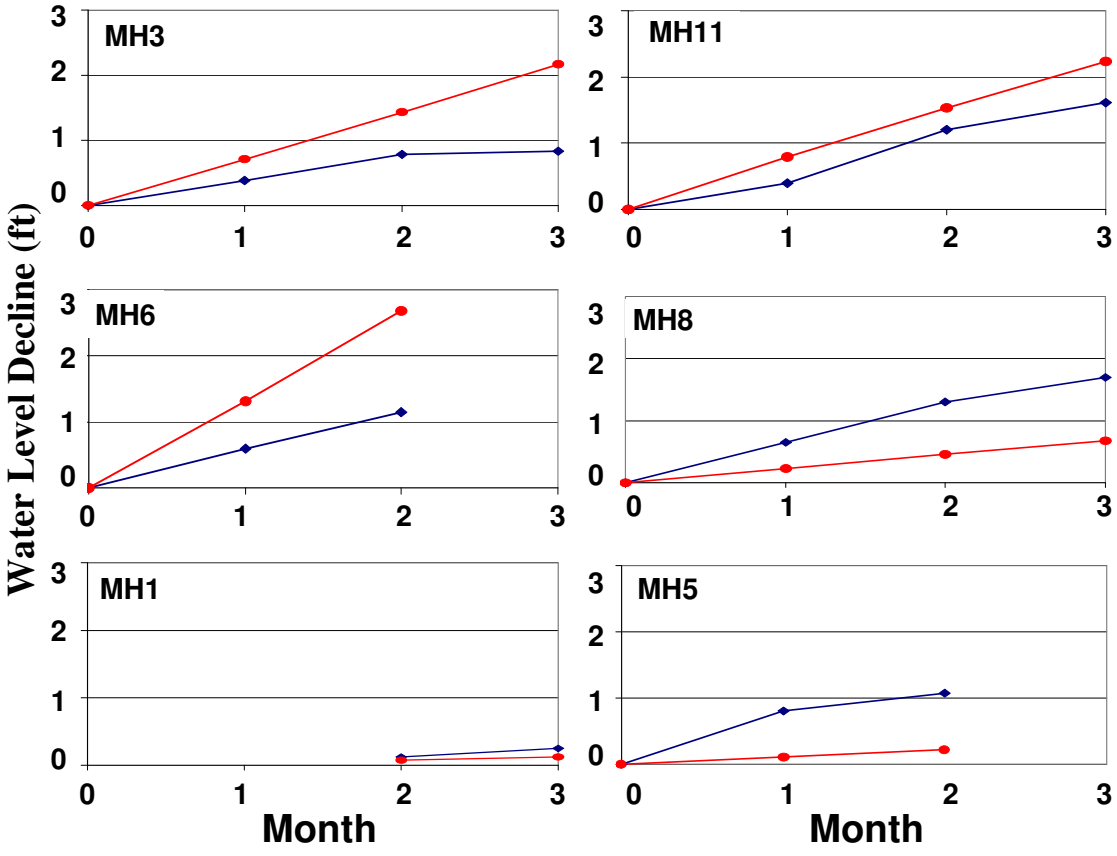

Figure 4.23 Simulated water level decline (red lines) vs. observed water level decline (blue lines) for each month.

CHAPTER 5: DISCUSSION AND CONCLUSIONS

5.1 Research Goal

This research focused on using low-cost data to identify the spatial distribution and magnitude of recharge, hydraulic conductivity, water consumption, and storage in an attempt to quantify sustainability of the TCB aquifer. For a system to be sustainable, recharge to the system must be greater than water consumption. During times of drought when water use exceeds recharge, sustainability will be dependent on storage and the rate that storage declines, which is a function of transmissivity. In order to assess sustainability, each of these factors was evaluated.

5.2 Recharge

Recharge in the Turkey Creek Basin appears to vary significantly with location. Based on the fit of ground-water flow models to head and flow observations, spatially uniform recharge does not adequately represent the system. Calculating recharge from elevation, and slope aspect improves model fit, as evaluated by comparing the sum-of-squared residuals and average head residual at the observation wells. The uniform based recharge model had values of 191 (SOS) and 47 ft (average head residual), the elevation based recharge model, 99 and 28 ft, and the Elevation/Aspect based recharge model 38 and 28 ft. However, addition of other physical parameters (e.g. land use; soil moisture potential; snow pack; and vegetation) degraded model fit. The PRMS recharge model produced an SOS of 210 and an average head residual of 47 ft; while the SWAT recharge model yielded 143 and 39 ft.

The unexpected degradation of model fit when recharge distribution is estimated from surface water models may result from a constant recharge value applied to each HRU (average of 0.42 mi^2) while the other functions (Elevation and Elevation/Aspect)

apply a unique recharge value to each model cell (0.01 mi^2). Alternatively, degradation of fit may be an artifact of the calibration process. The surface water models were calibrated independently of the ground-water model, limiting the number of surface water model parameters that could be calibrated along with the ground-water parameters such as hydraulic conductivity of aquifer units. Calibration of the recharge parameters of the surface water models in conjunction with ground-water parameters may improve model fit.

The magnitude of recharge produced by surface water models, PRMS model (9.6 cfs; 6,945 AFY; 2.75 in/yr EUD) and SWAT (2.37 cfs; 1,694 AFY; 0.67 in/yr EUD) appear larger than field conditions can support. Bossong et al., (2003) calculated values of recharge for three water years (7.8 in/yr, 0.31 in/yr, and 0.16 in/yr, respectively for 1999, 2000 and 2001). These were averaged for input into the steady state ground-water model, yielding a value of 2.75 in/yr with a spatial variation ranging from 0.49 to 8.9 in/yr. The SWAT model used a total recharge equivalent to 0.67 in/yr, with spatial variation ranging from 0.043 in/yr to 1.53 in/yr. In order to evaluate whether the spatial distributions of recharge determined with the surface water models are representative of the true distribution, their results were incorporated into a ground-water model and calibrated with a recharge multiplier, constrained by a stream base flow value of 0.35 ft^3/sec. Magnitudes of recharge resulting from each model were: 1) Uniform distribution, 0.54 ft^3/sec, 389 AFY; 2) Elevation based distribution, 0.52 ft^3/sec, 375 AFY; 3) Elevation/Aspect based distribution, 0.77 ft^3/sec, 556 AFY; 4) PRMS, Precipitation Runoff Modeling System, 0.56 ft^3/sec, 406 AFY; and 5) SWAT, Soil Water Assessment Tool, 0.66 ft^3/sec, 474 AFY. The EA model produced the best fit.

Based on current modeling and field observations, long-term average recharge is expected to be between 0.1 in/yr and 2.25 in/yr (252 to 5664 AFY). A rate of 2.25 in/yr is considered to be a substantial overestimation, resulting from the combination of maximum values for all parameters. This range includes the range of recharge rates (0.1 –

1.0 in/yr) estimated by Poeter et al. (2003), 0.6 in/yr estimated by Hofstra and Hall (1976) and 0.67 in/yr estimated by Murray (2003) using the SWAT surface water model.

5.3 Hydraulic Conductivity

Hydraulic conductivities for the best-fit model were compared to average hydraulic conductivities from Freeze and Cherry (1979). Using the hydraulic conductivity of the coarse-grained granitic rock group ($3.0x10^{-3}$ ft/day) for comparison, hydraulic conductivities are at the lower end of the hydraulic conductivity range for fractured rocks. Consequently, drainage from the basin will be relatively slow, which should enhance sustainability through droughts.

5.4 Water Consumption

The present population in TCB utilizes individual water wells and individual septic disposal systems (ISDS). Estimating that each home uses 150 GPD/home (the lowest estimated water use from the water budget), for 4900 homes, with a 90% return rate, provides a minimum water use of approximately 105 AFY. A high use is provided by the USGS estimate of 1900 AFY with a 90% return, which is a use of 190 AFY (Bossong et al., 2003). However recent measurements suggest return rate may be as low as 70% (Dano, 2003), yielding an estimated range of water consumption of 315 to 570 AFY (maximum water budget and USGS values respectively).

5.5 Specific Yield

The estimated range of specific yield in TCB is 0.2 – 2.5%. Calibration of observed water level decline to simulated water level decline in a ground-water model produced a smaller (0.6%) specific yield than aquifer tests (IHWD, 2.4% and Lewis, 2.5%). This is to be expected because multi-well aquifer tests were only successful in

wells that are preferentially located in high transmissivity and storage zones. Whereas storage calculated by the ground-water model is an average value assigned uniformly throughout the basin.

The range of specific yield (0.2% -2.5%) calculated from aquifer-test analysis and the ground-water model are larger than porosity values reported by Bossong et al., (2003) and Caine et al., (2003). They report porosity for the intrusive rock unit (equivalent to the granitic rock) to be constrained between two calculated end members, (0.0025% and 0.246%). These values were calculated by FracMan (Dershowitz et al., 1998) based on fracture data from surface outcrops, using a range of apertures (10μm – 1mm). Discrepancies between estimates published by Bossong and Caine and values measured in the field could occur because published estimates did not account for the following: fractures could decrease in aperture with increased depth due to overburden pressure; fractures that are not seen by the naked eye are not incorporated into estimated porosity; and matrix porosity is not included. The first two problems would cause published estimates to be larger than measured, which is not the case. Given that published estimates are smaller than measured values, contribution to storage from matrix porosity is a likely cause of the discrepancy. Values measured with pump tests reflect shallow storage. If water levels were to continue to decline, specific yield is likely to decrease.

5.6 Sustainability

Water use ranges from 105 AFY to 190 AFY given 90% return, or from 315 AFY to 570 AFY given a 70% return. The long-term average recharge rate in the Turkey Creek Basin appears to be above 0.1 in/yr. Given this recharge; TCB could sustain average water use of 250 AFY (the acre-feet resulting from 0.1 inch/yr recharge). Estimated values using a 90% return are both sustainable with 0.1 in/yr of recharge, but neither

estimate is sustainable using a 70% return rate. Continued investigation will reduce the uncertainty.

Given that the current use is near the low estimate of the possible range of recharge to TCB, the long-term water level declines likely reflect a transition to a new equilibrium condition. In a fractured environment this may result in individual wells going dry (well yield below sustainable use), but deepening or relocating wells should yield a sufficient supply once a well-connected fracture is tapped by the well. Given that the long-term average recharge is likely greater than average water consumption in TCB, storage is estimated to be relatively high for a fractured rock aquifer, and hydraulic conductivity is estimated to be relatively low, the current population appears to be sustainable in TCB. However, specific yield is likely to decrease as water levels decline, and the maximum estimated current water use exceeds the minimum estimated recharge, thus additional work to refine these estimates will be needed before further development in the Turkey Creek Basin.

REFERENCES CITED

Anderson, Mary P., Woessner, William W. Applied Ground Water Modeling. London: Academic Press, 1992

Arnold, J.G., Srinivasan, R., Muttiah, R.S., Allen, P.M. Continental Scale Simulation of the Hydrologic Balance. Journal of the American Water Resources Association, 35(5): 1037-1051, 1999.

Arnold, J.G., Srinivasan, R., Muttiah, R.S., Williams, J.R. Large area hydrologic Modeling and Assessment Part I: Model Development. Journal of the American Water Resources Association, 34(1):73-89, 1998.

Bossong, Clifford R., Caine, Jonathan S., Stannard, David I., Flynn, Jennifer L., Stevens, Michael R., Dash-Heiny, Janet S. Hydrologic conditions and Assemssment of Water Resources in the Turkey Creek Watershed, Jefferson County, Colorado, 1998-2001. U.S. Geological Survey Water-Resources Investigations Report 03-4034, 2003

Brigham Young University, 2002, Ground Water Modeling System, http://emrl.byu.edu

Bryant, Bruce. Reconnaissance Geologic Map of the Conifer Quadrangle, Jefferson County, Colorado. U.S. Geological Survey Misc. Field Studies Map Mf-598. 1974.

Caine, Jonathan S., Tomusiak, Stephanie R.A. Brittle Structures and Their Role in controlling Porosity and Permeability in a Complex Precambrian Crystalline Rock Aquifer System in the Colorado Rocky Mountain Front Range. Geological Society of America Bulletin, 2003

Dershowitz B., G. Lee, G., Geier, J., Foxford, T., P. LaPointe, P, and A. Thomas, 1998, FracMan – interactive discrete feature data analysis, geometric modeling, and exploration simulation, version 2.6, Golder Associates Inc. 1-184

ESRI, ArcMap, http://www.esri.com, 2003

Fetter, C.W. Applied Hydrogeology. New Jersey: Prentice-Hall Publishing Company, 2000.

Folger, Peter F. A Multidisciplinary Study of the Variability of Dissolved222Rn in Ground Water in a Fractured Crystalline Rock Aquifer and its Impact on Indoor Air. Colorado School of Mines PH. D, T4696, 1995.

Freeze, Allen R., Cherry, John A., Groundwater New Jersey: Prentice-Hall Publishing Company, 1979.

Harbaugh, Arlen W., Banta, Edward R., Hill, Mary C., McDonald, Micheal G. MODFLOW 2000, The U.S. Geological Survey Modular Ground-Water Model User Guide to Modularization Concepts and the Ground-Water Flow Process. Open-File Report 00-92, 2000.

Hicks, John R. Hydrogeology of Igneous and Metamorphic Rocks in the Shaffers Crossing Area and Vicinity Near Conifer, Colorado. Colorado School of Mines M.S. thesis, T-3319, 1987.

Hill, Mary C., Banta, Edward R., Harbaugh, Arlen W., Anderman, Evan R. User Guide to the Observation, Sensitivity, and Parameter-Estimation Processes and Three Post-Processing Programs. U.S. Geological Survey Open-File Report 00-184, 2000.

Hill, Mary C. Methods and Guidelines for Effective Model Calibration. U.S. Geological Survey Water-Resources Investigations Report 98-4005, 1998.

Hofstra, Warren E., Hall, Dennis C. Geologic Control of Supply and Quality of Water in the Mountainous part of Jefferson County, Colorado. Colorado Geological Survey, Bulletin 36, 1975.

King, K.W., Arnold, J.G., Binger, R.L. Comparison o fthe Green-Ampt and Curve Number Methods on Goodwin Creek Watershed using SWAT. 919-925, 1999.

Laws, Roy. Environmental protection agency, personal comm., November 2003

McDonald, Michael G., Harbaugh, Arlen W. A Modular Three-Dimensional Finite-Difference Ground-Water Flow Model. Washington: United States Government Printing Office, 1988.

Morgan, Karen. Spatial Analysis and Modeling of Geochemical Distribution to Assess Fracture Flow in Turkey Creek Basin, Jefferson County, Colorado. Colorado School of Mines M.S. thesis, T-5421, 2000.

Murray, Kyle, unpublished data communicated via electronic files, 2003

Poeter, Eileen P. http://www.mines.edu/~epoeter/583/11/index.shtml, 2003.

Poeter, Eileen P. "Low-Cost Data for Characterization and Management of Fractured Cystalline Aquifers" Proceedings of the 2002 NGWA Fractured-Rock Aquifers Conference, http://www.mines.edu/fs_home/epoeter/research/TC/FracAqConf_Poeter_etal_2002.pdf, 2002.

Poeter, Eileen P., Hill, Mary C. Documentation of UCODE, A computer Code for Universal Inverse Modeling. U.S. Geological Survey Water-Resources Investigations Report 98-4080, 1998

Poeter, Eileen P. unpublished data communicated via electronic files, 2003

Poeter, Eileen P., Thyne, Geoffory., VanderBeek, Greg A., Guler, Cyunt. Ground Water in the Turkey Creek Basin of the Rocky Mountain Front Range in Colorado. Engineering Geology in Colorado: Contributions, Trends, and Case Histories, ed.

Douglas Boyer, Paul Santi, and Pat Rogers Association of Engineering Geologists Special Publication and Colorado Geological Survey Special Publication 55, In Press.

U.S.D.A. Agricultural Research Service. SWAT Software, http://www.brc.tamus.edu/swat/swatbase.html, 2002.

U.S. Geological Survey, Division of Water Resources, Planning and Zoning Department Jefferson County. Mountain Ground Water Resource Study, Phase I Report Summary Water Resources Assessment of the Turkey Creek Watershed 1998 to 2000, 2001.

U.S. Geological Survey. GIS Data, http://gisdata.usgs.net/ned/default.asp

U.S. Geological Survey. Documentation of Precipitation Runoff Modeling System modules for the Modular Modeling System modified for the Watershed and River Systems Management Program. USGS Open-File Report 02-362, 2002

U.S. Geological Survey. Gauging Station 06710992, http://waterdata.usgs.gov/co/nwis/dv?format=gif&period=450&site_no=06710992, 2002.

Theis, C. V., The Relation Between the Lowering of the Piezometric Surface and the Rate and Duration of Discharge of a Well Using Ground-Water Storage. The American Geophysical Union, 1935.

Wang, Herbert F., Anderson, Mary P. Introduction to Ground Water Modeling. London: Academic Press, 1982.

Wellman, T. P., Colorado School of Mines, oral comm., October 2003.

CD-ROM CONTENT

APPENDIX A Newton single-well aquifer test

APPENDIX B Vogal/Johnston single-well aquifer test

APPENDIX C IHWD multi-well aquifer test

APPENDIX D Lewis multi-well aquifer test

APPENDIX E Elevation recharge model code

APPENDIX F Elevation/Slope/Aspect recharge model code

APPENDIX G Water Budget

APPENDIX H Uniform recharge steady state MODFLOW model

APPENDIX I Elevation recharge steady state MODFLOW model

APPENDIX J Elevation/Slope/Aspect recharge steady state MODFLOW model

APPENDIX K SWAT recharge steady state MODFLOW model

APPENDIX L PRMS recharge steady state MODFLOW model

APPENDIX M Transient MODFLOW model